

# **Bulk viscous matter and recent acceleration of the universe**

Thesis submitted to  
**Cochin University of Science and Technology**  
in partial fulfillment of the requirements  
for the award of the degree of

**DOCTOR OF PHILOSOPHY**

by

**Athira Sasidharan**  
Department of Physics  
Cochin University of Science and Technology  
Kochi - 682022

March 2019

*Bulk viscous matter and recent acceleration of the universe*

PhD thesis in the field of Cosmology

Author

**Athira Sasidharan**

Department of Physics

Cochin University of Science and Technology

Kochi-682022

athirasnair91@cusat.ac.in, athirasnair91@gmail.com

Research Supervisor

**Prof. Titus K Mathew**

Department of Physics

Cochin University of Science and Technology

Kochi-682022

titus@cusat.ac.in

**Front Cover:** SN 1994D in NGC 4526.

Credit: High-Z Supernova Search Team/HST/NASA

*Dedicated to my Amma and Achan.*





## CERTIFICATE

Certified that the work presented in this thesis entitled “**Bulk viscous matter and recent acceleration of the universe**” is a bonafide research work done by Ms. Athira Sasidharan, under my guidance in the Department of Physics, Cochin University of Science and Technology, Kochi- 682022, India, and has not been included in any other thesis submitted previously for the award of any degree. All the relevant corrections and modifications suggested by the audience during the pre-submission seminar and recommendations by the doctoral committee have been incorporated in this thesis.

Kochi-682022  
March, 2019

Prof. Titus K Mathew  
(Supervising Guide)



## DECLARATION

I hereby declare that the work presented in this thesis entitled “**Bulk viscous matter and recent acceleration of the universe**” is based on the original research work done by me under the guidance of Prof. Titus K Mathew, Department of Physics, Cochin University of Science and Technology, Kochi- 682022, India, and has not been included in any other thesis submitted previously for the award of any degree.

Kochi-682022  
March, 2019

Athira Sasidharan



# Contents

<b>Table of Contents</b>	<b>ix</b>
<b>List of Tables</b>	<b>xi</b>
<b>List of Figures</b>	<b>xiii</b>
<b>Preface</b>	<b>xix</b>
<b>List of publications</b>	<b>xxiii</b>
<b>Acknowledgments</b>	<b>xxv</b>
<b>1 Introduction</b>	<b>1</b>
1.1 Einstein's Field equation . . . . .	4
1.2 FLRW metric of the Universe . . . . .	5
1.3 Friedmann models . . . . .	5
1.4 Accelerating Universe and Dark energy . . . . .	8
1.4.1 Evidences for Accelerating Universe / Dark energy	9
1.4.2 Standard $\Lambda$ CDM model . . . . .	14
1.4.3 Alternative dark energy models . . . . .	19
1.4.4 Modified gravity models . . . . .	23
1.4.5 Mystery of dark energy and possible remedy . . . . .	26
<b>2 Bulk Viscous Universe</b>	<b>27</b>
2.1 FLRW Universe dominated with bulk viscous matter . . . . .	29
2.2 Behavior of scale factor . . . . .	32
2.3 Parameter estimation using Type Ia Supernovae data . . . . .	37
2.4 Age of the bulk viscous universe . . . . .	42
2.5 Evolution of cosmological parameters . . . . .	44
2.5.1 Deceleration parameter . . . . .	44
2.5.2 Equation of state . . . . .	48
2.5.3 Matter density . . . . .	49
2.5.4 The curvature scalar . . . . .	50
2.6 Statefinder analysis . . . . .	51

<b>3</b>	<b>Thermodynamics of bulk viscous matter dominated universe</b>	<b>57</b>
3.1	Local second law of thermodynamics . . . . .	57
3.2	Entropy and Generalized second law of thermodynamics . . . . .	59
3.3	Entropy evolution for some special cases of viscosity . . . . .	63
<b>4</b>	<b>Dynamical system analysis of bulk viscous matter dominated universe</b>	<b>71</b>
4.1	Phase space analysis of bulk viscous matter dominated universe . . . . .	72
4.2	Phase space analysis of the bulk viscous model including radiation . . . . .	81
4.3	Estimate of the bulk viscosity $\zeta = \zeta_0$ of the cosmic fluid . . . . .	91
<b>5</b>	<b>Bayesian analysis of bulk viscous matter dominated universe</b>	<b>95</b>
5.1	Bayesian model comparison . . . . .	95
5.2	Bayesian analysis of bulk viscous models . . . . .	99
<b>6</b>	<b>Bulk viscous matter with cosmological constant</b>	<b>107</b>
6.1	$\Lambda$ vCDM model . . . . .	107
6.2	The case with constant bulk viscosity . . . . .	111
6.2.1	Age of the universe . . . . .	112
6.2.2	Thermodynamics . . . . .	112
6.2.3	Phase space analysis . . . . .	115
6.3	The case with $\zeta = \zeta_1 H$ . . . . .	116
6.3.1	Equation of state parameter and Deceleration parameter . . . . .	117
6.3.2	Age of the universe . . . . .	119
<b>7</b>	<b>Conclusions and Future scope</b>	<b>121</b>
7.1	Conclusions . . . . .	122
7.1.1	Future scope . . . . .	130
	<b>Bibliography</b>	<b>133</b>

# List of Tables

2.1	Best estimates of the bulk viscous parameters and $H_0$ and also $\chi^2$ minimum value for the two cases of the limiting conditions of the viscous parameters. $\chi_{d.o.f}^2 = \frac{\chi_{min}^2}{n-m}$ , where $n = 307$ , the number of data and $m = 3$ , the number of parameters in the model. For the best estimation we have used SCP “Union” 307 SNe Ia data sets. We have also shown the best estimates of the corresponding parameters for the $\Lambda$ CDM model for comparison, where $\Omega_{m0}$ is the present mass density parameter. The subscript d.o.f stands for degrees of freedom. . . . .	39
3.1	Best estimates of the bulk viscous parameters and $H_0$ and also $\chi^2$ minimum value corresponding to the above different cases of $\zeta$ . $\chi_{d.o.f}^2 = \frac{\chi_{min}^2}{n-m}$ , where $n = 307$ , the number of data and $m$ is the number of parameters in the model. The subscript d.o.f stands for degrees of freedom. For the best estimation we have used SCP “Union” 307 SNe Ia data sets. $\Omega_{m0}$ is the present mass density parameter. . . . .	64
4.1	Critical points for case 1, with $\zeta = \zeta_0 + \zeta_1 \frac{\dot{a}}{a} + \zeta_2 \frac{\ddot{a}}{a}$ . . . . .	75
4.2	Critical points for case 2, with $\zeta = \zeta_0 + \zeta_1 \frac{\dot{a}}{a}$ . . . . .	78
4.3	Critical points for case 3, with $\zeta = \zeta_0$ . . . . .	81
4.4	Critical points for case 1: with $\zeta = \zeta_0$ . . . . .	84
4.5	Critical points for case 2: with $\zeta = \zeta_0 + \zeta_1 \frac{\dot{a}}{a}$ . . . . .	87
4.6	Critical points for case 3: with $\zeta = \zeta_0 + \zeta_1 \frac{\dot{a}}{a} + \zeta_2 \frac{\ddot{a}}{a}$ . . . . .	88
5.1	Best estimates of the bulk viscous parameters, $H_0$ and also $\chi^2$ minimum value corresponding to the cases 4 and 5 of $\zeta$ . $\chi_{d.o.f}^2 = \frac{\chi_{min}^2}{n-m}$ , where $n = 307$ , the number of data and $m$ is the number of parameters in the model. The subscript d.o.f stands for degrees of freedom. For the best estimation we have used SCP “Union” 307 SNe Ia data sets. . . . .	100
5.2	Bayes factors with respect to $\Lambda$ CDM model corresponding to three different priors . . . . .	104

---

5.3	Best estimates of the bulk viscous parameters, $H_0$ and also $\chi^2$ minimum value corresponding to the different cases of $\zeta$ for high redshift. $\chi_{d.o.f}^2 = \frac{\chi_{min}^2}{n-m}$ , where $n = 150$ , the number of data and $m$ is the number of parameters in the model. The subscript d.o.f stands for degrees of freedom. . . . .	105
5.4	Bayes factors with respect to $\Lambda$ CDM model corresponding to two different priors for high redshift. . . . .	105
6.1	Critical values and the corresponding eigen values for the bulk viscous model with $\Lambda$ for $\zeta = \zeta_0$ . . . . .	115
6.2	Best estimates of the bulk viscous parameter $\tilde{\zeta}_1$ , $H_0$ , $\Omega_\Lambda$ , $\Omega_m = 1 - \Omega_\Lambda$ and also $\chi^2$ minimum value for $\zeta = \zeta_1 \frac{a}{a_0}$ $\chi_{d.o.f}^2 = \frac{\chi_{min}^2}{n-m}$ , where $n = 307$ , the number of data and $m$ is the number of parameters in the model. The subscript d.o.f stands for degrees of freedom. For the best estimation we have used SCP “Union” 307 SNe Ia data sets. . . . .	117

# List of Figures

1.1	Hubble diagram (distance modulus vs redshift) from the Supernova Cosmology Project team (SCP) and from High-Z Supernova Search team. . . . .	11
2.1	Behavior of the scale factor for the first set of limiting conditions of parameters $\rightarrow \tilde{\zeta}_0 > 0, \tilde{\zeta}_0 + \tilde{\zeta}_{12} < 3, \tilde{\zeta}_{12} < 3, \tilde{\zeta}_2 < 2$ . Solid line corresponds to the best fit parameters $(\tilde{\zeta}_0, \tilde{\zeta}_1, \tilde{\zeta}_2) = (7.83, -5.13, -0.51)$ . Dashed line corresponds to parameter values $(5, -4, 1)$ and the dotted line corresponds to values $(4, -2, -3)$ . The parameter values are selected so that the transition to the accelerated epoch happens in the past. . . . .	35
2.2	Behavior of the scale factor for the second set of limiting conditions of parameters $\rightarrow \tilde{\zeta}_0 < 0, \tilde{\zeta}_0 + \tilde{\zeta}_{12} > 3, \tilde{\zeta}_{12} > 3, \tilde{\zeta}_2 > 2$ . Solid line corresponds to the best fit parameters $(\tilde{\zeta}_0, \tilde{\zeta}_1, \tilde{\zeta}_2) = (-4.68, 4.67, 3.49)$ . Dashed line corresponds to parameter values $(-6, 4, 6)$ and the dotted line corresponds to values $(-5, 6, 3)$ . The parameter values are selected so that the transition to the accelerated epoch happens in the past. . . . .	35
2.3	Evolution of the second derivative of the scale factor with respect to $y = H_0(t - t_0)$ for the first limiting conditions of parameters, $\tilde{\zeta}_0 > 0, \tilde{\zeta}_0 + \tilde{\zeta}_{12} < 3, \tilde{\zeta}_{12} < 3, \tilde{\zeta}_2 < 2$ . The curve corresponding to $\tilde{\zeta}_0 + \tilde{\zeta}_{12} \geq 3$ represents a universe which is eternally accelerating. If $\tilde{\zeta}_0 + \tilde{\zeta}_1 > 1$ , the transition to the accelerating epoch happens in the past. If $\tilde{\zeta}_0 + \tilde{\zeta}_1 < 1$ the transition will be in the future. If $\tilde{\zeta}_0 + \tilde{\zeta}_1 = 1$ , the transition occurs at present. . . . .	36

- 2.4 Evolution of the second derivative of the scale factor with respect to  $y = H_0(t - t_0)$  for the second limiting conditions of parameters,  $\tilde{\zeta}_0 < 0$ ,  $\tilde{\zeta}_0 + \tilde{\zeta}_{12} > 3$ ,  $\tilde{\zeta}_{12} > 3$ ,  $\tilde{\zeta}_2 > 2$ . The curve corresponding to  $\tilde{\zeta}_0 + \tilde{\zeta}_{12} \leq 3$  represents a universe which is eternally accelerating. If  $\tilde{\zeta}_0 + \tilde{\zeta}_1 < 1$ , the transition to the accelerating epoch happens in the past. If  $\tilde{\zeta}_0 + \tilde{\zeta}_1 > 1$  the transition will be in the future. If  $\tilde{\zeta}_0 + \tilde{\zeta}_1 = 1$ , the transition occurs at present. . . . . 36
- 2.5 Confidence intervals for the parameters  $(\tilde{\zeta}_1, \tilde{\zeta}_2)$  for the first set of limiting conditions, for the bulk viscous matter dominated universe using the SCP “Union” data set composed of 307 data points. The best estimated values of the parameters are  $\tilde{\zeta}_1 = -5.13_{-0.06}^{+0.056}$  and  $\tilde{\zeta}_2 = -0.51_{-0.14}^{+0.13}$  and are indicated by the point. The confidence intervals shown corresponds to 68.3%, 95.4%, 99.73% and 99.99% of probabilities. . . . . 40
- 2.6 Confidence intervals for the parameters  $(\tilde{\zeta}_1, \tilde{\zeta}_2)$  for the second set of limiting conditions, for the bulk viscous matter dominated universe using the SCP “Union” data set composed of 307 data points. The best estimated values of the parameters are  $4.67_{-0.03}^{+0.04}$  and  $3.49_{-0.071}^{+0.089}$  and are indicated by the point. The confidence intervals shown corresponds to 68.3%, 95.4%, 99.73% and 99.99% of probabilities. . . . . 41
- 2.7 Plot of the age of the universe in Gyr with  $H_0$  in units of  $\text{kms}^{-1}\text{Mpc}^{-1}$  for the best fit values of the bulk viscous parameters. The plots are identical for the best estimated values of the parameters from both the limiting conditions. The point located in the figure corresponds to an age 10.5 Gyr for the best estimate value of  $H_0$ , obtained as  $70.49 \text{ kms}^{-1}\text{Mpc}^{-1}$ . The shaded region corresponds to the interval  $H_0(55, 75) \text{ kms}^{-1}\text{Mpc}^{-1}$  and age (10, 15.8) Gyr, which are the permitted intervals for  $H_0$  and age, derived using observations on Galactic globular clusters from the Hipparcos parallaxes [14]. . . . . 43

2.8	Evolution of the deceleration parameter with red shift for the first limiting conditions of viscous parameters, $\tilde{\zeta}_0 > 0$ , $\tilde{\zeta}_0 + \tilde{\zeta}_{12} < 3$ , $\tilde{\zeta}_{12} < 3$ , $\tilde{\zeta}_2 < 2$ . $q$ enters the negative region in the recent past if $\tilde{\zeta}_0 + \tilde{\zeta}_1 > 1$ , at present if $\tilde{\zeta}_0 + \tilde{\zeta}_1 = 1$ and in the future if $\tilde{\zeta}_0 + \tilde{\zeta}_1 < 1$ . Evolution of $q$ for the best estimated values of the bulk viscous parameters is also shown. The redshift at which the $q$ enters the negative region for the best estimated values of the bulk viscous parameters corresponds to $z_T = 0.49^{+0.075}_{-0.057}$ . . . . .	45
2.9	Evolution of the deceleration parameter with red shift for the second limiting conditions of viscous parameters, $\tilde{\zeta}_0 < 0$ , $\tilde{\zeta}_0 + \tilde{\zeta}_{12} > 3$ , $\tilde{\zeta}_{12} > 3$ , $\tilde{\zeta}_2 > 2$ . $q$ enters the negative region in the recent past if $\tilde{\zeta}_0 + \tilde{\zeta}_1 < 1$ , at present if $\tilde{\zeta}_0 + \tilde{\zeta}_1 = 1$ and in the future if $\tilde{\zeta}_0 + \tilde{\zeta}_1 > 1$ . Evolution of $q$ for the best estimated values of the bulk viscous parameters is also shown. The redshift at which the $q$ enters the negative region for the best estimated values of the bulk viscous parameters corresponds to $z_T = 0.49^{+0.064}_{-0.066}$ . . . . .	46
2.10	Evolution of the equation of state parameter with red shift for the best estimates of the bulk viscous parameters. It is found that the evolution of $\omega$ are identical for the best estimates from both the limiting conditions. . . . .	49
2.11	Evolution of the mass density parameter with scale factor for the best estimated values of the bulk viscous parameters. It is found that the variation of the mass density coincides for the best estimated values from the two limiting conditions. . . . .	50
2.12	Evolution of the curvature scalar with scale factor for the best estimate parameters. It is found that the evolution of the curvature scalar are identical for the best estimated values from the two limiting conditions. . . . .	51
2.13	The evolution of the model in the r-s plane for the best estimates of the parameters. The curves are coinciding with each other for the best estimated values of the parameters from both the limiting conditions. . . . .	53

3.1	Evolution of the total dimensionless bulk viscous parameter with the red shift for the best estimated values corresponding to the two limiting conditions. $\tilde{\zeta}$ is positive for $z \leq 0.8$ .	58
3.2	Evolution of the first derivative of entropy with the scale factor for the best estimated values corresponding to the two limiting conditions. . . . .	62
3.3	Evolution of the second derivative of entropy with the scale factor for the best estimated values corresponding to the two limiting conditions. . . . .	63
3.4	Evolution of the first derivative of entropy with the scale factor for the best estimated values corresponding to the case $\zeta = \zeta_0 + \zeta_1 \frac{\dot{a}}{a}$ . . . . .	65
3.5	Evolution of the second derivative of entropy with the scale factor for the best estimated values corresponding to the case $\zeta = \zeta_0 + \zeta_1 \frac{\dot{a}}{a}$ . . . . .	65
3.6	Evolution of the first derivative of entropy with the scale factor for the best estimated values corresponding to the case $\zeta = \zeta_0$ . . . . .	66
3.7	Evolution of the second derivative of entropy with the scale factor for the best estimated values corresponding to the case $\zeta = \zeta_0$ . . . . .	67
3.8	Plot of $T(\dot{S}_E + \dot{S}_m)$ with the scale factor $a$ when event horizon is considered as the boundary. . . . .	70
4.1	The figure shows the phase space structure in the $u - v$ plane corresponding to the Case 1 ( $\zeta = \zeta_0 + \zeta_1 \frac{\dot{a}}{a} + \zeta_2 \frac{\ddot{a}}{a}$ ). The critical point (1,1) in the upper right corner of the plot is a past attractor and the point (1,0.475), below the first critical point, is a future attractor. The direction of the trajectories is shown by the arrow head. . . . .	76
4.2	The figure shows the phase space structure in the $u - v$ plane corresponding to the Case 2 ( $\zeta = \zeta_0 + \zeta_1 \frac{\dot{a}}{a}$ ). The critical point (1,1) in the upper right corner of the plot is a past attractor and the point (1,0.475), below the first critical point, is a future attractor. The direction of the trajectories is shown by the arrow head. . . . .	78

4.3	The figure shows the phase space structure in the $u - v$ plane corresponding to the Case 3 ( $\zeta = \zeta_0$ ). The direction of the trajectories is shown by the arrow head. . . . .	80
4.4	The evolution of the model in the r-s plane for the best estimates of the parameter $\tilde{\zeta}_0$ . . . . .	94
5.1	Marginal Likelihood of the parameters $\tilde{\zeta}_0, \tilde{\zeta}_1$ and $\tilde{\zeta}_2$ corresponding to the case 1, when $\zeta = \zeta_0 + \zeta_1 \frac{\dot{a}}{a} + \zeta_2 \frac{\ddot{a}}{a}$ . . . . .	101
5.2	Marginal Likelihood of the parameters $\tilde{\zeta}_0$ and $\tilde{\zeta}_1$ corresponding to the case 2, when $\zeta = \zeta_0 + \zeta_1 \frac{\dot{a}}{a}$ . . . . .	102
5.3	Marginal Likelihood of the parameter $\tilde{\zeta}_0$ corresponding to the case 3, when $\zeta = \zeta_0$ , a constant. . . . .	102
5.4	Marginal Likelihood of the parameter $\tilde{\zeta}_1$ corresponding to the case 4, when $\zeta = \zeta_1 \frac{\dot{a}}{a}$ , a constant. . . . .	103
5.5	Marginal Likelihood of the parameters $\tilde{\zeta}_0$ and $\tilde{\zeta}_2$ corresponding to the case 5, when $\zeta = \zeta_0 + \zeta_2 \frac{\ddot{a}}{a}$ . . . . .	103
6.1	The figure shows the variation of age with $H_0$ for different values of $(\tilde{\zeta}_0, \Omega_\Lambda)$ . Black line corresponds to $(\tilde{\zeta}_0, \Omega_\Lambda) = (0.1, 0.68)$ . The orange line and blue line corresponds to $(\tilde{\zeta}_0, \Omega_\Lambda) = (0.2, 0.7)$ and $(-0.5, 0.7)$ respectively. . . . .	113
6.2	Evolution of the first derivative of entropy with the scale factor for different values of $(\tilde{\zeta}_0, \Omega_\Lambda)$ subjected to the constrain (6.20). . . . .	114
6.3	Evolution of the second derivative of entropy with the scale factor for different values of $(\tilde{\zeta}_0, \Omega_\Lambda)$ subjected to the constrain (6.20). . . . .	114
6.4	Plot of the equation of state with the redshift for the best estimated values of $\tilde{\zeta}_1$ and $\Omega_\Lambda$ . . . . .	118
6.5	Plot of the deceleration parameter with the redshift for the best estimated values of $\tilde{\zeta}_1$ and $\Omega_\Lambda$ . . . . .	119



## PREFACE

An important milestone in cosmology was the Hubble's discovery of expanding universe in 1929. Recent surprise in modern cosmology occurred in the year 1998, when two teams - the Supernova Cosmology Project lead by Saul Perlmutter and the High-Z Supernova Search Team lead by Brian P. Schmidt and Adam G. Riess, based on their observations on Type I a Supernovae, independently reported that the universe is undergoing an accelerated expansion. For this remarkable discovery, they were awarded with Nobel prize in the year 2011. For explaining this discovery, an additional component called "Dark energy" has been introduced. But its nature and evolution still remains a mystery.

The simplest and the most successful candidate for the dark energy is the cosmological constant  $\Lambda$ , as in the standard model, known as the  $\Lambda$ CDM. This model is successful in predicting the recent acceleration and other cosmological parameters of the recent universe. However, the model has two major flaws: (i) cosmological constant problem, which refers to the huge discrepancy between the theoretical and observed value of the density of the  $\Lambda$  and (ii) cosmic coincidence problem, which refers to the inability of the model to explain the coincidence of the densities of the dark energy and dark matter, irrespective of their different evolutionary status, in the current epoch of the universe. This motivates the dynamical dark energy models like Quintessence, K-essence, Tachyon field, Phantom ghost field, Dilatonic dark energy, Chaplygin gas model, Holographic dark energy model etc. Another method to explain the accelerating universe is to modify the form of gravity. Such models are called alternative theories of gravity and these include  $f(R)$  gravity,  $f(T)$  gravity, Gauss-Bonnet theory, Lovelock gravity, Horava-Lifshitz gravity, scalar-tensor theories, brane world model etc. In spite of all these attempts the nature of dark energy still continues to be a mystery.

At this juncture, attempts were started to explain the recent acceleration without invoking any exotic components. It was suggested that bulk viscous matter could be a potential candidate to realize the recent acceleration of the universe, where one may not need an exotic cosmic component or a modified gravity theory. An additional advantage of this approach

is that it unifies dark energy and dark matter and thereby solving the coincidence problem automatically.

In this thesis we studied the bulk viscous matter dominated model in detail. First we analyze the background evolution of the model and then performed a dynamical system analysis. We have found that the model gives reasonable description of the universe if the viscosity of the dark matter is a constant. We also studied the thermal evolution of the model and have shown that the generalized second law of thermodynamics is satisfied and the model describes a universe which evolves as an ordinary macroscopic system. Due to slight problem in the prediction of age of the universe, we have extended the model by incorporating a bare cosmological constant as an additional component and have found that age has been improved substantially. Below we give a brief account of the facts analyzed in different chapters of the thesis.

**Chapter 1 :** This chapter gives a brief introduction to cosmology. It starts from Einstein's field equation and ends by giving a brief motivation to the bulk viscous model. The chapter briefly discuss the discovery of accelerating universe, the component dark energy and motivates the bulk viscous model of the universe.

**Chapter 2 :** This chapter describes our work on the the analysis of the background evolution of the bulk viscous matter dominated universe. We consider the total bulk viscosity coefficient,  $\zeta$ , as proportional to both the velocity and acceleration of the expansion of the universe as,

$$\zeta = \zeta_0 + \zeta_1 \frac{\dot{a}}{a} + \zeta_2 \frac{\ddot{a}}{\dot{a}}.$$

Following Eckart's approach in accounting the viscosity, we found two limiting conditions for the viscous coefficients ( $\zeta_0$ ,  $\zeta_1$ ,  $\zeta_2$ ) corresponding to a universe having a Big-Bang at the origin, followed by an early decelerated epoch and then making a smooth transition into an accelerating epoch. We have constrained the model with the Type Ia Supernovae data, hence evaluated the best estimated values of the bulk viscous parameters and also the present Hubble parameter corresponding to the two limiting conditions. We found that the evolution of the cosmological parameters are the same for the two limiting conditions. The transition into the late accelerating phase

occurs around a red-shift of  $z_T \sim 0.49$ , which is in the concordance range. The present value of the deceleration parameter and equation of state are found to be around,  $q_0 \sim -0.68$  and  $\omega_0 \sim -0.78$  respectively.  $q_0$  is in the concordance range but  $\omega_0$  is comparatively high. However the end state of the model is a de Sitter epoch, with equation of state  $\omega = -1$  and deceleration parameter  $q = -1$ , as indicating by almost all the recent cosmological observations. The age of the universe predicted by this model is relatively less than that predicted from the oldest galactic globular clusters, however it is within the concordance limit. We also made a statefinder analysis and found that the model is distinguishably different from the standard  $\Lambda$ CDM model at present, but shows a de Sitter type behavior in the far future of the evolution.

**Chapter 3 :** This chapter is devoted to the analysis of the thermodynamics of the model. A preliminary analysis shows a violation of local second law of thermodynamics during the early epoch when  $z > 0.8$  and is due to the behavior of total viscosity of the dark matter. But is only a local phenomenon. On extending the analysis to the generalized second law, we found that it is fully satisfied throughout the evolution of the universe. For a thermodynamically consistent system, the second derivative of the entropy must be negative at least in the long run of the evolution, i.e.  $\ddot{S} < 0$ . In the case of the present viscous model we found that this condition is obeyed so that the model describes a universe which evolve like an ordinary macroscopic system. However, when  $\zeta = \zeta_0$ , both the local second law and the generalized second law of thermodynamics are found to be valid throughout the evolution of the universe and also obeys the convexity condition (maximization of entropy).

**Chapter 4 :** In this chapter, we discussed the dynamical system analysis of the model to understand its asymptotic behavior. Converse to the earlier analysis, here we have included the radiation component besides matter. It was found that the model predicts a conventional evolution of the universe, i.e., a universe having an initial radiation dominated phase followed by a decelerated matter dominated phase and then finally evolving to an accelerated epoch, only when the coefficient of bulk viscosity  $\zeta = \zeta_0$ , a constant. We compute the evo-

lutionary behavior of the cosmic parameters corresponding to this case and also obtained the range of values for  $\zeta_0$  of the matter to represent a conventional universe.

**Chapter 5 :** There exists many models of dark energy in the literature which are giving almost same background evolution for the universe. To check the relative status of a model, Bayesian analysis has been used. This chapter deals with the Bayesian analysis of the bulk viscous matter dominated universe, where we contrast the model with the standard  $\Lambda$ CDM model of the universe. We have shown that, even though the viscous model gives a reasonable back ground evolution of the universe, the Bayes factor of the model indicates that it is not so superior over the  $\Lambda$ CDM model, but have a slight advantage over it.

**Chapter 6 :** In this chapter, we extended the analysis given in the second chapter by introducing an additional cosmic component, the cosmological constant,  $\Lambda$  into the bulk viscous matter dominated universe. This model, as many authors have interpreted, may be called as  $\Lambda$ vCDM model, which is  $\Lambda$  viscous cold dark matter model. We mainly studied the evolution of the cosmological parameters by finding the limiting conditions on the viscous parameters. We also consider two special cases for  $\zeta$  ( $\zeta = \zeta_0$  and  $\zeta = \zeta_1(\frac{\dot{a}}{a})$ ). We then obtain the evolution of the cosmological parameters and the age of the universe subjected to the range of the viscous parameters. The evolution of the entropy has also been studied and found that both the generalized second law and entropy maximization condition are satisfied.

**Chapter 7 :** In this chapter we summarized the overall work and presents our conclusions. We have also presented the future scope of the work.

## List of publications

Papers published in refereed international journals and those presented in seminars and conferences are listed below.

### Refereed Journals.

1. Athira Sasidharan and Titus K Mathew, “Bulk viscous matter and recent acceleration of the universe, *Eur. Phys. J. C.* **75**, 348 (2015).
2. Athira Sasidharan and Titus K Mathew, “Phase space analysis of bulk viscous matter dominated universe, *JHEP* **06**, 138 (2016).
3. Athira Sasidharan, N. D. Jerin Mohan, Money V. John and Titus K Mathew, “Bayesian analysis of bulk viscous matter dominated universe, *Eur. Phys. J. C.* **78**, 628 (2018).
- 4 -Paper under preparation:  
Athira Sasidharan and Titus K Mathew, “Bulk viscous universe with cosmological constant”, Article under preparation.

### Conferences.

1. *Bulk viscosity - a cause for recent acceleration*, National workshop on Dark energy, 5-6 September 2016, Cochin University of Science and Technology.
2. *Bulk viscosity and recent acceleration of the universe*, Post-Planck Cosmology:Enigma, Challenges and Visions, Inter University Center for Astronomy and Astrophysics (IUCAA), Pune, India, October 9-12, 2017
3. *Bulk viscosity as an alternate to Dark energy*, Regional Astronomers meeting on Astronomy Research Opportunities and Challenges-IV, 1-2 December, 2017, Wayanad.
4. *Analysis of Bulk viscous matter dominated universe*, theory thoughts, 27-28 February, 2018, St. Paul’s College, Kalamassery.
5. *Asymptotic behavior of bulk viscous matter dominated universe*, National seminar on Astronomy and Astrophysics (NSAA 2018), 21-22 November, 2018, Farook College, Kozhikode.
6. *Fixing the value of bulk viscosity in the context of late acceleration*, Regional Astronomy Meet-V : Opportunities and Challenges, 8-9 February, 2019, Cochin University of Science and Technology.



## ACKNOWLEDGMENTS

This thesis was completed with the help, support and prayers of several people.

First and foremost, I express my sincere thanks to my supervisor, Prof. Titus K Mathew, for the patient guidance, encouragement and advice he has provided throughout my research period. I have been extremely lucky to have a supervisor who cared so much about my work, and who responded to my questions and queries so promptly.

I would like to thank Prof. Moncy V John, School of Pure and Applied Physics, Mahatma Gandhi University, Kottayam, India who has introduced me the concept of Bayesian Analysis and thereby extending warm hands for doing a collaborative research work.

I gratefully acknowledge all the funding sources - Cochin University of Science and Technology for providing me UJRF, KSCSTE and DST for DST-INSPIRE fellowship, that made my Ph.D. work possible.

I express my heart-felt gratitude to Prof. M. Junaid Bushiri, Head of the Department of Physics and all the former Heads of this Department

for providing the necessary facilities for my research work. I thank all the members of the faculty, library and office staff of the department for the help they rendered during the entire period of my research study. Special thanks to Dr. Ramesh Babu T, Dr. M. Sabir and Dr. Godfrey Louis for their help and always being available with their comments and suggestions for the improvement of the present work. I would also like to acknowledge all the teachers I learnt from since my childhood, I would not have been here without their guidance, blessing and support.

I also like to thank Inter University Center for Astronomy and Astrophysics (IUCAA), Pune for support they have extended in using the computational facility for many of our computations. We have also used the excellent library in IUCAA for reference purposes.

I would like to thank all my fellow researchers, Jerin, Paxy, Manosh, Athul, Sarath, Dinto, Thaskeena, Rajagopalan Nair, Krishna, etc for their moral support and motivation which helps me to bring the best in me. I also like to thank all my seniors, specially Lini, for all the support and guidance. I would also like to thank all other research scholars, M. Phil. and M. Sc. students of the Department for the moments I had with them.

Last, but by no means least, this thesis would not have been possible without the confidence, endurance and support of my family. Thank you Achan and Amma (N Sasidharan Nair and G Saralakumari) for all the sacrifices you have made for me. Thank you for always being there for me and understanding me and also for giving me an environment to grow up

in where I was able to think the way I chose. I owe my deepest gratitude towards my soul mate, Muralikrishnan for his eternal support and understanding of my goals and aspirations. My heart felt regard also goes to my in laws (Sivaprasad and Jayasree) for their love and moral support.

Above all, I express my gratefulness to the Almighty God for providing me the needful and giving me strength to face every phases of my life.

Athira Sasidharan



# 1

## Introduction

*In this chapter we are giving necessary introduction to the cosmological model and also discussing the discovery of the recent acceleration of the universe. Following this, we describe the standard  $\Lambda$ CDM model, its success and short comings and also motivates the bulk viscous model which is the subject of the thesis.*

Cosmology is the study of the origin, evolution and ultimate fate of the entire universe, which has been lead by theoretical as well as observational advances. It deals with the large scale properties of the universe. Even though the area had it's uplift with the Newtonian theory of gravity, the modern era of cosmology began with the introduction of General theory of relativity by Albert Einstein in 1915. Earlier it was strongly believed, even by Einstein, that the universe is static, steady and infinite. On understanding that his own equations of gravity would lead to a dynamical universe, Einstein modified the field equations by introducing  $\Lambda$ , the cosmological constant in order to get a solution corresponding to a static universe. Five years later, using Einstein's theory of general relativity, Alexander Friedmann developed a model of expanding universe which is having an origin at time  $t = 0$ , often called as the Big Bang. About the same time, Georges Lematre also get the same conclusions. The first observational evidence for an expanding universe was given by

Edwin Hubble in the year 1929, in which he found that the galaxies are receding from us with a velocity proportional to their distance. Following this, Einstein withdraw the cosmological constant from his equation by considering it as his “greatest blunder”. Later Robertson and Walker re-discovered the Friedmann model of the universe and verified that Hubble’s discovery was exactly in accordance with this model of the universe. This ignited a plethora of research in the Friedmann model of the universe, which was then called as the standard hot Big Bang model or Friedmann-Lamatre-Robertson-Walker (FLRW) model of the universe. By combining it with the thermodynamics, George Gamow predicted the presence of a background radiation that would be left over from the early stage of the universe and also argued that the light elements like H, He, Li etc. were synthesized in the early universe. In 1965, Arno Penzias and Robert Wilson detect this Cosmic Microwave Background (CMB) radiation left over from the birth of the universe, which provide a strong evidence for the expanding model of the universe. Later observations on stars of varied metallicity concluded that the abundances of the light elements were in good agreement with the prediction from the FLRW model of the universe. All these were finally proved beyond doubt that our universe is an expanding one.

Due to the attractive nature of gravity, it was expected that the expansion to be decelerating. So, the ultimate fate of the universe depends mainly on two factors, the amount of curvature of the space of the universe (which depends on the matter content of the universe) and the amount at which the expansion is decelerating. Thus the major aim is to find these two parameters, however to achieve it was a ‘Gedanken’ task. The first challenge was to find suitable type of star which can be used as standard candle to chart the distances to far away locations of the universe. The Cepheid variables used by Hubble was not so visible over larger distances

and also the luminosity of them is not so constant to read the history of the universe in an accurate way. During last century, astronomers were fortunate enough to find one such suitable candidate, Type Ia supernovae. These objects are basically exploding white dwarf and because of the constancy of mass, their luminosity is almost constant and more over they are visible over huge distances. Searches were proposed to find out the amount of deceleration of the universe by finding out the velocities and distances of Type Ia supernovae.

In the year 1998, the Supernova Cosmology Project, lead by Saul Perlmutter [1] and the High-Z Supernova Search Team lead by Brian P. Schmidt and Adam G. Riess [2], based on their observations on Type Ia Supernova, independently reported that the Universe is undergoing an accelerated expansion and this extraordinary phenomenon began only in the recent past of the universe, about five billion years ago. This discovery is one of the most important development/milestone in recent cosmology as it is a surprise against the then existed expectation that the expansion would be decelerating. This discovery lead to the search of an exotic form of matter called “Dark Energy”, which is considered to be the cosmic component responsible for the accelerated expansion of the universe. However, the physical origin and the nature of dark energy still remains a deep mystery. The immediate candidate for dark energy was the cosmological constant,  $\Lambda$ . The cosmological constant was then re-introduced into the FLRW model to explain the late acceleration of the universe and the model thus arised is known as the standard  $\Lambda$ CDM model. Though  $\Lambda$ CDM is the most successful model in explaining the recent acceleration of the universe, it has some serious flaws. So, rooms are open for some new models that could explain the current acceleration and its associative properties of the universe. Many looked for some known properties of matter, that could cause this acceleration without invoking the exotic

dark energy. One such simple property is the bulk viscosity of matter and our research work is based on this. Before detailing our work, we present the basics of cosmology and an introduction to accelerating universe. We briefly describe the standard  $\Lambda$ CDM model and have a quick look at some other models which were proposed to explain the recent acceleration of the universe.

## 1.1 Einstein's Field equation

Einstein's general theory of relativity reformulated gravity as the space-time curvature. The dynamics of the gravitational field is described by the Einstein's field equation,

$$G_{\mu\nu} = \frac{8\pi G}{c^4} T_{\mu\nu}, \quad (1.1)$$

which relates the curvature of space-time to the matter content of the universe which causes it. Here  $G_{\mu\nu} = R_{\mu\nu} - \frac{1}{2}g_{\mu\nu}R$ , is the Einstein tensor representing the curvature of space-time,  $R_{\mu\nu}$  is the Ricci curvature tensor,  $g_{\mu\nu}$  is the metric tensor which specifies the space-time geometry,  $R$  is the Ricci scalar,  $G$  is the Newton's gravitational constant,  $c$  is the speed of light and  $T_{\mu\nu}$  is the energy - momentum tensor of matter. The solutions to this equation is primarily depending on the form of  $T_{\mu\nu}$ . In the case of the universe with a uniform distribution with perfect fluid, a homogeneous and isotropic distribution of matter was assumed, which implies  $T_{\mu\nu} = P g_{\mu\nu} + (\rho + P)u_\mu u_\nu$ , where  $u^\mu$  is the four velocity of an observer comoving with the fluid,  $\rho$  and  $P$  are the energy density and pressure of the matter, respectively.

## 1.2 FLRW metric of the Universe

Little was known about the distribution of matter in the universe and hence Einstein's theory of gravity was found to be too difficult to solve. In order to proceed, early cosmologists used the idea called cosmological principle. According to this principle, universe is homogeneous and isotropic at large scales. This principle make easier to define a metric that describes the spacetime of a matter filled universe. Such a metric, in spherical co-ordinates using the sign convention (+,-,-) takes the form,

$$ds^2 = c^2 dt^2 - a(t)^2 \left( \frac{dr^2}{1 - kr^2} + r^2 d\theta^2 + r^2 \sin^2 \theta d\phi^2 \right), \quad (1.2)$$

where  $t$  is cosmic time,  $a(t)$  is the scale factor which is a function of time,  $(r, \theta, \phi)$  are the comoving spacial co-ordinates,  $k$  is the curvature parameter, a constant, which can be scaled in such a way that it takes only the values 1,0 and -1. This metric was proposed by four scientist at various times, Alexander Friedmann, Georges Lematre, Howard P. Robertson and Arthur Geoffrey Walker and hence known as FLRW metric. Here  $k = 1$  corresponds to positive curvature and such a universe is known as a closed universe,  $k = 0$  corresponds to zero curvature and it represents a flat universe and  $k = -1$  corresponds to constant negative curvature and it represents an open universe. The evolution of the universe with different  $k$  value are different.

## 1.3 Friedmann models

Using FLRW metric and assuming that that Universe is filled with perfect fluid, Alexander Friedmann solved Einstein's field equation and thus he obtained the equations which governs the evolution of an expanding

universe, known as the Friedmann equations. These equations are,

$$\frac{\dot{a}^2}{a^2} + \frac{k}{a^2} = \frac{8\pi G}{3}\rho, \quad (1.3)$$

$$2\frac{\ddot{a}}{a} + \frac{\dot{a}^2}{a^2} + \frac{k}{a^2} = -8\pi GP. \quad (1.4)$$

Here overdot represents derivative with respect to the cosmic time  $t$ ,  $\rho$  represents the density of all the contents of the universe and  $P$  represents the corresponding pressure. The above two equations can be combined to form,

$$\frac{\ddot{a}}{a} = -\frac{4\pi G}{3}(\rho + 3P). \quad (1.5)$$

From this equation, it is clear that if  $(\rho + 3P) > 0$ ,  $\ddot{a} < 0$ , implying a decelerating expansion and if  $(\rho + 3P) < 0$ ,  $\ddot{a} > 0$ , implying an accelerating expansion of the universe. For normal matter  $P = 0$  (provided it is an ideal fluid), so  $(\rho + 3P) > 0$ , and hence it produces a decelerating expansion of the universe.

Friedmann model implies that the size of the universe tends to zero, i.e.  $a \rightarrow 0$ , at the beginning of the cosmic time at which the densities of the cosmic constituents and curvature become infinity. This corresponds to a space-time singularity in the beginning of the universe and is called the ‘Big Bang’. For positive curvature corresponds to  $k = 1$ , the universe expands from zero size to a maximum and then contracts back to the original conditions, hence the universe is said to be a closed one [3]. For  $k = 0$ , space is flat and infinite, and the universe expands forever and for  $k = -1$ , space is negatively curved and infinite, and universe expands forever in much faster speed than flat universe. We could define dimensionless density parameter  $\Omega = \frac{\rho(t)}{\rho_c(t)}$ , where  $\rho_c = \frac{3H^2}{8\pi G}$ , is the critical density, where  $H = \frac{\dot{a}}{a}$  is the Hubble parameter and it measures the rate of expansion of the universe. From the equation (1.3). it is clear that when  $\Omega > 1$  or  $\rho > \rho_c$ , then  $k = +1$ . If  $\Omega = 1$  i.e.,  $\rho = \rho_c$ , then  $k = 0$  and if

$\Omega < 1$  or  $\rho < \rho_c$ , then  $k = -1$ . Observations and considerations of early inflationary scenario shows that the value of  $k$  is close to zero [4]. So we assume  $k = 0$ , i.e., a flat universe in our further discussions.

From the Friedmann equations, we can obtain a relation,

$$\frac{d}{da}(\rho a^3) = -3a^2 P. \quad (1.6)$$

If we assume the barotropic equation of state  $P = \omega\rho$ , with constant equation of state parameter  $\omega$ , then the above relation leads to,

$$\begin{aligned} \rho &\propto a^{-3(1+\omega)}, \\ H &= \frac{2}{3(1+\omega)(t-t_0)}, \\ a(t) &\propto (t-t_0)^{\frac{2}{3(1+\omega)}}, \end{aligned} \quad (1.7)$$

where  $t_0$  is the present time. For non-relativistic matter  $\omega = 0$  and for radiation,  $\omega = -\frac{1}{3}$ . It can easily be seen that for matter,  $\rho_m \propto a^{-3}$ ,  $a(t) \propto (t-t_0)^{2/3}$  and for radiation,  $\rho_r \propto a^{-4}$  and  $a(t) \propto (t-t_0)^{1/2}$ . So we see that radiation density is decreasing faster than the matter density as time evolves. This difference is due to the additional decrease in the energy density of radiation due to stretching of wavelength (redshift) as the universe expands. Currently the radiation density is very small but if one moves back in time, the radiation density would increase at a faster rate than matter and a stage occurs where radiation density dominates over matter. Thus we could divide the universe into two era, early radiation dominated epoch and later matter dominated epoch. If  $\omega = 1$ , then  $P = \rho$  and  $\rho \propto a^{-6}$ . This is called a ‘stiff’ equation of state. In such a medium, the speed of sound is the same as the speed of light.

Differentiating equation (1.3) and using equation (1.5), we get

$$\dot{\rho} + 3H(\rho + P) = 0 \quad (1.8)$$

This equation is known as conservation or continuity equation, which gives the variation in density of any given cosmic components with time during the expansion. One of the important observational parameter is the current value of the Hubble parameter,  $H_0$ . Theoretical considerations indicate that it is in the range,  $50 - 100 \text{ kms}^{-1}\text{Mpc}^{-1}$ . Recent observation shows that its value is around  $68 \text{ kms}^{-1}\text{Mpc}^{-1}$  [5].

The FLRW model was successful, (i) in explaining the expansion of the universe, (ii) in predicting the abundance of light-element produced during primordial nucleosynthesis, (iii) explaining the origin of the cosmic microwave background radiation and (iv) also helps in understanding the formation of galaxies and other cosmic structures. However, the model breakdown at the origin of the universe and failed to predict the evolution of the universe before Planck time. It also fails to explain the horizon size of the present universe (horizon problem) and yet couldn't find possible solution to the question why the universe is close to being flat. But the most important challenge is the one regarding the recent discovery on the accelerated expansion of the current universe.

## 1.4 Accelerating Universe and Dark energy

As mentioned before, in hope of measuring the rate at which universe is decelerating, two teams, the Supernova Cosmology Project and the High-Z Supernova Search Team, observed the Type I a Supernovae, which are exploding white dwarfs. Because of the constant mass of Type I a Supernovae, their luminosity will be constant and large. So they can act as good standard candles, which are visible over large distances. Observing their redshift and flux at farther and farther distances, it is possible to read the history of the universe and also will be able to predict the future of the evolution of the universe. These teams measure the redshift and magni-

tude of various Type I a Supernovae and, to their surprise, they found that the expansion of the current universe is actually speeding up. They independently reported their conclusion of accelerating universe [1, 2, 6, 7]. For this remarkable discovery, they were awarded with the Nobel Prize in the year 2011. This acceleration of the universe was further confirmed by the observations on cosmic microwave background radiations (CMBR)[8], large scale structure (LSS)[9], the Sloan Digital Sky Survey (SDSS)[10], the Wilkinson Microwave Anisotropy Probe (WMAP)[11], Baryon Acoustic Oscillation (BAO)[12] etc.

The physical origin of the cosmic acceleration is still remains a deep mystery. To cause such an acceleration, universe must contain some hitherto unknown components that could counteract the gravitational force. Such type of exotic cosmic constituent, called “Dark energy”, has been proposed, which is different from ordinary matter and radiation in the sense that it is having a negative pressure, thereby counteracting the gravitational force. The nature and dynamics of dark energy is still not clearly understood, however, there exists various models in the literature trying to explain it. Before explaining various models, let us first look in detail at the various evidences for accelerating universe.

### **1.4.1 Evidences for Accelerating Universe / Dark energy**

Many observations leads to the conclusion that the universe is accelerating and hence dominated by dark energy in the later stage of the evolution [13]. This section discusses some of the observational evidences that leads to this conclusion.

#### **1. Observations on Type I a Supernovae**

Type Ia Supernovae are those formed when white dwarf exceed the mass of the Chandrasekhar limit by the process of mass accretion

form its binary companion. The spectrum of these supernovae are characterized by absence of Hydrogen spectrum line and presence of absorption line of singly ionized silicon. These are having a constant absolute luminosity or magnitude independent of the redshift and so distance to a SN Ia can be determined by measuring the apparent magnitude, and hence they are treated as “standard candles”. The relation between apparent magnitude  $m$ , absolute magnitude  $M$  and the luminosity distance  $d_L$  is given as,

$$m - M = 5 \text{Log}_{10}\left(\frac{d_L}{\text{Mpc}}\right) + 25. \quad (1.9)$$

Upto 1998, Perlmutter et.al.(Supernova Cosmology project (SCP) team) observed 42 SN Ia in the redshift range  $z = 0.18 - 0.83$  and Riess et.al (High-z Supernova search team (HSST)) discovered 14 SN Ia in the range  $z = 0.16 - 0.62$  and 34 low redshift SN Ia . They observed that the high redshift supernovae was fainter than expected, in addition to the statistical and systematic errors. They obtained the luminosity distance and redshift relation of many high redshift supernova and the results are given in Figure 1.1. Their data clearly point towards a recent cosmic acceleration, with the luminosity distance to the the high-z sample 10-15% larger than expected for a low-mass density universe without dark energy, say  $\Lambda$ .

From the Figure 1.1, it is clear that a matter dominated universe without cosmological constant do not fit the observed data. The observational data in the high redshift regime favor the luminosity distance larger than the one predicted by the CDM model ( $\Omega_m^{(0)} = 1$  and  $\Omega_\Lambda^{(0)} = 0$ ). From the likelihood analysis of the SN Ia data accumulated by the year 1998, Perlmutter et al.[1] found the present density parameter of non-relativistic matter as  $\Omega_m^{(0)} = 0.28^{+0.09}_{-0.08}$  in

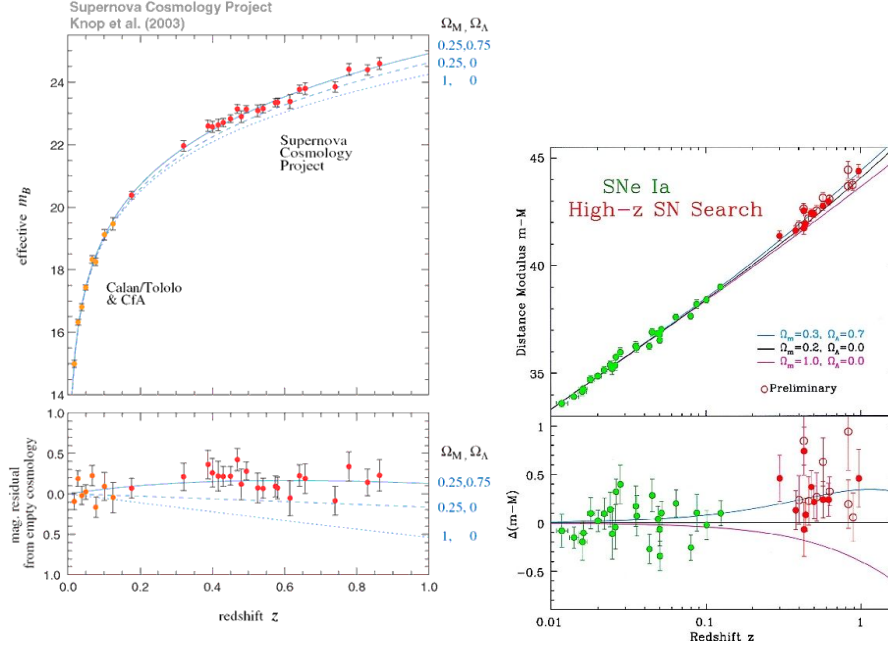


Figure 1.1: Hubble diagram (distance modulus vs redshift) from the Supernova Cosmology Project team (SCP) and from High-Z Supernova Search team.

the flat universe with the cosmological constant.

## 2. Age of the universe

If one use the standard cosmology without dark energy/cosmological constant, then the age of the universe is,

$$t_0 = \frac{2}{3}H_0^{-1}. \quad (1.10)$$

This is found to be in the range  $8.2 \text{ Gyr} < t_0 < 10.2 \text{ Gyr}$ . Compared to the age of the oldest globular cluster, the above range is inconsistent. The age of most of the globular clusters are found to be larger than 11 Gyr and generally lie in the range  $12.9 \pm 2.9 \text{ Gyr}$ [14]. This

discrepancy can easily be eliminated, if one consider a flat universe with cosmological constant or dark energy with equation of state  $\omega_{DE}$  close to  $-1$ . In that case the age becomes,

$$t_0 = \frac{2H_0^{-1}}{3\sqrt{\Omega_\Lambda}} \ln \left( \frac{1 + \sqrt{\Omega_\Lambda}}{\sqrt{\Omega_m}} \right), \quad (1.11)$$

satisfying the constraint  $\Omega_m + \Omega_\Lambda = 1$ . Under asymptotic conditions we have  $H_0 t_0 \rightarrow \infty$  as  $\Omega_m \rightarrow 0$  and  $H_0 t_0 \rightarrow 2/3$  as  $\Omega_m \rightarrow 1$ . It is then seen that the age of the universe increases as  $\Omega_m$  decreases. When  $\Omega_m = 0.3$  and  $\Omega_\Lambda = 0.7$ ,  $t_0 = 0.964H_0^{-1} = 13.1$  Gyr for  $h = 0.72$ . It is clearly evident that, the presence of dark energy is inevitable for the age of the universe to be in range higher than  $t_0 > 11$  Gyr, as indicated by the present day cosmological observation.

### 3. Cosmic microwave Background (CMB)

Cosmic Microwave Background radiations are the primordial radiation left over from the Big Bang which fill the entire universe. These radiation are those which were strongly coupled with baryons in the very early stage of the universe and were decoupled at an epoch around  $z \simeq 1090$ . In 1963, Penzias and Wilson [15] first detected these photons and was found to be almost uniform in distribution with a temperature of about 2.7 K. The slight temperature anisotropies of the CMB were first measured by the COBE satellite in 1992[16]. The angular power spectrum of CMB temperature anisotropies measured by Wilkinson Microwave Anisotropy Probe (WMAP) [11, 17–19] implies that it is dominated by acoustic peaks arising from gravity-driven sound waves in the photon-baryon fluid. And then the positions of these acoustic peaks are shifted by cosmic expansion. Thus the positions and amplitudes of acoustic peaks contain important cosmic information. The combination of CMB

and supernova observations indicates that the universe is accelerating and also the presence of an exotic energy about 70% of the universe.

#### 4. Baryon Acoustic Oscillations (BAO)

The baryons were strongly coupled with the photons before the recombination epoch. As a result of this early stage coupling there arise density fluctuations in the visible baryonic sector of the universe and are called baryon acoustic oscillations. These sound waves must have their effect in the baryonic perturbations which lead to the large scale structure formation as well as in the CMB temperature anisotropies. The length of this wave is given by the largest distance the acoustic waves could travel in the primordial universe before recombination, at which time it stopped. The Sloan Digital Sky Survey (SDSS) [12] catalog gives us a picture of distribution of galaxies upto  $z = 0.47$  and also for a BAO signal. Both CMB and BAO signals indicate that the sound horizon today is about 150 Mpc. The combined analysis of SNe+BAO+CMB constrains the equation of state of the dark energy as  $-1.097 < \omega_{DE} < -0.858$  at 95% confidence level [20].

#### 5. Large Scale Structure (LSS)

Measurements of galaxy clustering can also be a probe of dark energy. The initial fluctuations in the energy density of the early universe grow through gravitational instability into the structure seen today. The sizes, densities and distribution of the structures depends on cosmological parameters, matter density and dark energy and also on the physics of the galaxy formation and evolution. Thus measuring these would constrains the cosmological parameters. Measurement of LSS involves cross-correlations of the galaxy distribution

with the shear field measured by lensing (so-called galaxy-galaxy lensing) or with the cosmic microwave background. At present the largest redshift surveys of galaxies at low redshift are the two Degree Field Galaxy Redshift Survey (2dFGRS) [21] and the Sloan Digital Sky Survey (SDSS)[12]. These provide the current map of large scale structure in the universe.

### 1.4.2 Standard $\Lambda$ CDM model

In order to understand the nature of the recent acceleration, there are basically two approaches. The first one is to modify energy-momentum tensor  $T_{\mu\nu}$  in the right hand side of the Einstein's equation by including suitable forms, which can produce a negative pressure to cause the recent acceleration. The second approach is to modify the left hand side of the Einstein's equation, i.e., the geometry of the space-time and are thus known as modified gravity models or alternative theories of gravity. Some of the models belonging to first and second approach are briefly discussed below. First, we will discuss the standard  $\Lambda$ CDM model, which can incorporate either in first class or in the second method. But we will consider here it as the first approach. The Standard model is considering the cosmological constant,  $\Lambda$ , as the one responsible for the late acceleration of the universe.

The simplest and the most successful candidate for dark energy is the so-called cosmological constant  $\Lambda$ , which was introduced earlier by Einstein to realize a static universe and was omitted due the discovery of expanding universe. But it can also be used to account for the late acceleration of the universe. Incorporating  $\Lambda$  in to the Einstein equation leads to,

$$R_{\mu\nu} - \frac{1}{2}g_{\mu\nu}R + \Lambda g_{\mu\nu} = 8\pi GT_{\mu\nu}. \quad (1.12)$$

In the above equation even though  $\Lambda$  appears in the left hand of Einstein's

equation, it is not a part of the geometry. The cosmological constant actually arise as the vacuum energy. Since vacuum energy should not have any preferred direction, the energy-momentum tensor of it contain only the pressure term, i.e  $T_{\mu\nu} = p_{\text{vac}}g_{\mu\nu} = -\rho_{\text{vac}}g_{\mu\nu}$ . As a result the total energy momentum tensor is  $T_{\mu\nu} = T_{\mu\nu}^{\text{matter}} - \rho_{\text{vac}}g_{\mu\nu} = T_{\mu\nu}^{\text{matter}} - \Lambda g_{\mu\nu}$ . Correspondingly, the Friedmann equations becomes,

$$\frac{\dot{a}^2}{a^2} + \frac{k}{a^2} = \frac{8\pi G}{3}\rho + \frac{\Lambda}{3} \quad (1.13)$$

$$\frac{\ddot{a}}{a} = -\frac{4\pi G}{3}(\rho + 3P) + \frac{\Lambda}{3}. \quad (1.14)$$

From these equations, it is clear that the cosmological constant  $\Lambda$  produces acceleration and thereby counteracting the gravitational effect of normal components of the universe. The equation of state of the cosmological constant  $\omega = -1$ , i.e.,  $P_\Lambda = -\rho_\Lambda = -\frac{\Lambda}{8\pi G}$ . Defining the dimensionless density parameters as,

$$\Omega_m = \frac{8\pi G\rho_m}{3H_0^2}, \quad \Omega_\Lambda = \frac{\Lambda}{3H_0^2}, \quad \Omega_k = \frac{-k}{H_0^2 a^2} \quad (1.15)$$

for matter, cosmological constant and the curvature respectively, then the first Friedmann equation(1.13) can be re-written as,

$$H^2 = H_0^2 (\Omega_{r0}a^{-4} + \Omega_{m0}a^{-3} + \Omega_{k0}a^{-2} + \Omega_\Lambda), \quad (1.16)$$

where the quantities with subscript '0' refers to the values of the corresponding mass parameter in the present time and it is assumed that  $\rho_m \sim a^{-3}$ ,  $\rho_r \sim a^{-4}$ . For a flat universe, i.e.  $k = 0$  and neglecting radiation component since we are interested in the late evolution of the universe, the scale factor evolves as,

$$a(t) = \left(\frac{\Omega_m}{\Omega_\Lambda}\right)^{1/3} \left[ \sinh\left(\frac{3}{2}\sqrt{\Omega_\Lambda}H_0t\right) \right]^{2/3}. \quad (1.17)$$

It is now easy to see that this solution implies a prior decelerated epoch followed by a late accelerated epoch as warranted by the observation. In the asymptotic limit corresponding to the past, i.e.  $H_0 t \ll 1$ , the scale factor reduces to  $a(t) \sim (H_0 t)^{2/3}$  which corresponds to a prior decelerated epoch dominated by matter. On the other hand in the future asymptotic limit,  $H_0 t \gg 1$ , the scale factor takes the form,  $a(t) \sim \exp(\sqrt{\Omega_\Lambda} H_0 t)$ , and is corresponding to the end de-Sitter phase of the universe which expands exponentially. Thus the model predicts the transition from the deceleration to accelerating phase of the universe.

The model is also good in predicting the age of the universe. Putting  $a = a_0 = 1$  in equation (1.17), we get the expression for the age as,

$$t_0 = \frac{2}{3\sqrt{\Omega_\Lambda}} H_0^{-1} \sinh^{-1} \sqrt{\frac{\Omega_\Lambda}{\Omega_m}}. \quad (1.18)$$

By assuming  $\Omega_m + \Omega_\Lambda = 1$  for flat universe, the age of the universe reduces to,

$$t_0 = \frac{2}{3\sqrt{\Omega_\Lambda}} H_0^{-1} \ln \left( \frac{1 + \sqrt{\Omega_\Lambda}}{\sqrt{1 - \Omega_\Lambda}} \right). \quad (1.19)$$

In constraining the age one need to know the observational constraints on the mass density parameters. Using the latest observational data from Planck 2015+Lensing+BAO+JLA+HST, the best fit values of  $\Omega_m = 0.3070 \pm 0.0061$  and  $H_0 = 67.87 \pm 0.46 \text{ kms}^{-1}\text{Mpc}^{-1}$  [22]. If one use the most conventional values,  $\Omega_\Lambda \sim 0.7$ ,  $\Omega_m \sim 0.3$ ,  $H_0 = 70 \text{ kms}^{-1}\text{Mpc}^{-1}$  then according to the above obtained formula the age of the present universe becomes around 13 Gyr, which is close the age deduced from the oldest globular clusters. The above constraints on the mass parameters implies that, that  $\Lambda$  contributes 70% of the energy of the universe and matter contributes the remaining 30% which would be further divided into dark matter (25%) and baryonic matter (5%).

The model is also reasonably successful in predicting all other cosmological parameters. The model by default accounting for a dark en-

ergy with equation of state,  $\omega_\Lambda = -1$ . From the combined analysis of SNe+CMB+BAO, the WMAP [19] has obtained the range for the equation of state of dark energy as,  $-1.097 < \omega_{DE} < -0.858$  which in fact supporting the  $\Lambda$ CDM value.

Another important parameter is the transition redshift, characterizing the transit of the universe from the matter dominated decelerated epoch to the late accelerating phase. The early observations of Permutter et al and Riess et al. have shown that, the transition into the late accelerating epoch occurred at around five billion years ago. From the scale factor derived above one can extract the transition redshift by using the condition,

$$\frac{d\dot{a}}{da} = 0. \quad (1.20)$$

Using equation (1.17) it can be easily shown that the transition redshift  $z_T$  is,

$$z_T = \left( \frac{2\Omega_\Lambda}{\Omega_m} \right)^{1/3} - 1 \quad (1.21)$$

and is corresponding to a redshift of around,  $z_T = 0.56$ .

The nature of expansion as whether it is decelerated or accelerated is characterized by the deceleration parameter and is defined as,

$$q = -1 - \frac{\dot{H}}{H^2}. \quad (1.22)$$

Using the expression for the Hubble parameter of the  $\Lambda$ CDM model, we get,

$$q = \frac{\Omega_m a^{-3} - 2\Omega_\Lambda}{2(\Omega_m a^{-3} + \Omega_\Lambda)}. \quad (1.23)$$

For  $\Lambda$ CDM model, the present value of deceleration parameter is found to be  $q_0 = -0.5427$  [22].

The model is also successful in predicting the structure formation and matter distribution of the universe. In a  $\Lambda$ CDM universe, quasi-equilibrium dark matter clumps or otherwise called ‘‘halos grow by the

collapse and hierarchical aggregation to more massive systems [23]. At the center of these dark halos, galaxies are formed by the cooling and condensation of gas which fragments into stars once it becomes sufficiently dense. As these halos aggregate, groups and clusters of galaxies are formed. They are arranged in the cosmic web, the larger-scale pattern of filaments and sheets which is a nonlinear gravitational sharpening of the pattern already present in the Gaussian random field of initial fluctuations.

### Shortcomings of the $\Lambda$ CDM model

Even though this model explains the recent acceleration of the universe and find close similarities with the observations, it suffers from two major flaws- cosmological constant problem and coincidence problem.

#### 1. Cosmological constant problem

This problem refers to the disagreement of theoretical and observational values of the cosmological constant. From the view of particle physics, the cosmological constant appears as vacuum energy density [24–27]. So in order to find the value of the vacuum density, we add up the zero-point energies of all normal modes of the quantum fields and we assume the momentum at the Planck scale as the cut-off scale and the value is estimated to be

$$\rho_{vac} \approx 10^{74} \text{GeV}^4. \quad (1.24)$$

Observationally, the cosmological constant is found to be

$$\rho_{\Lambda} = \frac{\Lambda m_{pl}^2}{8\pi} \approx 10^{-47} \text{GeV}^4. \quad (1.25)$$

This is about  $10^{121}$  orders of magnitude less than the predicted value. What accounts for this lesser value of  $\rho_{\Lambda}$  is still unknown.

## 2. Cosmic Coincidence problem

This problem refers to the coincidence of the densities of the two dark sectors - dark energy and dark matter. The nature of both the dark energy and dark matter are still unknown [28–30]. However we assume dark energy as cosmological constant and dark matter is modeled as a non-relativistic fluid [31]. So even though their evolution are different, the ratio of their densities is found to be closer to unity in the present time. In the standard model, the dark energy density is assumed to be constant and the dark matter density varies as inverse third power of the scale factor. In the very early universe they differ by many orders. But why they coincide now is still an unexplained fact.

Since the  $\Lambda$ CDM model has the above two major flaws, people started looking for other candidate that could cause the universe to accelerate. Some even consider dynamical approach to this Cosmological constant. In such models, “cosmological constant” remains no longer a constant but varies with time (may be with scale factor, the Hubble parameter, etc). These methods are expected to solve the cosmological constant problem and many other problems faced by constant  $\Lambda$  [32].

### 1.4.3 Alternative dark energy models

Due to the drawback of the  $\Lambda$ CDM model, there introduced varying dark energy models, where both the density of the dark energy and the corresponding equation of state are supposed to vary with the cosmic time. These includes Quintessence, k-essence, Tachyon field, Phantom ghost field, Dilatonic dark energy, Chaplygin gas model, Holographic dark energy model etc. Of these, a brief account on Quintessence, K-essence and Chaplygin gas, which most dealt with in the recent literature are given below.

### 1. Quintessence

The word quintessence means the fifth element. It refers to the fifth dynamical component, in addition to the previously known baryonic matter, leptons, photons and dark matter. The basic idea of quintessence is that the dark energy is in the form of a time varying canonical scalar field  $\phi$  minimally coupled to gravity, which is slowly rolling down toward its potential minimum  $V(\phi)$  [28, 33, 34]. The corresponding action integral is given as,

$$S = \int d^4x \sqrt{-g} \left[ \frac{1}{16\pi G} R + L_\phi \right] + S_M, \quad (1.26)$$

where  $L_\phi = -\frac{1}{2}g^{\mu\nu}\partial_\mu\phi\partial_\nu\phi - V(\phi)$ ,  $R$  is the Ricci scalar and  $S_M$  is the matter action. The evolution of the scalar field is governed by the equation of motion,

$$\ddot{\phi} + 3H\dot{\phi} + V'(\phi) = 0 \quad (1.27)$$

where  $V'(\phi) = \frac{dV}{d\phi}$ . The energy density and pressure of the scalar field, respectively, are given as

$$\rho_Q = \frac{1}{2}\dot{\phi}^2 + V(\phi) \quad P_Q = \frac{1}{2}\dot{\phi}^2 - V(\phi) \quad (1.28)$$

This makes the equation of state parameter,

$$\omega_Q = \frac{\frac{1}{2}\dot{\phi}^2 - V(\phi)}{\frac{1}{2}\dot{\phi}^2 + V(\phi)} \quad (1.29)$$

This ranges in between  $-1 < \omega_Q < 1$ . However, we are interested in the negative pressure region for causing the late acceleration of the universe, i.e,  $-1 < \omega_Q < 0$ . If the scalar field evolves very slowly then the kinetic energy term  $\frac{1}{2}\dot{\phi}^2$  becomes much smaller than the potential energy term  $V(\phi)$ , then  $\omega$  is close to  $-1$  and then the

scalar field behaves just like the cosmological constant. In general the evolution of  $\omega$  depends on the quintessence potentials and the initial conditions[35].

## 2. k-essence

In k-essence, it is the scalar field kinetic energy that drives the acceleration of the universe [36]. The action for such models is characterised as [37],

$$S = \int d^4x \sqrt{-g} \left[ \frac{1}{16\pi G} R + P(\phi, X) \right] + S_m \quad (1.30)$$

Here  $P(\phi, X)$  (usually corresponds to a pressure density) is a function of  $\phi$ , the scalar field and  $X$ , its kinetic energy which is  $X = -\frac{1}{2}g^{\mu\nu}\partial_\mu\phi\partial_\nu\phi$  [37, 38]. The scalar field energy density can be obtained as,

$$\rho_\phi = 2X \frac{\partial P}{\partial X} - P. \quad (1.31)$$

Hence the equation of state for the k-essence scalar field becomes,

$$\omega_\phi = \frac{P_\phi}{\rho_\phi} = P \left( 2X \frac{\partial P}{\partial X} - P \right)^{-1} \quad (1.32)$$

Note that the function  $P$  plays the role of the scalar field pressure  $P_\phi$ . Here the allowed range and possible singularities strongly depend on the function  $P(X, \phi)$ . In literature, many forms for the k-essence Lagrangian have been considered. However, for applications for dynamical systems, we can broadly classify into three:  $P = XG(X/V(\phi))$ ,  $P(X, \phi) = K(\phi)\hat{p}(X)$  and  $P = F(X) - V(\phi)$ . However, String theory restricts the Lagrangian density  $P(\phi, X)$  to the second form  $K(\phi)\hat{p}(X)$ .

## 3. Chaplygin gas model

This is a type of fluid dark energy model [39], in which the universe

is assumed to be filled with perfect fluid, known as Chaplygin gas having an unusual equation of state,

$$P = -\frac{A}{\rho^\alpha}, \quad (1.33)$$

where  $A$  is a positive constant and  $\alpha$  is a parameter. Initially,  $\alpha = 1$  was considered. Later other values of  $\alpha$  was also considered. One of the main peculiarity of this model is that it is a unified model capable of accounting for both dark matter and dark energy. This single fluid behaves as dark matter in the early epoch and as dark energy in the later epoch. Using the conservation equation and the pressure equation noted above, one can obtain expression for the energy density as,

$$\rho(t) = \left[ A + \frac{B}{a^{3(1+\alpha)}} \right]^{\frac{1}{1+\alpha}}, \quad (1.34)$$

where  $B$  is an integration constant. From this equation, it is clear that in the early epoch corresponding to  $a \ll 1$  and the density behaves as,  $\rho \propto a^{-3}$ , which is corresponding to the prior matter dominated region with decelerated expansion. In the late epoch,  $a \gg 1$ , the energy density evolves as  $\rho \propto A^{1/1+\alpha}$ , which corresponds to the de Sitter universe. The effective speed of the sound for the Chaplygin gas is given as,

$$c_s^2 = \frac{dp}{d\rho} = -\alpha\omega = \alpha \left[ 1 + \frac{B/A}{a^{3(1+\alpha)}} \right]^{-1} \quad (1.35)$$

where  $\omega$  is the equation of state parameter of the Chaplygin gas. For this model, the sound speed is small at the early epoch and increases during the later epoch. This leads to the growth of inhomogeneities in the later epoch. An upper bound for  $\alpha$  is obtained in [40] as,  $|\alpha| \leq 10^{-5}$ . The role of the pressure in this model is very crucial. During

matter dominated region, for a successful structure formation, the effect of pressure needs to be strongly suppressed. However, in late time negative pressure is required. But it is difficult to satisfy these two condition simultaneously in this model.

#### 1.4.4 Modified gravity models

Yet another approach to explain the recent acceleration is to modify geometry part of the Einstein equation, which inevitably leads to various modified gravity theories. These include  $f(R)$  gravity,  $f(T)$  gravity, Gauss-Bonnet theory, Lovelock gravity, Horava-Lifshitz gravity, scalar-tensor theories, brane world model, etc. Of these a brief introduction on  $f(R)$ , Gauss-Bonnet theory and  $f(T)$  are given below.

##### 1. $f(R)$ gravity model

In this model, we replace the Ricci scalar  $R$  in the action integral with a function of  $R$ , i.e.  $f(R)$  [41, 42]. So the action becomes,

$$S = \frac{1}{16\pi G} \int d^4x \sqrt{-g} f(R) + S_m(g_{\mu\nu}, \Psi_m) \quad (1.36)$$

where  $S_m$  is a matter action with matter fields  $\Psi_m$ . The field equations can be derived from the above action using two methods or approaches - metric formalism and Palatini formalism [20]. In the metric formalism, the connections  $\Gamma_{\beta\gamma}^\alpha$  are defined in terms of the metric  $g_{\mu\nu}$ . So by varying the action (1.36) with respect to the metric  $g_{\mu\nu}$  we get the field equations as

$$F(R)R_{\mu\nu}(g) - \frac{1}{2}f(R)g_{\mu\nu} - \nabla_\mu \nabla_\nu F(R) + g_{\mu\nu} \square F(R) = 8\pi G T_{\mu\nu}, \quad (1.37)$$

where  $F(R) = \partial f / \partial R$ ,  $\nabla_\mu$  is the covariant derivative and  $\square = g^{\mu\nu} \nabla_\mu \nabla_\nu$  is the D'Alembert operator. The trace of this equation is

given by,

$$3\Box F(R) + F(R)R - 2f(R) = 8\pi GT, \quad (1.38)$$

where  $T = g_{\mu\nu}T_{\mu\nu} = -\rho + 3P$ . In the second approach, Palatini formalism,  $\Gamma_{\beta\gamma}^{\alpha}$  and  $g_{\mu\nu}$  are independent variables. In this approach, varying equation (1.36) with respect to  $g_{\mu\nu}$  gives,

$$F(R)R_{\mu\nu}(\Gamma) - \frac{1}{2}f(R)g_{\mu\nu} = 8\pi GT_{\mu\nu}, \quad (1.39)$$

where  $R_{\mu\nu}(\Gamma)$  is the Ricci tensor corresponding to the connections  $\Gamma_{\beta\gamma}^{\alpha}$ . The trace of this equation gives,

$$F(R)R - 2f(R) = 8\pi GT. \quad (1.40)$$

The de Sitter point corresponds to  $\Box F(R) = 0$ , for both the metric and the Palatini formalism and we get

$$F(R)R - 2f(R) = 0. \quad (1.41)$$

These leads to a plethora of investigations to throw light on the nature of the late acceleration of our universe.

## 2. Gauss-Bonnet (GB) theory

In this modified gravity theory, the gravitational action is modified by adding an arbitrary function  $f(G)$ , where  $G$  is the Gauss-Bonnet invariant defined as  $G \sim R^2 - 4R^{ab}R_{ab} + R^{abcd}R_{abcd}$  [43]. This modification can be explained by considering effective low-energy actions in string theory. The action becomes,

$$S = \int d^4x \sqrt{-g} \left( \frac{1}{2k^2} R + f(G) \right). \quad (1.42)$$

It is found that such modified GB gravity can describe late-time acceleration of the universe [44]. For different functions of  $f$ , it is

found to be possible to describe the transition from deceleration to acceleration or from non-phantom phase to phantom phase in the late universe [45].

### 3. $f(T)$ gravity model

$F(T)$  type of modified gravity is based on the teleparallel equivalent of general relativity (TEGR) Lagrangian, where the torsion will be responsible for the observed acceleration of the universe, and the field equations will always be 2nd order equations. The action of these models is given as [46, 47],

$$S = \frac{1}{16\pi G} \int dx^4 e f(T) + S_m \quad (1.43)$$

where  $e = \det(e^i_\mu) = \sqrt{-g}$  and  $T$  is the torsion scalar and  $f(T)$  is a function of the torsion.  $e^i_\mu$  is the vierbein field which is a dynamical object in teleparallel gravity, which has the following orthonormal property,

$$e_i \cdot e_j = \eta_{ij}, \quad (1.44)$$

where  $\eta_{ij} = \text{diag}(1, -1, -1, -1)$ . The metric tensor is also obtained from the dual vierbein,  $g_{\mu\nu} = \eta_{ij} e^i_\mu(x) e^j_\nu(x)$ . The torsion scalar is defined as [48]

$$T = S^{\mu\nu} T_{\mu\nu}^\rho \quad (1.45)$$

where  $S_\rho^{\mu\nu} = \frac{1}{2}(K_\rho^{\mu\nu} + \delta_\rho^\mu T_\theta^{\nu\mu} - \delta_\rho^\nu T_\theta^{\mu\nu})$ ,  $K_\rho^{\mu\nu} = -\frac{1}{2}(T_\rho^{\mu\nu} - T_\rho^{\nu\mu} - T_\rho^{\mu\nu})$  and  $T_{\mu\nu}^\lambda = \Gamma_{\nu\mu}^{\omega\lambda} - \Gamma_{\mu\nu}^{\omega\lambda}$ .

For a spatially flat FLRW metric the field equations reduces to,

$$\begin{aligned} 12H^2 f_T(T) + f(T) &= 16\pi G \rho \\ 48H^2 \dot{H} f_{TT}(T) - (12H^2 + 4\dot{H}) f_T(T) - f(T) &= 16\pi G p \end{aligned} \quad (1.46)$$

for  $i = 0$  and  $i = 1$ , respectively, where  $f_T(T) = \frac{df(T)}{dT}$  and  $f_{TT}(T) = \frac{d^2 f(T)}{dT^2}$ . Here  $\rho$  and  $p$  are the total energy density and pressure of the

matter content of the universe respectively and satisfies the usual conservation equation (1.8). The equation of state parameter due to torsion is defined as

$$\omega_T = -1 + \frac{4\dot{H}(2Tf_{TT} + f_T - 1)}{2Tf_T - f - T}. \quad (1.47)$$

This model is good in predicting a varying equation of state for the late accelerating universe.

### 1.4.5 Mystery of dark energy and possible remedy

All the above attempts either propose an exotic cosmic component for dark energy or modifying the Einstein's theory of gravity. In spite of these varied approaches, the nature and evolution of dark energy still remains a mystery. Still further problem is that of dark matter which also remains as mysterious as the dark energy. Even though Chaplygin gas model made an attempt to solve this double edged problem of dark matter and dark energy, a clear way out is still lacking. So searches were diverted to check whether it is possible to account at least for the recent acceleration by invoking already known simple properties of matter itself. Dissipative models of cosmology, in which one invoke the bulk viscous property of the matter is promising in this direction. Like Chaplygin gas, this unifies dark energy and dark matter thereby solving the coincidence problem because there is no separate dark energy component. But unlike Chaplygin gas here one doesn't use any exotic fluid, instead the late acceleration is caused by the viscosity of the matter sector.

# 2

## Bulk Viscous Universe

*This chapter gives an account of our work on bulk viscous matter dominated model. We have extracted the values of the model parameters involved using the observational data. Then evaluated the evolution of the cosmological parameters. In addition to this, the state finder analysis of the model is also done to distinguish it from the conventional dark energy models, especially the standard  $\Lambda$ CDM model.*

Misner (1968) [49] was probably the first to introduce viscosity in cosmological theory. Later Murphy, in the year 1973 [50], have found that the bulk viscous pressure is capable of producing expansion in the universe. However it acquired much attention when viscosity has been used to cause the the early inflation of the universe [51–55]. This idea was later extended to explain the late acceleration of the universe [56–61, 78]. Of the fluid dissipative phenomena, bulk viscosity is the most favorable one compatible with the symmetry requirements of the homogeneous and isotropic Friedmann-Lemaitre-Robertson-Walker (FLRW) universe. But a viable mechanism for the origin of bulk viscosity in the expanding universe is still to be sorted out. From the theoretical point of view, bulk viscosity can arise due to deviations from the local thermodynamic equilibrium [62, 63]. In cosmology, bulk viscosity arises as an effective pressure to restore the system back to its thermal equilibrium, which was broken when

the cosmological fluid expands (or contract) too fast. This bulk viscosity pressure generated, ceases as soon as the fluid reaches the thermal equilibrium [64, 65]. In [66, 67], the authors have considered an alternative mechanism for the generation of bulk viscosity due to the decay of a dark matter particle into relativistic products.

In this chapter, we analyze matter dominated cosmological model with bulk viscosity with the aim to understand the recent acceleration of the universe. The non-relativistic matter is basically a pressureless fluid comprising both baryonic and dark matter components. If the bulk viscous matter can produce the recent acceleration of the universe, then it would leads to a unified description of both dark matter and dark energy sectors thereby eliminating the unlikely introduction of any exotic fluid. The additional advantage is that it automatically solves the coincidence problem because there is no separate dark energy component. Since viscosity is basically a transport phenomenon, we took the bulk viscosity coefficient as proportional to both the velocity (characterized by the parameter  $\zeta_1$ ) and acceleration (characterized by the parameter  $\zeta_2$ ) of the expansion of the universe, along with an additive constant ( $\zeta_0$ ). Recently a similar model was studied by Avelino et al. [68], but in constraining the parameters,  $(\zeta_0, \zeta_1, \zeta_2)$  using the observational data the authors fixed either  $\zeta_1$  or  $\zeta_2$  as zero. So it is effectively a two parameter model, which consequently obscured many of the generic properties of the model. In that reference the authors have ruled out the possibility of predicting the conventional evolution of the universe towards a stable late accelerating epoch. However, to get the actual generic behavior of the model, we think that one should study it by evaluating all the parameters simultaneously, which may lead to a more mature conclusion regarding the status of bulk viscous dark matter taking the role of dark energy. In the present work we aim to such an analysis in studying the evolution of all the cosmological

parameters by simultaneously evaluating all the constant parameters on which the total bulk viscosity depends on.

## 2.1 FLRW Universe dominated with bulk viscous matter

We consider a spatially flat universe described by the Friedmann-Lemaitre-Robertson-Walker (FLRW) metric,

$$ds^2 = -dt^2 + a(t)^2(dr^2 + r^2d\theta^2 + r^2\sin^2\theta d\phi^2), \quad (2.1)$$

where  $(r, \theta, \phi)$  are the co-moving coordinates,  $t$  is the cosmic time and  $a(t)$  is the scale factor of the universe dominated with bulk viscous matter, which can produce an effective pressure [69, 70],

$$P^* = P - 3\zeta H, \quad (2.2)$$

where  $P$  is the normal pressure, which is zero for non-relativistic matter and  $\zeta$  is the coefficient of bulk viscosity, which can be a function of Hubble parameter and its derivatives in an expanding universe. We have not considered the radiation component, as it is a reasonable simplification as long as we are concerned with late time acceleration. The form of equation (2.2) was originally proposed by Eckart in 1940 [71]. A similar theory was also proposed by Landau and Lifshitz [72]. However, Eckart theory suffer from pathologies. One of them is that in this theory, dissipative perturbations propagate at infinite speed [73]. Another one is that the equilibrium states in the theory are unstable [74, 75]. In 1979, Israel and Stewart [76, 77] developed a more general theory which was causal and stable and one can obtain the Eckart theory from it in the first order limit, when the relaxation time goes to zero. So, in the limit of vanishing relaxation time, the Eckart theory is a good approximation to the Israel-Stewart theory.

Even though Eckart theory have drawbacks, it is less complicated than the Israel-Stewart theory. So it has been used widely by many authors to characterize the bulk viscous fluid. For example in references [56, 78–80], Eckart approach has been used in dealing with the accelerating universe with the bulk viscous fluid. In this context, it is reasonable to point out that Hiscock et.al.[81] have found that pathological Eckart theory and also truncated Israel- Stewart theory (avoiding the non-linear terms) can produce early inflation. However, as pointed out by the same authors, in the truncated version of Israel-Stewart theory, the relaxation time stands to be a constant which is in fact not logically correct in an expanding universe. However, there exist some later studies [82, 83] which deals with the importance of equation of state in such theories in order to explain the acceleration. But, it should be checked whether these theories will produce the late acceleration of the universe as observed today. One should also note at this juncture that a more general formulation than Israel-Stewart model was proposed by Pavon et al. [84] for irreversible process, especially in dealing with thermodynamic equilibrium of dissipative fluid.

The Friedmann equations describing the evolution of flat universe dominated with bulk viscous matter are,

$$H^2 = \frac{\rho_m}{3}, \quad (2.3)$$

$$2\frac{\ddot{a}}{a} + \left(\frac{\dot{a}}{a}\right)^2 = -P^*, \quad (2.4)$$

where we have taken  $8\pi G = 1$ ,  $\rho_m$  is the matter density and overdot represents the derivative with respect to cosmic time  $t$ . The conservation equation is

$$\dot{\rho}_m + 3H(\rho_m + P^*) = 0. \quad (2.5)$$

From the Fluid mechanics, it is clear that the bulk viscosity coefficient,  $\zeta$  is related to the rate of compression or expansion of the fluid [85]. In the

present model, the fluid is comoving with the expanding universe. So, the velocity and acceleration of the fluid is the same as that of the expanding universe, which are  $\dot{a}$  and  $\ddot{a}$ , respectively. Since there is no conclusive microscopic theory to calculate the transport coefficient, it is logical to consider  $\zeta$  to be depending on the velocity and acceleration,  $\dot{a}$  and  $\ddot{a}$ . The best way is to take a linear combination of the three terms: the first term is a constant  $\zeta_0$ , the second term is proportional to the Hubble parameter, which characterizes the dependence of the bulk viscosity on velocity, and the third is proportional to  $\frac{\ddot{a}}{\dot{a}}$ , characterizing the effect of acceleration on the bulk viscosity [68, 86, 87] as,

$$\zeta = \zeta_0 + \zeta_1 \frac{\dot{a}}{a} + \zeta_2 \frac{\ddot{a}}{\dot{a}}. \quad (2.6)$$

Using the relation  $H = \frac{\dot{a}}{a}$ ,  $\zeta$  becomes,

$$\zeta = \zeta_0 + \zeta_1 H + \zeta_2 \left( \frac{\dot{H}}{H} + H \right). \quad (2.7)$$

On taking this form of time dependent bulk viscosity, the equation of state assumes the most general form [86, 88–90],

$$P_{eff} = \omega\rho + P_0 + w_H H + w_{H2} H^2 + w_{dH} \dot{H}. \quad (2.8)$$

By comparing equations (2.8), (2.2) and (2.7), we could identify,  $w_H = -3\tilde{\zeta}_0$ ,  $w_{H2} = -3(\tilde{\zeta}_1 + \tilde{\zeta}_2)$  and  $w_{dH} = -3\tilde{\zeta}_2$ .

From Friedmann equations, and from equations (2.2), (2.5) and (2.7), we can obtain a first order differential equation for Hubble parameter by replacing  $\frac{d}{dt}$  with  $\frac{d}{d \ln a}$  through  $\frac{d}{dt} = H \frac{d}{d \ln a}$  as,

$$\frac{dH}{d \ln a} - \left( \frac{\tilde{\zeta}_1 + \tilde{\zeta}_2 - 3}{2 - \tilde{\zeta}_2} \right) H - \left( \frac{\tilde{\zeta}_0}{2 - \tilde{\zeta}_2} \right) H_0 = 0, \quad (2.9)$$

where

$$\tilde{\zeta}_0 = \frac{3\zeta_0}{H_0}, \quad \tilde{\zeta}_1 = 3\zeta_1, \quad \tilde{\zeta}_2 = 3\zeta_2, \quad (2.10)$$

are the dimensionless bulk viscous parameters and  $H_0$  is the present value of the Hubble parameter. The above equation can be integrated to obtain the Hubble parameter as,

$$H(a) = H_0 \left[ a^{\frac{\tilde{\zeta}_1 + \tilde{\zeta}_2 - 3}{2 - \tilde{\zeta}_2}} \left( 1 + \frac{\tilde{\zeta}_0}{\tilde{\zeta}_1 + \tilde{\zeta}_2 - 3} \right) - \frac{\tilde{\zeta}_0}{\tilde{\zeta}_1 + \tilde{\zeta}_2 - 3} \right]. \quad (2.11)$$

This equation shows that when  $\tilde{\zeta}_0$ ,  $\tilde{\zeta}_1$  and  $\tilde{\zeta}_2$  are all zeros, the Hubble parameter,  $H = H_0 a^{-\frac{3}{2}}$  which corresponds to the ordinary matter dominated universe. When  $\tilde{\zeta}_1 = \tilde{\zeta}_2 = 0$ , the Hubble parameter reduces to [59]

$$H(a) = H_0 \left[ a^{-\frac{3}{2}} \left( 1 - \frac{\tilde{\zeta}_0}{3} \right) + \frac{\tilde{\zeta}_0}{3} \right]. \quad (2.12)$$

The asymptotic behavior of the Hubble parameter given by equation (2.11) is as follows. As  $a \rightarrow 0$  the  $H \rightarrow a^{-3/2}$  which corresponds to the prior decelerated epoch, on the other hand as  $a \rightarrow \infty$  the  $H \rightarrow \frac{\tilde{\zeta}_0}{\tilde{\zeta}_1 + \tilde{\zeta}_2 - 3}$ , a constant, corresponding to a late accelerating epoch. This shows that with suitable choice of the viscous parameters, it is possible to predict a prior decelerated epoch and late accelerated epoch from the more general Hubble parameter given in equation (2.11).

## 2.2 Behavior of scale factor

In this section we analyze the behavior of scale factor in the bulk viscous matter dominated universe. Using the definition of Hubble parameter, equation (2.11) becomes,

$$\frac{1}{a} \frac{da}{dt} = H_0 \left[ a^{\frac{\tilde{\zeta}_{12} - 3}{2 - \tilde{\zeta}_2}} \left( 1 + \frac{\tilde{\zeta}_0}{\tilde{\zeta}_{12} - 3} \right) - \frac{\tilde{\zeta}_0}{\tilde{\zeta}_{12} - 3} \right], \quad (2.13)$$

where  $\tilde{\zeta}_{12} = \tilde{\zeta}_1 + \tilde{\zeta}_2$ . Integrating the above equation to solve for the scale factor we get,

$$a(t) = \left[ \left( \frac{\tilde{\zeta}_0 + \tilde{\zeta}_{12} - 3}{\tilde{\zeta}_0} \right) + \left( \frac{3 - \tilde{\zeta}_{12}}{\tilde{\zeta}_0} \right) e^{\frac{\tilde{\zeta}_0}{2-\tilde{\zeta}_2} H_0(t-t_0)} \right]^{\frac{2-\tilde{\zeta}_2}{3-\tilde{\zeta}_{12}}}, \quad (2.14)$$

where  $t_0$  is the present cosmic time. Assuming,  $y = H_0(t - t_0)$  and taking second derivative of the scale factor  $a$  (equation (2.14)) with respect to  $y$ , we obtain

$$\begin{aligned} \frac{d^2 a}{dy^2} = \frac{e^{\frac{\tilde{\zeta}_0 y}{2-\tilde{\zeta}_2}}}{2-\tilde{\zeta}_2} \left[ \tilde{\zeta}_0 + \tilde{\zeta}_{12} - 3 + (2-\tilde{\zeta}_2) e^{\frac{\tilde{\zeta}_0 y}{2-\tilde{\zeta}_2}} \right] \\ \left[ \frac{\tilde{\zeta}_0 + \tilde{\zeta}_{12} - 3 + (3-\tilde{\zeta}_{12}) e^{\frac{\tilde{\zeta}_0 y}{2-\tilde{\zeta}_2}}}{\tilde{\zeta}_0} \right]^{\frac{2(\tilde{\zeta}_1-2)+\tilde{\zeta}_2}{3-\tilde{\zeta}_{12}}} \end{aligned} \quad (2.15)$$

From the behavior of the scale factor and the Hubble parameter, it is possible to identify two limiting conditions on  $\tilde{\zeta}_0$ ,  $\tilde{\zeta}_1$  and  $\tilde{\zeta}_2$  which corresponds to a universe that would start with a Big-Bang followed by an early decelerated epoch, then making a transition into the accelerated epoch in the later times. These two conditions are,

$$\tilde{\zeta}_0 > 0, \tilde{\zeta}_{12} < 3, \tilde{\zeta}_2 < 2 \quad (2.16)$$

$$\tilde{\zeta}_0 < 0, \tilde{\zeta}_{12} > 3, \tilde{\zeta}_2 > 2. \quad (2.17)$$

The first condition is to be simultaneously satisfied with  $\tilde{\zeta}_0 + \tilde{\zeta}_{12} < 3$  and the second condition with  $\tilde{\zeta}_0 + \tilde{\zeta}_{12} > 3$ . Instead of these, if the first condition, equation (2.16) is satisfied simultaneously with  $\tilde{\zeta}_0 + \tilde{\zeta}_{12} > 3$  or the second condition, equation (2.17) with  $\tilde{\zeta}_0 + \tilde{\zeta}_{12} < 3$ , then the universe will undergo an eternally accelerated expansion, see the curve for  $\tilde{\zeta}_0 + \tilde{\zeta}_{12} = 3$  in figures 2.3 and 2.4. We have obtained the best estimates of the bulk viscous parameters  $(\tilde{\zeta}_0, \tilde{\zeta}_1, \tilde{\zeta}_2)$  corresponding to the cases, equations (2.16)

and (2.17) separately, using the SCP “Union” SNe Ia data set, about which we will discuss in section 2.3.

For both the cases of bulk viscous parameters, as given by equations (2.16) and (2.17), the Hubble parameter given in equation (2.11) becomes infinity as the scale factor  $a \rightarrow 0$ , which implies that the density becomes infinity at the origin, indicating the presence of a Big-Bang at the origin. The behavior of the scale factor as given in equation (2.14) are shown in figures 2.1 and 2.2 for the two conditions of parameters respectively. As  $(t - t_0) \rightarrow 0$ , the scale factor in both the cases reduces to

$$a(t) \rightarrow \left[ 1 + \frac{3 - \tilde{\zeta}_{12}}{2 - \tilde{\zeta}_2} H_0(t - t_0) \right]^{\frac{2 - \tilde{\zeta}_2}{3 - \tilde{\zeta}_{12}}}, \quad (2.18)$$

which corresponds to an early decelerated expansion. In both the cases of limiting conditions, as  $(t - t_0) \rightarrow \infty$ , the scale factor tends to,

$$a(t) \rightarrow e^{\frac{\tilde{\zeta}_0}{2 - \tilde{\zeta}_2} H_0(t - t_0)}. \quad (2.19)$$

This corresponds to acceleration similar to the de Sitter phase which implies that the bulk viscous dark matter behaves similar to the cosmological constant as  $(t - t_0) \rightarrow \infty$ , at least at the background level. An important point to be noted is that the evolution of the scale factor is the same for the best estimates of the bulk viscous coefficient from the two limiting conditions, see figures 2.1 and 2.2.

The scale factor and red shift corresponding to the transition from decelerated to accelerated expansion can be obtained as shown below. From the Hubble parameter (equation (2.11)) the derivative of  $\dot{a}$  with respect to  $a$  can be obtained as,

$$\frac{d\dot{a}}{da} = H_0 \left[ \left( \frac{\tilde{\zeta}_1 - 1}{2 - \tilde{\zeta}_2} \right) \left( \frac{\tilde{\zeta}_0 + \tilde{\zeta}_{12} - 3}{\tilde{\zeta}_{12} - 3} \right) a^{\frac{\tilde{\zeta}_{12} - 3}{2 - \tilde{\zeta}_2}} - \frac{\tilde{\zeta}_0}{\tilde{\zeta}_{12} - 3} \right]. \quad (2.20)$$

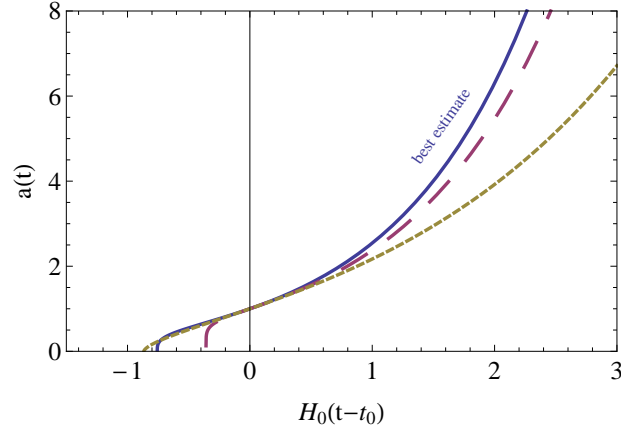


Figure 2.1: Behavior of the scale factor for the first set of limiting conditions of parameters  $\rightarrow \tilde{\zeta}_0 > 0$ ,  $\tilde{\zeta}_0 + \tilde{\zeta}_{12} < 3$ ,  $\tilde{\zeta}_{12} < 3$ ,  $\tilde{\zeta}_2 < 2$ . Solid line corresponds to the best fit parameters  $(\tilde{\zeta}_0, \tilde{\zeta}_1, \tilde{\zeta}_2) = (7.83, -5.13, -0.51)$ . Dashed line corresponds to parameter values  $(5, -4, 1)$  and the dotted line corresponds to values  $(4, -2, -3)$ . The parameter values are selected so that the transition to the accelerated epoch happens in the past.

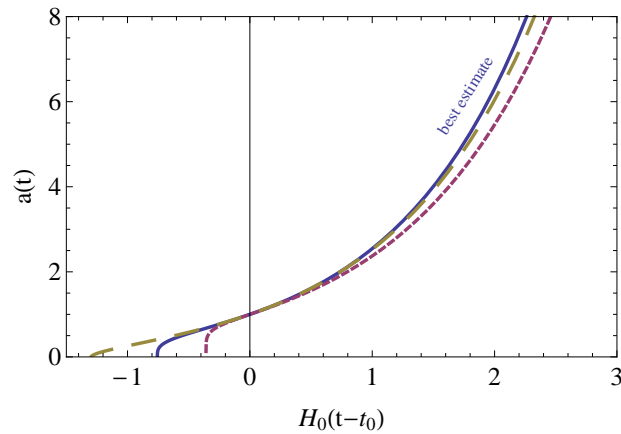


Figure 2.2: Behavior of the scale factor for the second set of limiting conditions of parameters  $\rightarrow \tilde{\zeta}_0 < 0$ ,  $\tilde{\zeta}_0 + \tilde{\zeta}_{12} > 3$ ,  $\tilde{\zeta}_{12} > 3$ ,  $\tilde{\zeta}_2 > 2$ . Solid line corresponds to the best fit parameters  $(\tilde{\zeta}_0, \tilde{\zeta}_1, \tilde{\zeta}_2) = (-4.68, 4.67, 3.49)$ . Dashed line corresponds to parameter values  $(-6, 4, 6)$  and the dotted line corresponds to values  $(-5, 6, 3)$ . The parameter values are selected so that the transition to the accelerated epoch happens in the past.

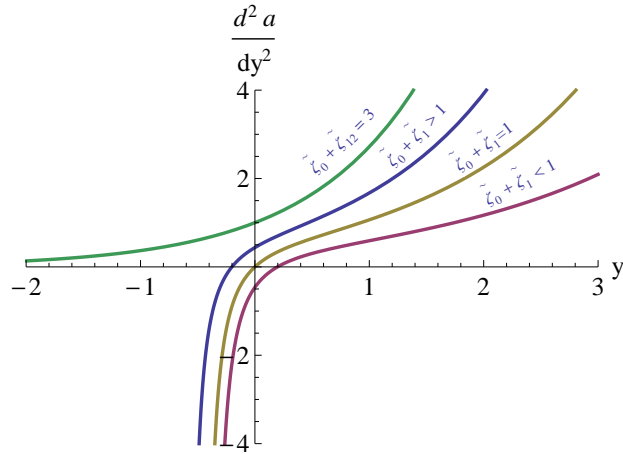


Figure 2.3: Evolution of the second derivative of the scale factor with respect to  $y = H_0(t - t_0)$  for the first limiting conditions of parameters,  $\tilde{\zeta}_0 > 0$ ,  $\tilde{\zeta}_0 + \tilde{\zeta}_{12} < 3$ ,  $\tilde{\zeta}_{12} < 3$ ,  $\tilde{\zeta}_2 < 2$ . The curve corresponding to  $\tilde{\zeta}_0 + \tilde{\zeta}_{12} \geq 3$  represents a universe which is eternally accelerating. If  $\tilde{\zeta}_0 + \tilde{\zeta}_1 > 1$ , the transition to the accelerating epoch happens in the past. If  $\tilde{\zeta}_0 + \tilde{\zeta}_1 < 1$  the transition will be in the future. If  $\tilde{\zeta}_0 + \tilde{\zeta}_1 = 1$ , the transition occurs at present.

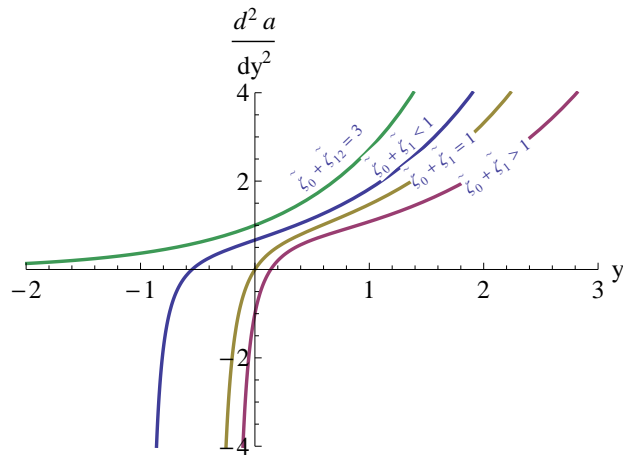


Figure 2.4: Evolution of the second derivative of the scale factor with respect to  $y = H_0(t - t_0)$  for the second limiting conditions of parameters,  $\tilde{\zeta}_0 < 0$ ,  $\tilde{\zeta}_0 + \tilde{\zeta}_{12} > 3$ ,  $\tilde{\zeta}_{12} > 3$ ,  $\tilde{\zeta}_2 > 2$ . The curve corresponding to  $\tilde{\zeta}_0 + \tilde{\zeta}_{12} \leq 3$  represents a universe which is eternally accelerating. If  $\tilde{\zeta}_0 + \tilde{\zeta}_1 < 1$ , the transition to the accelerating epoch happens in the past. If  $\tilde{\zeta}_0 + \tilde{\zeta}_1 > 1$  the transition will be in the future. If  $\tilde{\zeta}_0 + \tilde{\zeta}_1 = 1$ , the transition occurs at present.

Equating this to zero, we obtain the transition scale factor  $a_T$ ,

$$a_T = \left[ \frac{\tilde{\zeta}_0 (2 - \tilde{\zeta}_2)}{(\tilde{\zeta}_1 - 1) (\tilde{\zeta}_0 + \tilde{\zeta}_{12} - 3)} \right]^{\frac{2 - \tilde{\zeta}_2}{\tilde{\zeta}_{12} - 3}} \quad (2.21)$$

and the corresponding transition red shift  $z_T$  is,

$$z_T = \left[ \frac{\tilde{\zeta}_0 (2 - \tilde{\zeta}_2)}{(\tilde{\zeta}_1 - 1) (\tilde{\zeta}_0 + \tilde{\zeta}_{12} - 3)} \right]^{-\frac{2 - \tilde{\zeta}_2}{\tilde{\zeta}_{12} - 3}} - 1. \quad (2.22)$$

From equations (2.21) and (2.22), it is clear that if  $\tilde{\zeta}_0 + \tilde{\zeta}_1 = 1$ , the transition from decelerated phase to accelerated phase occurs at  $a_T = 1$  and  $z_T = 0$ , which corresponds to the present time of the universe. For the first case of limiting conditions of parameters with  $\tilde{\zeta}_0 > 0$ , the transition would take place in the past if  $\tilde{\zeta}_0 + \tilde{\zeta}_1 > 1$  and in the future if  $\tilde{\zeta}_0 + \tilde{\zeta}_1 < 1$ . For the second case of limiting conditions of parameters, that corresponds to  $\tilde{\zeta}_0 < 0$ , the above conditions are reversed such that transition would take place in the future if  $\tilde{\zeta}_0 + \tilde{\zeta}_1 > 1$  and in the past if  $\tilde{\zeta}_0 + \tilde{\zeta}_1 < 1$ . These are shown in figures 2.3 and 2.4 respectively, where we have plotted  $\frac{d^2 a}{dy^2}$  (equation 2.15) with  $y$ .

### 2.3 Parameter estimation using Type Ia Supernovae data

In this section we have obtained the best fit of the parameters,  $\tilde{\zeta}_0$ ,  $\tilde{\zeta}_1$ ,  $\tilde{\zeta}_2$  and  $H_0$  using the type Ia Supernovae observations. The goodness-of-fit of the model is obtained by the  $\chi^2$ -minimization. We did the statistical analysis using the Supernova Cosmology Project (SCP) ‘‘Union’’ SNe Ia data set [91], composed of 307 type Ia Supernovae from 13 independent data sets.

In a flat universe, the luminosity distance  $d_L$  is defined as

$$d_L(z, \tilde{\zeta}_0, \tilde{\zeta}_1, \tilde{\zeta}_2, H_0) = c(1+z) \int_0^z \frac{dz'}{H(z', \tilde{\zeta}_0, \tilde{\zeta}_1, \tilde{\zeta}_2, H_0)}, \quad (2.23)$$

where  $H(z, \tilde{\zeta}_0, \tilde{\zeta}_1, \tilde{\zeta}_2, H_0)$  is the Hubble parameter and  $c$  is the speed of light. The theoretical distance moduli  $\mu_t$  for the  $k$ -th Supernova with redshift  $z_k$  is given as,

$$\begin{aligned} \mu_t(z_k, \tilde{\zeta}_0, \tilde{\zeta}_1, \tilde{\zeta}_2, H_0) &= m - M \\ &= 5 \log_{10} \left[ \frac{d_L(z_k, \tilde{\zeta}_0, \tilde{\zeta}_1, \tilde{\zeta}_2, H_0)}{Mpc} \right] + 25, \end{aligned} \quad (2.24)$$

where,  $m$  and  $M$  are the apparent and absolute magnitudes of the SNe respectively. Then we can construct  $\chi^2$  function as,

$$\chi^2(\tilde{\zeta}_0, \tilde{\zeta}_1, \tilde{\zeta}_2, H_0) \equiv \sum_{k=1}^n \frac{[\mu_t(z_k, \tilde{\zeta}_0, \tilde{\zeta}_1, \tilde{\zeta}_2, H_0) - \mu_k]^2}{\sigma_k^2} \quad (2.25)$$

where  $\mu_k$  is the observational distance moduli for the  $k$ -th Supernova,  $\sigma_k^2$  is the variance of the measurement and  $n$  is the total number of data, here  $n = 307$ . The  $\chi^2$  function thus obtained is then minimized to obtain the best estimate of the parameters,  $\tilde{\zeta}_0$ ,  $\tilde{\zeta}_1$ ,  $\tilde{\zeta}_2$  and  $H_0$ . From the behavior of scale factor and other cosmological parameters, we found that there exists two possible sets of conditions which describes a universe having a Big-Bang at the origin, then entering an early stage of decelerated expansion followed by acceleration. These two sets of conditions are mentioned in section 2.2. We have used these two conditions separately in minimizing the  $\chi^2$  function. This leads to two sets of values for the best estimates of the parameters  $\tilde{\zeta}_0$ ,  $\tilde{\zeta}_1$ ,  $\tilde{\zeta}_2$  but  $H_0$  is same in both the cases. In addition to  $H_0$ , the other cosmological parameters, scale factor, deceleration parameter, equation of state parameter, matter density and curvature scalar are all showing identical behavior for both the sets of best fit of parameters.

Model $\rightarrow$	Bulk viscous model with $\tilde{\zeta}_0 > 0, \tilde{\zeta}_0 + \tilde{\zeta}_{12} < 3, \tilde{\zeta}_{12} < 3, \tilde{\zeta}_2 < 2$	Bulk viscous model with $\tilde{\zeta}_0 < 0, \tilde{\zeta}_0 + \tilde{\zeta}_{12} > 3, \tilde{\zeta}_{12} > 3, \tilde{\zeta}_2 > 2$	$\Lambda$ CDM
$\tilde{\zeta}_0$	7.83	-4.68	-
$\tilde{\zeta}_1$	$-5.13^{+0.056}_{-0.060}$	$4.67^{+0.04}_{-0.03}$	-
$\tilde{\zeta}_2$	$-0.51^{+0.13}_{-0.14}$	$3.49^{+0.089}_{-0.071}$	-
$\Omega_{m0}$	1	1	0.316
$H_0$	70.49	70.49	70.03
$\chi^2_{min}$	310.54	310.54	311.93
$\chi^2_{d.o.f}$	1.02	1.02	1.02

Table 2.1: Best estimates of the bulk viscous parameters and  $H_0$  and also  $\chi^2$  minimum value for the two cases of the limiting conditions of the viscous parameters.  $\chi^2_{d.o.f} = \frac{\chi^2_{min}}{n-m}$ , where  $n = 307$ , the number of data and  $m = 3$ , the number of parameters in the model. For the best estimation we have used SCP ‘‘Union’’ 307 SNe Ia data sets. We have also shown the best estimates of the corresponding parameters for the  $\Lambda$ CDM model for comparison, where  $\Omega_{m0}$  is the present mass density parameter. The subscript d.o.f stands for degrees of freedom.

The values of the parameters are given in Table 2.1. In order to compare the results of the present model, we have also estimated the values for  $\Lambda$ CDM model using the same data set and the results are also shown in Table 2.1. We find that the values of  $H_0$  and Goodness-of-fit  $\chi^2_{d.o.f}$  for  $\Lambda$ CDM model are very close to those obtained from the present bulk viscous model. The value of the present Hubble parameter,  $H_0$  for both the cases of parameters are found to be  $70.49 \text{ kms}^{-1}\text{Mpc}^{-1}$ , which is in close agreement with the corresponding WMAP value ( $H_0 = 70.5 \pm 1.3 \text{ kms}^{-1}\text{Mpc}^{-1}$ ) [93].

We have constructed the confidence interval plane for the bulk viscous parameters ( $\tilde{\zeta}_1, \tilde{\zeta}_2$ ) by keeping  $\tilde{\zeta}_0$  as a constant equal to its best estimated value obtained by minimizing the  $\chi^2$  function. From figure 2.5, corresponding to the first set of limiting conditions and figure 2.6, correspond-

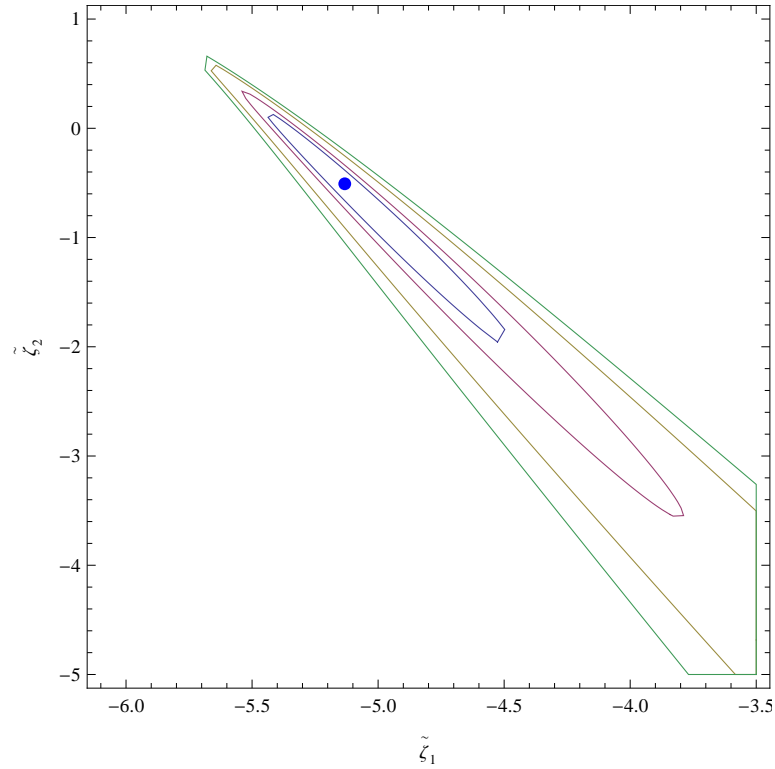


Figure 2.5: Confidence intervals for the parameters  $(\tilde{\zeta}_1, \tilde{\zeta}_2)$  for the first set of limiting conditions, for the bulk viscous matter dominated universe using the SCP “Union” data set composed of 307 data points. The best estimated values of the parameters are  $\tilde{\zeta}_1 = -5.13_{-0.06}^{+0.056}$  and  $\tilde{\zeta}_2 = -0.51_{-0.14}^{+0.13}$  and are indicated by the point. The confidence intervals shown corresponds to 68.3%, 95.4%, 99.73% and 99.99% of probabilities.

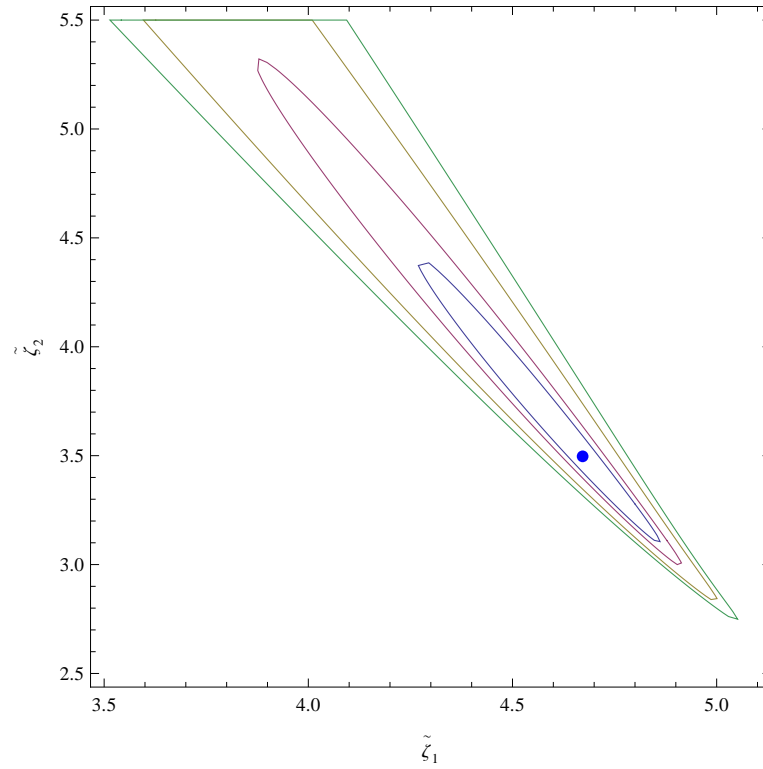


Figure 2.6: Confidence intervals for the parameters  $(\tilde{\zeta}_1, \tilde{\zeta}_2)$  for the second set of limiting conditions, for the bulk viscous matter dominated universe using the SCP “Union” data set composed of 307 data points. The best estimated values of the parameters are  $4.67_{-0.03}^{+0.04}$  and  $3.49_{-0.071}^{+0.089}$  and are indicated by the point. The confidence intervals shown corresponds to 68.3%, 95.4%, 99.73% and 99.99% of probabilities.

ing to the second set of limiting conditions, it is seen that the fitting of the confidence intervals corresponding to 99.73% and 99.99% probabilities are poor. But the confidence intervals corresponding to 68.3% and 95.4% probabilities are showing a fairly good behavior.

For the first case of parameters with  $\tilde{\zeta}_0 > 0$ , it is found that  $\tilde{\zeta}_1 = -5.13_{-0.06}^{+0.056}$  and  $\tilde{\zeta}_2 = -0.51_{-0.14}^{+0.13}$ , for  $\tilde{\zeta}_0 = 7.83$  with 68.3% probability. In the second case with  $\tilde{\zeta}_0 < 0$ , the values of  $\tilde{\zeta}_1$  and  $\tilde{\zeta}_2$  are obtained as  $4.67_{-0.03}^{+0.04}$  and  $3.49_{-0.071}^{+0.089}$ , respectively, for  $\tilde{\zeta}_0 = -4.68$  with 68.3% probability.

## 2.4 Age of the bulk viscous universe

Age of the universe can be deduced from the scale factor equation (2.14) by equating it to zero. The time elapsed since the Big-Bang is,

$$t_B = t_0 + \left( \frac{2 - \tilde{\zeta}_2}{H_0 \tilde{\zeta}_0} \right) \ln \left( 1 - \frac{\tilde{\zeta}_0}{3 - \tilde{\zeta}_{12}} \right). \quad (2.26)$$

Hence, the age of the universe since Big-Bang is

$$Age \equiv t_0 - t_B = - \left( \frac{2 - \tilde{\zeta}_2}{H_0 \tilde{\zeta}_0} \right) \ln \left( 1 - \frac{\tilde{\zeta}_0}{3 - \tilde{\zeta}_{12}} \right). \quad (2.27)$$

A plot of the age of the universe with  $H_0$  for the best estimates of the bulk viscous parameters is shown in figure 2.7 (the evolution is the same for the best estimates from the two limiting conditions). The age of the universe corresponding to the best estimates of the present Hubble parameter is found to be 10.90 Gyr and is marked in the plot. This value is less compared to the age deduced from CMB anisotropy data [92] and also that from the oldest globular clusters [14], which is around  $12.9 \pm 2.9$  Gyr. For comparison, we have also extracted the value of the Hubble parameter for the  $\Lambda$ CDM model using the same data set (see Table 2.1) from which

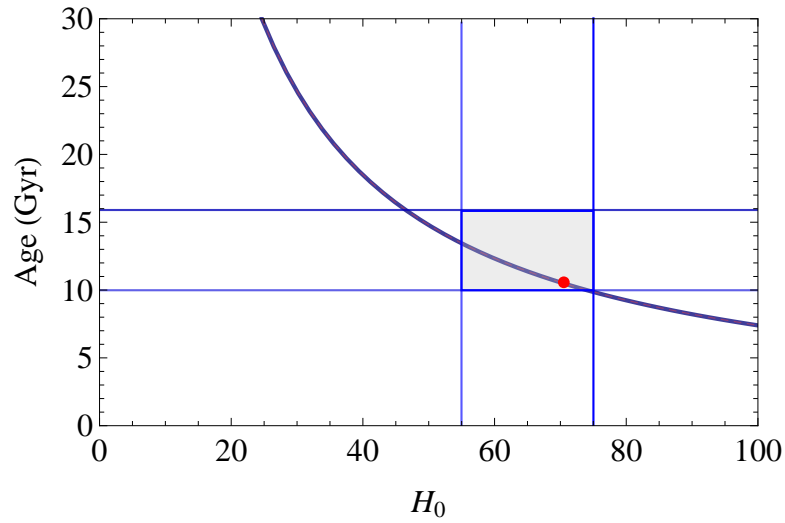


Figure 2.7: Plot of the age of the universe in Gyr with  $H_0$  in units of  $\text{kms}^{-1}\text{Mpc}^{-1}$  for the best fit values of the bulk viscous parameters. The plots are identical for the best estimated values of the parameters from both the limiting conditions. The point located in the figure corresponds to an age 10.5 Gyr for the best estimate value of  $H_0$ , obtained as  $70.49 \text{ kms}^{-1}\text{Mpc}^{-1}$ . The shaded region corresponds to the interval  $H_0(55, 75) \text{ kms}^{-1}\text{Mpc}^{-1}$  and age (10, 15.8) Gyr, which are the permitted intervals for  $H_0$  and age, derived using observations on Galactic globular clusters from the Hipparcos parallaxes [14].

the age of the universe is found to be around 13.85 Gyr. So compared to the age of the universe from globular clusters and the standard  $\Lambda$ CDM model, the present model, where the bulk viscous matter replaces the dark energy, predicts a relatively low age.

## 2.5 Evolution of cosmological parameters

### 2.5.1 Deceleration parameter

The results regarding the transition of the universe into the accelerated epoch discussed in the previous section can be further verified by studying the evolution of the deceleration parameter  $q$ , which is defined as,

$$q(a) = -\frac{\ddot{a}a}{\dot{a}^2} = -\frac{\ddot{a}}{a} \frac{1}{H^2} = -1 - \frac{\dot{H}}{H^2}. \quad (2.28)$$

For the bulk viscous matter dominated universe, using the Friedmann equations, one can obtain,

$$\frac{\ddot{a}}{a} = -\frac{1}{6} \left[ \rho_m - 9H \left( \zeta_0 + \zeta_1 H + \zeta_2 \left( \frac{\dot{H}}{H} + H \right) \right) \right]. \quad (2.29)$$

Using the dimensionless bulk viscous parameters as defined in equation (2.10) and using equations (2.3) and (2.29), the deceleration parameter becomes,

$$q = \frac{1}{2} \left[ 1 - \left( \frac{H_0}{H} \tilde{\zeta}_0 + \tilde{\zeta}_1 + \frac{\tilde{\zeta}_2}{H} \left( \frac{\dot{H}}{H} + H \right) \right) \right]. \quad (2.30)$$

Substituting equations (2.9) and (2.11), we can obtain the deceleration parameter in terms of  $a$ ,  $\tilde{\zeta}_0$ ,  $\tilde{\zeta}_1$  and  $\tilde{\zeta}_2$  as,

$$q(a) = \frac{1}{2 - \tilde{\zeta}_2} \left[ 1 - \tilde{\zeta}_1 - \frac{\tilde{\zeta}_0}{a^{\frac{\tilde{\zeta}_{12}-3}{2-\tilde{\zeta}_2}} \left( 1 + \frac{\tilde{\zeta}_0}{\tilde{\zeta}_{12}-3} \right) - \frac{\tilde{\zeta}_0}{\tilde{\zeta}_{12}-3}} \right]. \quad (2.31)$$

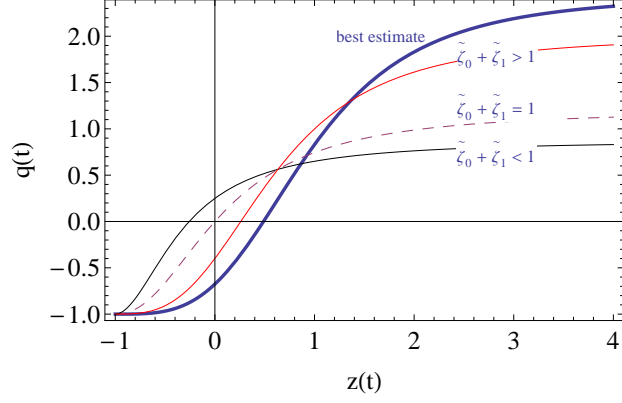


Figure 2.8: Evolution of the deceleration parameter with red shift for the first limiting conditions of viscous parameters,  $\tilde{\zeta}_0 > 0$ ,  $\tilde{\zeta}_0 + \tilde{\zeta}_{12} < 3$ ,  $\tilde{\zeta}_{12} < 3$ ,  $\tilde{\zeta}_2 < 2$ .  $q$  enters the negative region in the recent past if  $\tilde{\zeta}_0 + \tilde{\zeta}_1 > 1$ , at present if  $\tilde{\zeta}_0 + \tilde{\zeta}_1 = 1$  and in the future if  $\tilde{\zeta}_0 + \tilde{\zeta}_1 < 1$ . Evolution of  $q$  for the best estimated values of the bulk viscous parameters is also shown. The redshift at which the  $q$  enters the negative region for the best estimated values of the bulk viscous parameters corresponds to  $z_T = 0.49^{+0.075}_{-0.057}$ .

In terms of red shift, the above equation becomes,

$$q(z) = \frac{1}{2 - \tilde{\zeta}_2} \left[ 1 - \tilde{\zeta}_1 - \frac{\tilde{\zeta}_0}{(1+z)^{-\frac{\tilde{\zeta}_{12}-3}{2-\tilde{\zeta}_2}} \left( 1 + \frac{\tilde{\zeta}_0}{\tilde{\zeta}_{12}-3} \right) - \frac{\tilde{\zeta}_0}{\tilde{\zeta}_{12}-3}} \right]. \quad (2.32)$$

The variation of  $q$  with  $z$  for the two sets of limiting conditions of the viscous parameters are shown in figures 2.8 and 2.9. The evolution corresponding to the best estimates from both limiting conditions are identical as it is clear from the figures. When all the bulk viscous parameters are zero, the deceleration parameter  $q = 1/2$ , which corresponds to a decelerating epoch of the universe.

The present value of the deceleration parameter corresponds to  $z = 0$  or  $a = a_0 = 1$  is,

$$q_0 = q(a = 1) = \frac{1 - (\tilde{\zeta}_0 + \tilde{\zeta}_1)}{2 - \tilde{\zeta}_2}. \quad (2.33)$$

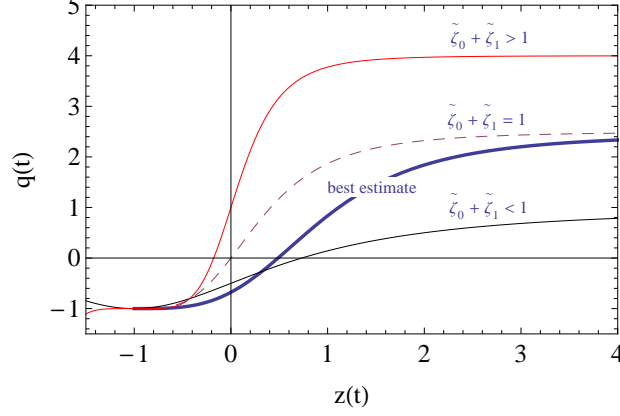


Figure 2.9: Evolution of the deceleration parameter with red shift for the second limiting conditions of viscous parameters,  $\tilde{\zeta}_0 < 0$ ,  $\tilde{\zeta}_0 + \tilde{\zeta}_{12} > 3$ ,  $\tilde{\zeta}_{12} > 3$ ,  $\tilde{\zeta}_2 > 2$ .  $q$  enters the negative region in the recent past if  $\tilde{\zeta}_0 + \tilde{\zeta}_1 < 1$ , at present if  $\tilde{\zeta}_0 + \tilde{\zeta}_1 = 1$  and in the future if  $\tilde{\zeta}_0 + \tilde{\zeta}_1 > 1$ . Evolution of  $q$  for the best estimated values of the bulk viscous parameters is also shown. The redshift at which the  $q$  enters the negative region for the best estimated values of the bulk viscous parameters corresponds to  $z_T = 0.49_{-0.066}^{+0.064}$ .

This equation shows that for  $\tilde{\zeta}_0 + \tilde{\zeta}_1 = 1$ , the deceleration parameter  $q = 0$ . This implies that the transition into the accelerating phase would occur at the present time and is true for both the cases of the parameters.

For the first case of limiting conditions of the parameters (2.16) with  $\tilde{\zeta}_0 > 0$  and  $\tilde{\zeta}_2 < 2$ , the current deceleration parameter  $q_0 < 0$  if  $\tilde{\zeta}_0 + \tilde{\zeta}_1 > 1$ , implying that the present universe is in the accelerating epoch and it entered this epoch at an early stage. But  $q_0 > 0$  if  $\tilde{\zeta}_0 + \tilde{\zeta}_1 < 1$ , implying that the present universe is decelerating and it will be entering the accelerating phase at a future time, see figure 2.8 which shows the behavior of  $q$  with  $z$ . For the best estimate of the bulk viscous parameters, the behavior of  $q$  (figure 2.8) shows that the universe transit from decelerated to accelerated epoch at a recent past. The best estimate of the bulk viscous parameters corresponding to the first limiting case, equation 2.16 were extracted using the Supernova data and are ( $\tilde{\zeta}_0 = 7.83$ ,  $\tilde{\zeta}_1 = -5.13$ ,  $\tilde{\zeta}_2 = -0.51$ ) (see Table

2.1), which indicate that  $\tilde{\zeta}_0 + \tilde{\zeta}_1 > 1$ . So the model predicts a universe which is accelerating at present and has entered this phase of accelerating expansion at a recent past.

For the second case of limiting conditions of the viscous parameters (2.17) with  $\tilde{\zeta}_0 < 0$  and  $\tilde{\zeta}_2 > 2$ , the current deceleration parameter  $q_0 > 0$  if  $\tilde{\zeta}_0 + \tilde{\zeta}_1 > 1$ , implies that the present universe is in the decelerating epoch and it will be entering the accelerating phase at a future time, see figure 2.9 which shows the behavior of  $q$  with  $z$ . But  $q_0 < 0$  if  $\tilde{\zeta}_0 + \tilde{\zeta}_1 < 1$ , implying that the present universe is accelerating and it entered this phase at an early time. From the behavior of  $q$  (figure 2.9) for the best estimate of the bulk viscous parameters corresponding to the second limiting condition, equation 2.17, it is clear that the transition of the universe from the decelerated to accelerated epoch was in the recent past. The best estimate of the bulk viscous parameters in this case are ( $\tilde{\zeta}_0 = -4.68$ ,  $\tilde{\zeta}_1 = 4.67$ ,  $\tilde{\zeta}_2 = 3.49$ ) (see Table 2.1), which indicate that  $\tilde{\zeta}_0 + \tilde{\zeta}_1 < 1$ . So, for this case also, the model predicts a universe which is accelerating at present and has entered this phase of accelerating expansion at a recent past.

These results confirm the earlier conclusion with respect to the behavior of  $d^2a/dy^2$ . For the best estimated values of the bulk viscous parameters, the present value of the deceleration parameter is found to be about  $-0.68 \pm 0.06$  and  $-0.68_{-0.050}^{+0.066}$  corresponding to the first and second limiting conditions respectively (see equation (2.33)). This is comparable with the observational results on the present value of  $q$ , which is around  $-0.64 \pm 0.03$  [92, 93]. The transition red shift, at which  $q$  enters the negative value region, corresponding to an accelerating epoch, is found to be  $z_T = 0.49_{-0.057}^{+0.075}$  for the first case of limiting conditions of the bulk viscous parameters and  $z_T = 0.49_{-0.066}^{+0.064}$  for the second case of limiting conditions of the bulk viscous parameters (see equation (2.22) and figures 2.8 and

2.9). An analysis of the  $\Lambda$ CDM model with combined SNe+CMB data gives the transition red shift range as  $z_T = 0.45 - 0.73$  [94]. So the transition red shift predicted by the present model is agreeing with the lower limit of the corresponding  $\Lambda$ CDM range.

### 2.5.2 Equation of state

An accelerated expansion of the universe is possible only if the effective equation of state parameter,  $\omega < -1/3$ , or equivalently,  $3\omega + 1 < 0$ . The equation of state can be obtained using [95],

$$\omega = -1 - \frac{1}{3} \frac{d \ln h^2}{dx} = -1 - \frac{2}{3} \frac{\dot{H}}{H^2}, \quad (2.34)$$

where  $x = \ln a$  and  $h = \frac{H}{H_0}$ . Using equation (2.11) we get the equation of state as,

$$\omega = -1 - \frac{2}{3(2 - \tilde{\zeta}_2)} \left[ \tilde{\zeta}_1 + \tilde{\zeta}_2 - 3 + \frac{\tilde{\zeta}_0}{h} \right]. \quad (2.35)$$

The present value of the equation of state parameter  $\omega_0$ , can be obtained by taking  $h = 1$ . The condition for acceleration of the present universe can then be represented as,

$$3\omega_0 + 1 = -2 \left( \frac{\tilde{\zeta}_0 + \tilde{\zeta}_1 - 1}{2 - \tilde{\zeta}_2} \right) < 0. \quad (2.36)$$

For the first case of parameters with  $\tilde{\zeta}_0 > 0$ ,  $\tilde{\zeta}_2 < 2$ , this condition is satisfied if  $\tilde{\zeta}_0 + \tilde{\zeta}_1 > 1$  and for the second case with  $\tilde{\zeta}_0 < 0$ ,  $\tilde{\zeta}_2 > 2$ , this will be satisfied if  $\tilde{\zeta}_0 + \tilde{\zeta}_1 < 1$ . These conditions are compatible with that arrived in the analysis of deceleration parameter in section 2.5.1.

The evolution of the equation of state parameter with red shift for both the sets of the best fit values of the bulk viscous parameters are found to be identical and is shown in figure 2.10. It is clear from the figure that as  $z \rightarrow -1$  ( $a \rightarrow \infty$ ),  $\omega \rightarrow -1$  in the future which corresponds to the de Sitter

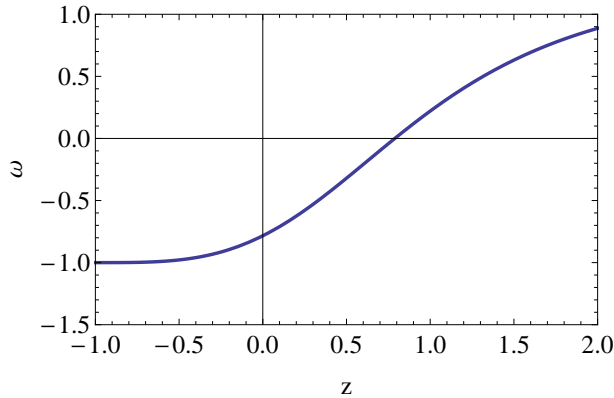


Figure 2.10: Evolution of the equation of state parameter with red shift for the best estimates of the bulk viscous parameters. It is found that the evolution of  $\omega$  are identical for the best estimates from both the limiting conditions.

universe and also coincides with that of the future behavior of the  $\Lambda$ CDM model [96], and also resembles the behavior of some scalar field models [13]. Since it is not crossing the phantom divide  $\omega \leq -1$ , the model is free from big rip singularity or little rip [97]. The present value of the equation of state parameter is around  $\omega_0 \sim -0.78^{+0.03}_{-0.045}$  and  $\omega_0 \sim -0.78^{+0.037}_{-0.043}$  for the best estimate of viscosity parameters corresponding to the first and second limiting conditions, respectively. This value is comparatively higher than that predicted by the joint analysis of WMAP+BAO+ $H_0$ +SNe data, which is around  $-0.93$  [11, 98].

### 2.5.3 Matter density

From the Friedmann equation (2.3) and the Hubble parameter, equation (2.11) we obtain the mass density parameter  $\Omega_m$  as,

$$\Omega_m(a) = \left[ a^{\frac{\tilde{\zeta}_{12}-3}{2-\tilde{\zeta}_2}} \left( 1 + \frac{\tilde{\zeta}_0}{\tilde{\zeta}_{12}-3} \right) - \frac{\tilde{\zeta}_0}{\tilde{\zeta}_{12}-3} \right]^2, \quad (2.37)$$

where,  $\Omega_m = \frac{\rho_m}{\rho_{crit}}$  and  $\rho_{crit} = 3H_0^2$  is the critical density. If  $\tilde{\zeta}_0 = \tilde{\zeta}_1 = \tilde{\zeta}_2 =$

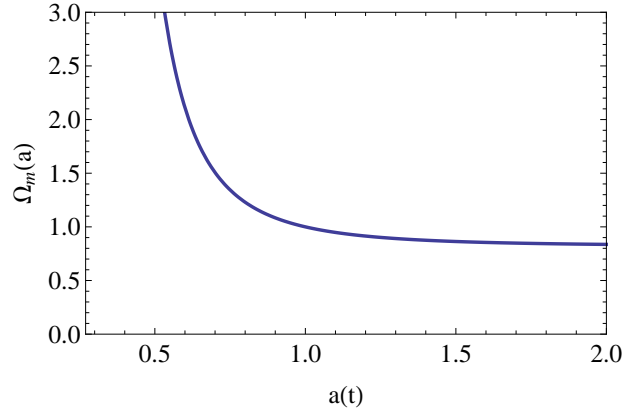


Figure 2.11: Evolution of the mass density parameter with scale factor for the best estimated values of the bulk viscous parameters. It is found that the variation of the mass density coincides for the best estimated values from the two limiting conditions.

0, the mass density parameter reduces to  $\Omega_m \sim a^{-3}$ , which corresponds to the matter dominated universe with null bulk viscosity. The evolution of the mass density parameter for the best estimated values corresponding to the two limiting conditions are shown in figure 2.11 and it is clear that their evolutions are coinciding with each other. As  $a \rightarrow 0$ , the matter density diverges. Figure 2.11 also indicating the same, which is a clear indication of the existence of the Big-Bang at the origin of the universe.

#### 2.5.4 The curvature scalar

The curvature scalar is the parameter used to confirm the presence of singularities in the model. For a flat universe, the curvature scalar is defined as,

$$R = 6 \left[ \frac{\ddot{a}}{a} + H^2 \right]. \quad (2.38)$$

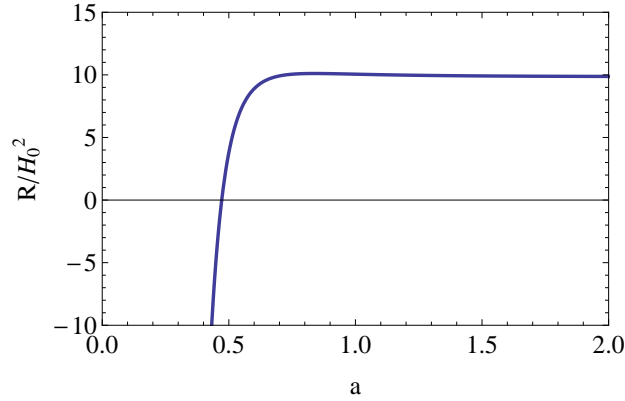


Figure 2.12: Evolution of the curvature scalar with scale factor for the best estimate parameters. It is found that the evolution of the curvature scalar are identical for the best estimated values from the two limiting conditions.

Using equations (2.9), (6.7), (2.11) and (2.29), we obtain the curvature scalar as,

$$R(a) = \frac{6H_0^2}{(2 - \tilde{\zeta}_2)(\tilde{\zeta}_{12} - 3)^2} [2\tilde{\zeta}_0^2(2 - \tilde{\zeta}_2) + (\tilde{\zeta}_0 + \tilde{\zeta}_{12} - 3) a^{\frac{\tilde{\zeta}_{12}-3}{2-\tilde{\zeta}_2}} [(\tilde{\zeta}_1 - \tilde{\zeta}_2 + 1)(\tilde{\zeta}_0 + \tilde{\zeta}_{12} - 3)a^{\frac{\tilde{\zeta}_{12}-3}{2-\tilde{\zeta}_2}} - \tilde{\zeta}_0(\tilde{\zeta}_1 - 3\tilde{\zeta}_2 + 5)]]]. \quad (2.39)$$

From the above equation it is clear that as  $a \rightarrow 0$ ,  $R \rightarrow \infty$ . The evolution of the curvature scalar for both the cases of best fit of the parameters coincides with each other as shown in figure 2.12. The behavior of  $R$  shows that the curvature scalar diverges as  $a \rightarrow 0$ . This indicates the existence of Big-Bang at the origin of the universe.

## 2.6 Statefinder analysis

In this section, we present our analysis on comparing the present model with other standard models of dark energy. We have used the statefinder parameter diagnostic introduced by Sahni et al [99]. The statefinder is

a geometrical diagnostic tool which allows us to characterize the properties of dark energy in a model-independent manner. The statefinder parameters  $\{r, s\}$  are defined as,

$$r = \frac{\ddot{a}}{aH^3}, \quad s = \frac{r-1}{3\left(q - \frac{1}{2}\right)}. \quad (2.40)$$

In terms of  $h = \frac{H}{H_0}$ ,  $r$  and  $s$  can be written as

$$r = \frac{1}{2h^2} \frac{d^2h^2}{dx^2} + \frac{3}{2h^2} \frac{dh^2}{dx} + 1 \quad (2.41)$$

$$s = -\frac{\frac{1}{2h^2} \frac{d^2h^2}{dx^2} + \frac{3}{2h^2} \frac{dh^2}{dx}}{\frac{3}{2h^2} \frac{dh^2}{dx} + \frac{9}{2}}. \quad (2.42)$$

Using the expression for  $h$  from equation (2.11), these parameters become,

$$r = \frac{(\tilde{\zeta}_0 + \tilde{\zeta}_{12} - 3)(\tilde{\zeta}_{12} - 3)}{h^2(2 - \tilde{\zeta}_2)^2} a^{\frac{\tilde{\zeta}_{12}-3}{2-\tilde{\zeta}_2}} \left[2h + \frac{\tilde{\zeta}_0}{\tilde{\zeta}_{12} - 3}\right] + \frac{3(\tilde{\zeta}_0 + \tilde{\zeta}_{12} - 3)}{h(2 - \tilde{\zeta}_2)} a^{\frac{\tilde{\zeta}_{12}-3}{2-\tilde{\zeta}_2}} + 1, \quad (2.43)$$

$$s = \frac{\frac{(\tilde{\zeta}_0 + \tilde{\zeta}_{12} - 3)(\tilde{\zeta}_{12} - 3)}{h^2(2 - \tilde{\zeta}_2)^2} a^{\frac{\tilde{\zeta}_{12}-3}{2-\tilde{\zeta}_2}} \left[2h + \frac{\tilde{\zeta}_0}{\tilde{\zeta}_{12} - 3}\right] + \frac{3(\tilde{\zeta}_0 + \tilde{\zeta}_{12} - 3)}{h(2 - \tilde{\zeta}_2)} a^{\frac{\tilde{\zeta}_{12}-3}{2-\tilde{\zeta}_2}}}{\frac{3(\tilde{\zeta}_0 + \tilde{\zeta}_{12} - 3)}{h(2 - \tilde{\zeta}_2)} a^{\frac{\tilde{\zeta}_{12}-3}{2-\tilde{\zeta}_2}} + \frac{9}{2}}. \quad (2.44)$$

The above equations show that in the limit  $a \rightarrow \infty$ , the statefinder parameters  $\{r, s\} \rightarrow \{1, 0\}$ , a value corresponding to the  $\Lambda$ CDM model of the universe. So the present model resembles the  $\Lambda$ CDM model in the future. The  $\{r, s\}$  plane trajectory of the model is shown in figure 2.13. The trajectories are coinciding with each other for the best estimates from both the sets of the limiting conditions of the parameters. The trajectory in the  $\{r, s\}$  plane are lying in the region  $r > 1, s < 0$ , a feature similar to the generalized Chaplygin gas model of dark energy [100]. The present model can also be discriminated from the Holographic dark energy model with event horizon as the I.R. cut off, in which the  $r - s$  evolution starts from a region  $r \sim 1, s \sim 2/3$  and end on the  $\Lambda$ CDM point [101]. The

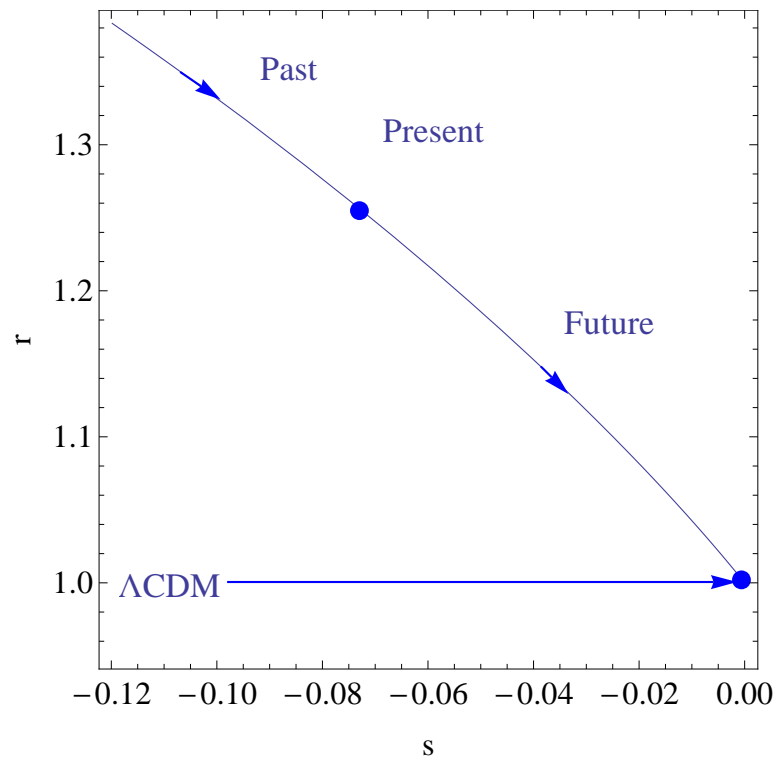


Figure 2.13: The evolution of the model in the  $r$ - $s$  plane for the best estimates of the parameters. The curves are coinciding with each other for the best estimated values of the parameters from both the limiting conditions.

present position of the universe dominated by the bulk viscous matter is noted in the plot and it corresponds to  $\{r_0, s_0\} = \{1.25, -0.07\}$ . This means that the present model is distinguishably different from the  $\Lambda$ CDM model.

## Appendix

Here we briefly analyze the effect of the model on the integrated Sachs - Wolfe (ISW) effect and has not gone into the details, hence added as appendix.

### ISW effect

Viscous dark matter will, in general, resist to the density perturbations. Consequently it will dilute the gravitational potential at the perturbed regions. This will subsequently affect the CMB radiation and leads to ISW effect [102].

The ISW Effect is the change in the energy of a CMB photon as it passes through the evolving gravitational potential wells. It is obtained as

$$\left(\frac{\Delta T}{T}\right)_{ISW} = 2 \int_{\eta_r}^{\eta_0} \Phi'[(\eta_0 - \eta)\hat{\mathbf{n}}, \eta] \mathbf{d}\eta, \quad (2.45)$$

where  $\hat{\mathbf{n}}$  is the photon trajectory and  $\eta_0$  is the conformal time today and  $\eta_r$  is the conformal time at recombination,  $\Phi$  is the gravitational potential and prime represents derivative with respect to the conformal time.

So the first step towards the calculation of the ISW Effect is to obtain the evolution of gravitational potential in an expanding universe. This can be obtained from Einstein's equation by taking care of the perturbations. Viscous dark matter may cause a fast decay of gravitational potential which modifies the CMB spectrum.

In Fourier space, the gravitational potential takes the form [103]

$$\Phi = \frac{3}{2} \frac{\Omega_{mo}}{a} \left(\frac{H_0}{k}\right)^2 \delta(k, \eta), \quad (2.46)$$

where density perturbation,  $\delta(k, \eta) = G(\eta)\delta(k, 0)$ .  $G(\eta)$  is the growth factor which is related to the Hubble parameter as,

$$G(\eta) \propto \frac{H(\eta)}{H_0} \int_{z(\eta)}^{\infty} dz' (1+z') \left(\frac{H_0}{H(z')}\right)^3. \quad (2.47)$$

In matter dominated universe,  $G \propto a$ , so  $\Phi$  remains a constant, hence no ISW effect.

In our model, by considering the bulk viscous coefficient  $\zeta = \zeta_0 + \zeta_1 \frac{\dot{a}}{a} + \zeta_2 \frac{\ddot{a}}{a}$ , the Hubble parameter evolves as equation (2.11). By using this relation, the integral in the growth factor becomes hypergeometric function. For simplification, let us consider the case when  $a$  is large, then  $H \propto a^{\frac{\tilde{\zeta}_1 + \tilde{\zeta}_2 - 3}{2 - \tilde{\zeta}_2}}$ . Then the growth factor becomes,

$$G \propto (1+z)^{\frac{\tilde{\zeta}_1 + \tilde{\zeta}_2 - 3}{2 - \tilde{\zeta}_2}} \left( \frac{(2 - \tilde{\zeta}_2) z^{\frac{-3\tilde{\zeta}_1 + \tilde{\zeta}_2 + 5}{2 - \tilde{\zeta}_2}}}{-3\tilde{\zeta}_1 - \tilde{\zeta}_2 + 5} \right). \quad (2.48)$$

So, potential becomes  $\Phi \propto z^{8.34}(1+z)^{4.45}$  (by using extracted parameter values). From the last scattering surface, which corresponds to  $z = 1091$ , to the present epoch  $z = 0$ , the potential will be rarefied. This causes ISW effect. However, only with an exact calculations and by obtaining the correlation function, one can get the total ISW effect and its effect on the structure formation.



# 3

## Thermodynamics of bulk viscous matter dominated universe

*This chapter deals with the thermodynamical analysis of the bulk viscous model by peeking into the entropy evolution. Here we have also considered two special cases for  $\zeta$ ,  $\zeta = \zeta_0 + \zeta_1 \frac{\dot{a}}{a}$  and  $\zeta = \zeta_0$ .*

Dissipative process like viscosity will generate entropy in the system. In this chapter we presents a detailed analysis on the thermal evolution of the bulk viscous model. It mainly consist of the status of the local and generalized second laws of thermodynamics. Following this we also study the status of the convexity condition to check whether the thermal evolution leads to state of maximum entropy, indicating a stable thermal evolution.

### 3.1 Local second law of thermodynamics

In the FLRW space-time, the law of generation of the local entropy due to viscosity is given as [69, 70, 104],

$$T\nabla_\nu s^\nu = \zeta(\nabla_\nu u^\nu)^2 = 9H^2\zeta, \quad (3.1)$$

## 58 Thermodynamics of bulk viscous matter dominated universe

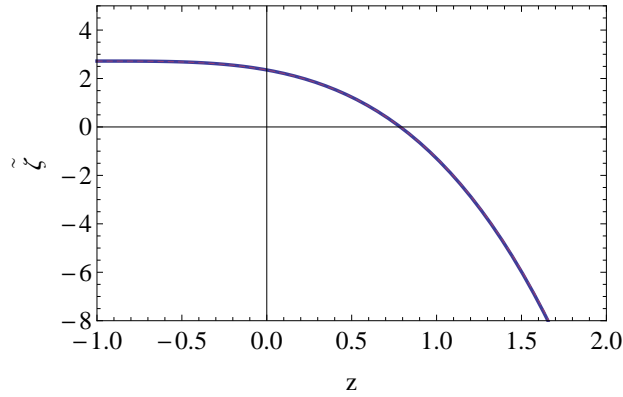


Figure 3.1: Evolution of the total dimensionless bulk viscous parameter with the red shift for the best estimated values corresponding to the two limiting conditions.  $\tilde{\zeta}$  is positive for  $z \leq 0.8$ .

where  $T$  is the temperature and  $\nabla_{\nu}s^{\nu}$  is the rate of generation of entropy in unit volume. The local second law of thermodynamics will be satisfied if,

$$T\nabla_{\nu}s^{\nu} \geq 0, \quad (3.2)$$

which implies that, the viscosity of matter must satisfies the condition,

$$\zeta \geq 0. \quad (3.3)$$

Using equations (2.9) and (2.11), the total dimensionless bulk viscous parameter (equation (2.6)), can be obtained as

$$\tilde{\zeta}(a) = \frac{1}{2 - \tilde{\zeta}_2} \left[ 2\tilde{\zeta}_0 + (2\tilde{\zeta}_1 - \tilde{\zeta}_2) \frac{H}{H_0} \right], \quad (3.4)$$

where  $\tilde{\zeta} = \frac{3\zeta}{H_0}$ , the total dimensionless bulk viscous parameter. We have studied the evolution of  $\tilde{\zeta}$  using the best estimated values for both cases of parameters and found that the evolution of the total bulk viscous parameter are coinciding for both the cases as shown in figure 3.2. It also shows that the total bulk viscous coefficient is evolving continuously from the negative value region to a positive region. When  $z \leq 0.8$ , the total bulk

viscous parameter becomes positive. This means that the rate of entropy production is negative in the early epoch and positive in the later epoch. Hence the local second law is violated in the early epoch and is obeyed in the later epoch. This seems to be a drawback of the present model. However, it can be considered only as a theoretical possibility [105]. This drawback will be rectified when one consider the entropy evolution of the whole system, which include both the local entropy and also the entropy of the boundary, the horizon of the universe.

But when  $\zeta = \zeta_0$ , such that  $\zeta_1 = 0$  and  $\zeta_2 = 0$  then it can be easily seen that  $\zeta$  always remains positive through out the evolution of the universe (since  $\zeta_0 > 0$ , see section 3.3) and hence satisfying the local second law of thermodynamics.

### **3.2 Entropy and Generalized second law of thermodynamics**

In an absolute way the status of the second law of thermodynamics should be considered along with the accounting of the entropy generation from the horizon. In that circumstances, the second law becomes the generalized second law of thermodynamics, which state that the total entropy of the fluid components of the universe plus that of the horizon should never decrease [106–109]. In the present model this means the rate of entropy change of the bulk viscous matter and that of the horizon must be greater than zero i.e.,

$$\frac{d}{dt}(S_m + S_h) \geq 0, \quad (3.5)$$

where,  $S_m$  is the entropy of the matter and  $S_h$  is that of the horizon. For a flat FLRW universe, the apparent horizon radius is given as [130]

$$r_A = \frac{1}{H}. \quad (3.6)$$

## 60 Thermodynamics of bulk viscous matter dominated universe

The entropy associated to the apparent horizon is [111],

$$S_h = 2\pi A = 8\pi^2 r_A^2 \quad (3.7)$$

where  $A = 4\pi r_A^2$  is the area of the apparent horizon and we have assumed  $8\pi G = 1$ . Using the first Friedmann equation and equations (2.2), (2.5), (2.7) and (3.6), we obtain the time derivative of  $r_A$  as,

$$\dot{r}_A = \frac{1}{2} r_A^3 H \left[ -H(\tilde{\zeta}_0 H_0 + \tilde{\zeta}_1 H + \tilde{\zeta}_2 \left( \frac{\dot{H}}{H} + H \right)) + \rho_m \right]. \quad (3.8)$$

The temperature of the apparent horizon can be defined as [112]

$$T_h = \frac{1}{2\pi r_A} \left( 1 - \frac{\dot{r}_A}{2Hr_A} \right). \quad (3.9)$$

Using equations (3.7), (3.8) and (3.9), we arrive

$$T_h \dot{S}_h = 4\pi r_A^3 H \left[ \rho_m - H(\tilde{\zeta}_0 H_0 + \tilde{\zeta}_1 H + \tilde{\zeta}_2 \left( \frac{\dot{H}}{H} + H \right)) \right] \left[ 1 - \frac{\dot{r}_A}{2Hr_A} \right]. \quad (3.10)$$

The change in entropy of the viscous matter inside the apparent horizon can be obtained using the Gibbs equation,

$$T_m dS_m = d(\rho_m V) + P^* dV \quad (3.11)$$

where  $T_m$  is the temperature of the bulk viscous matter,  $V = \frac{4}{3}\pi r_A^3$  is the volume enclosed by the apparent horizon and  $P^*$  is given by the equation (2.2). Using equations (2.2) and (2.7), the Gibbs equation becomes

$$T_m dS_m = V d\rho_m + (\rho_m - H(\tilde{\zeta}_0 H_0 + \tilde{\zeta}_1 H + \tilde{\zeta}_2 \left( \frac{\dot{H}}{H} + H \right))) dV. \quad (3.12)$$

Under equilibrium conditions, the temperature  $T_m$  of the viscous matter and that of the horizon  $T_h$  are equal,  $T_m = T_h$ . Then the Gibbs equation

(3.12) becomes

$$\begin{aligned}
 T_h \dot{S}_m = 4\pi r_A^3 H \left[ H(\tilde{\zeta}_0 H_0 + \tilde{\zeta}_1 H + \tilde{\zeta}_2 \left(\frac{\dot{H}}{H} + H\right) - \rho_m) \right] \\
 + 4\pi r_A^2 \dot{r}_A \left[ \rho_m - H(\tilde{\zeta}_0 H_0 + \tilde{\zeta}_1 H + \tilde{\zeta}_2 \left(\frac{\dot{H}}{H} + H\right)) \right].
 \end{aligned} \tag{3.13}$$

Adding equations (3.10) and (3.13), we get

$$T_h(\dot{S}_h + \dot{S}_m) = \frac{A}{4} H r_A^3 [\rho_m - H(\tilde{\zeta}_0 H_0 + \tilde{\zeta}_1 H + \tilde{\zeta}_2 \left(\frac{\dot{H}}{H} + H\right))]^2. \tag{3.14}$$

$A$ , the area of the apparent horizon,  $H$ , the Hubble parameter and the radius  $r_A$  are always positive, therefore,  $\dot{S}_h + \dot{S}_m \geq 0$  for a given temperature. This means that the generalized second law (GSL) is always valid. Hence the decrease in the entropy of the viscous matter is compensated by the increase in the entropy of the horizon. Even though the violation of the local second law of thermodynamics seems to be a drawback of this model, the validity of the Generalized second law for the entire causal region of the universe may safeguard the model.

Now we will check the status of the convexity condition or maximization condition of entropy. For a feasible thermodynamic system, the entropy must always increase. But for a stable evolution towards a state of stable thermodynamic equilibrium, the entropy evolution must satisfy [113],

$$\ddot{S} < 0 \quad \text{at least in the long run or last stage of the evolution.} \tag{3.15}$$

This is known as the convexity condition or condition of maximization of entropy, which implies an upper bound to the growth of entropy at least in the last stage of the evolution of the universe. The over dots in the above equation implies the derivative with respect to any suitable variable.

Following the expression for the Hubble parameter  $H$  (equation (2.11)), we can obtain the derivative of total entropy with respect to the time  $t$ ,

## 62 Thermodynamics of bulk viscous matter dominated universe

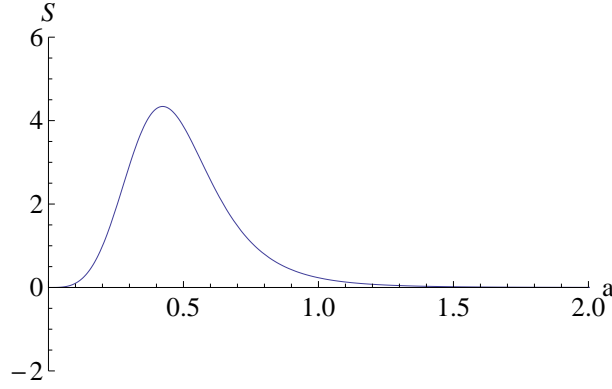


Figure 3.2: Evolution of the first derivative of entropy with the scale factor for the best estimated values corresponding to the two limiting conditions.

$\dot{S} = \dot{S}_h + \dot{S}_m$  as

$$\dot{S} = \frac{16\pi^2 a^{\frac{\tilde{\zeta}_1 + \tilde{\zeta}_2 + 6}{\tilde{\zeta}_2 - 2}} (\tilde{\zeta}_1 + \tilde{\zeta}_2 - 3)^3 (\tilde{\zeta}_0 + \tilde{\zeta}_1 + \tilde{\zeta}_2 - 3)^2}{H_0 (\tilde{\zeta}_2 - 2)^2 \left( a^{\frac{3}{\tilde{\zeta}_2 - 2}} (\tilde{\zeta}_0 + \tilde{\zeta}_1 + \tilde{\zeta}_2 - 3) - a^{\frac{\tilde{\zeta}_1 + \tilde{\zeta}_2}{\tilde{\zeta}_2 - 2}} \tilde{\zeta}_0 \right)^3}. \quad (3.16)$$

Using the estimated values of  $\tilde{\zeta}_0$ ,  $\tilde{\zeta}_1$  and  $\tilde{\zeta}_2$  from the Table 2.1, we plotted  $\dot{S}$  with the scale factor  $a$ , and is shown (same for both sets of values) in figure 3.2. It shows that the entropy always increases as  $\dot{S} > 0$ . This is desirable. Using the first derivative of entropy (equation (3.16)), we can calculate the second derivative of entropy  $\ddot{S}$  as,

$$\ddot{S} = \frac{16\pi^2 a^{\frac{6}{\tilde{\zeta}_2 - 2}} (\tilde{\zeta}_{12} - 3)^3 (\tilde{\zeta}_0 + \tilde{\zeta}_{12} - 3)^2 (2\tilde{\zeta}_0 a^{\frac{\tilde{\zeta}_{12}}{\tilde{\zeta}_2 - 2}} + (\tilde{\zeta}_0 + \tilde{\zeta}_{12} - 3) a^{\frac{3}{\tilde{\zeta}_2 - 2}})}{(\tilde{\zeta}_2 - 2)^3 ((\tilde{\zeta}_0 + \tilde{\zeta}_{12} - 3) a^{\frac{3}{\tilde{\zeta}_2 - 2}} - \tilde{\zeta}_0 a^{\frac{\tilde{\zeta}_{12}}{\tilde{\zeta}_2 - 2}})^3}, \quad (3.17)$$

where  $\tilde{\zeta}_{12} = \tilde{\zeta}_1 + \tilde{\zeta}_2$ . The result has been plotted in figure 3.3, and we see that  $\ddot{S} < 0$ , at the last stage of the evolution. Here  $\ddot{S}$  is approaching zero from below. which is implying that the growth of entropy is bounded and the system is approaching a stage of maximum finite entropy. Form this

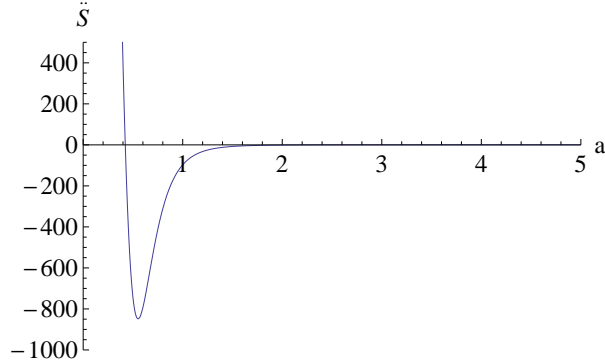


Figure 3.3: Evolution of the second derivative of entropy with the scale factor for the best estimated values corresponding to the two limiting conditions.

it can be concluded that the model predicts a universe which behaves as an ordinary macroscopic system[114].

### 3.3 Entropy evolution for some special cases of viscosity

Here we study the evolution of entropy for the special cases mentioned below:

**Case 1** -  $\zeta = \zeta_0 + \zeta_1 \frac{\dot{a}}{a}$  with  $\tilde{\zeta}_2 = 0$  where viscosity is not depending on the acceleration.

**Case 2** -  $\zeta = \zeta_0$  with  $\tilde{\zeta}_1 = \tilde{\zeta}_2 = 0$ , where viscosity is a constant.

For this the first step is to extract the values of the viscosity parameters subjected to the above conditions by the  $\chi^2$  minimization technique using the same data set of supernova used in the chapter 2. The extracted values are tabulated in the Table 3.1. For Case - 2, we see that the value of  $\zeta_0$  is positive and hence the total viscous coefficient always remains a positive constant through out the evolution of the universe, hence, the local second law of thermodynamics is valid throughout.

## 64 Thermodynamics of bulk viscous matter dominated universe

Cases	$\zeta = \zeta_0 + \zeta_1 \frac{a}{a}$	$\zeta = \zeta_0$
$\tilde{\zeta}_0$	6.26	1.92
$\tilde{\zeta}_1$	-3.91	0
$\tilde{\zeta}_2$	0	0
$\Omega_{m0}$	1	1
$H_0$	70.49	69.61
$\chi_{min}^2$	310.54	315.07
$\chi_{d.o.f}^2$	1.02	1.03

Table 3.1: Best estimates of the bulk viscous parameters and  $H_0$  and also  $\chi^2$  minimum value corresponding to the above different cases of  $\zeta$ .  $\chi_{d.o.f}^2 = \frac{\chi_{min}^2}{n-m}$ , where  $n = 307$ , the number of data and  $m$  is the number of parameters in the model. The subscript d.o.f stands for degrees of freedom. For the best estimation we have used SCP ‘‘Union’’ 307 SNe Ia data sets.  $\Omega_{m0}$  is the present mass density parameter.

For Case - 1, the first and second derivatives of the total entropy are obtained (using equations (3.16) and (3.17)) as,

$$\dot{S} = -\frac{4\pi^2 a^{\frac{3}{2} + \tilde{\zeta}_1} (\tilde{\zeta}_1 - 3)^3 (\tilde{\zeta}_0 + \tilde{\zeta}_1 - 3)^2}{H_0 (a^{3/2} \tilde{\zeta}_0 - a^{\frac{\tilde{\zeta}_1}{2}} (\tilde{\zeta}_0 + \tilde{\zeta}_1 - 3))^3}, \quad (3.18)$$

$$\ddot{S} = -\frac{2\pi^2 a^{\tilde{\zeta}_1} (\tilde{\zeta}_1 - 3)^3 (\tilde{\zeta}_0 + \tilde{\zeta}_1 - 3)^2 (2a^{\frac{3}{2}} \tilde{\zeta}_0 + a^{\frac{\tilde{\zeta}_1}{2}} (\tilde{\zeta}_0 + \tilde{\zeta}_1 - 3))}{(a^{\frac{\tilde{\zeta}_1}{2}} (\tilde{\zeta}_0 + \tilde{\zeta}_1 - 3) - a^{\frac{3}{2}} \tilde{\zeta}_0)^3}. \quad (3.19)$$

The plot of  $\dot{S}$  and  $\ddot{S}$  for the best estimated values of  $\zeta$ 's corresponding to this case are shown in the figures 3.4 and 3.5, respectively. The figures indicates that both the generalized second law and the maximization conditions are satisfied in this case.

For Case 2 - we have obtained the expression for  $\dot{S}$  and  $\ddot{S}$  by following the same procedure and are,

$$\dot{S} = \frac{108\pi^2 a^{\frac{3}{2}} (\tilde{\zeta}_0 - 3)^2}{H_0 \left( \left( a^{\frac{3}{2}} - 1 \right) \tilde{\zeta}_0 + 3 \right)^3}, \quad (3.20)$$

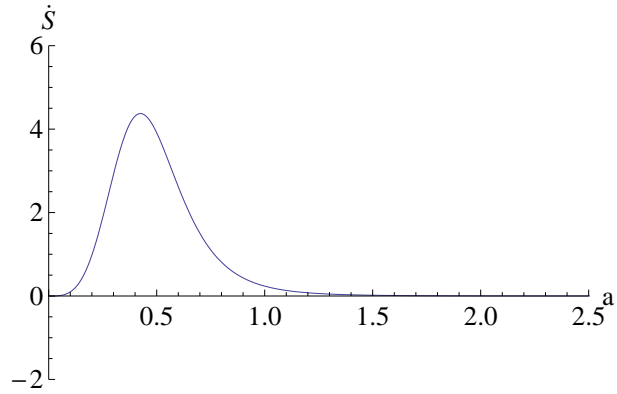


Figure 3.4: Evolution of the first derivative of entropy with the scale factor for the best estimated values corresponding to the case  $\zeta = \zeta_0 + \zeta_1 \frac{\dot{a}}{a}$ .

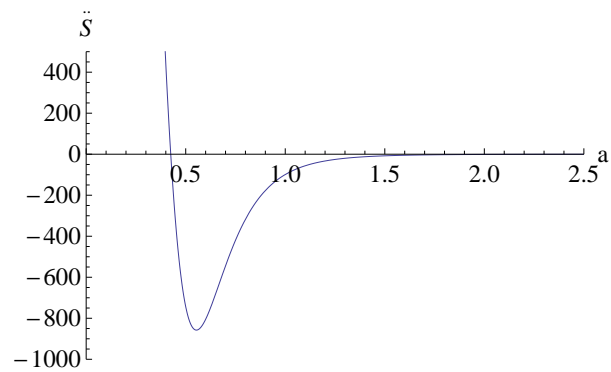


Figure 3.5: Evolution of the second derivative of entropy with the scale factor for the best estimated values corresponding to the case  $\zeta = \zeta_0 + \zeta_1 \frac{\dot{a}}{a}$ .

## 66 Thermodynamics of bulk viscous matter dominated universe

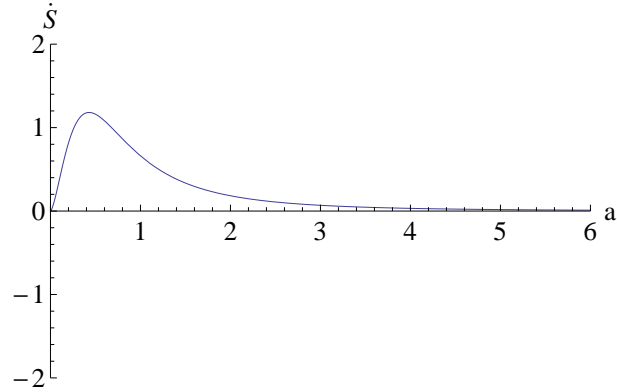


Figure 3.6: Evolution of the first derivative of entropy with the scale factor for the best estimated values corresponding to the case  $\zeta = \zeta_0$ .

$$\ddot{S} = -\frac{54\pi^2 (\tilde{\zeta}_0 - 3)^2 \left( (1 + 2a^{\frac{3}{2}}) \tilde{\zeta}_0 - 3 \right)}{\left( (a^{\frac{3}{2}} - 1) \tilde{\zeta}_0 + 3 \right)^3}. \quad (3.21)$$

The evolution of  $\dot{S}$  and  $\ddot{S}$  for the best estimated values of  $\tilde{\zeta}_0$  are shown in the figures 3.6 and 3.7, respectively.

We see that both the conditions,  $\dot{S} > 0$  and  $\ddot{S} < 0$  are satisfied, implying the validity of generalized second law and entropy maximization as in the previous case.

The entropy evolution behavior shows that the bulk viscous model predicts a stable thermal evolution for the universe. The validity of the maximization condition implies that, the universe evolves to an asymptotically stable thermal state at which the entropy is bounded. But with this alone is not sufficient to get the full potential of the model as a viable one to explain the late evolution of the current universe. Further we would like to study the dynamical system behavior of the model to see whether it gives a compatible evolutionary status.

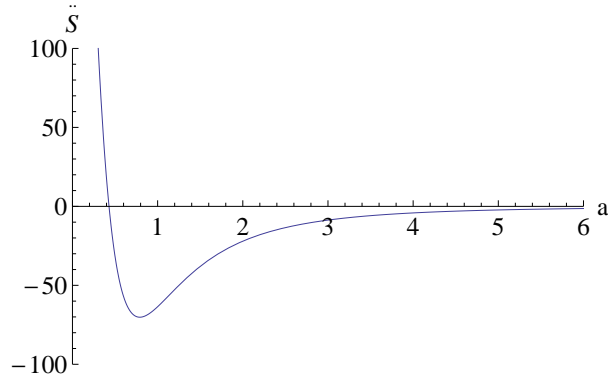


Figure 3.7: Evolution of the second derivative of entropy with the scale factor for the best estimated values corresponding to the case  $\zeta = \zeta_0$ .

## Appendix

### Generalized second law with event horizon as boundary

In this chapter, we have found out that the total  $\zeta$  is negative when  $z > 0.8$  for  $\zeta = \zeta_0 + \zeta_1 \frac{\dot{a}}{a} + \zeta_2 \frac{\ddot{a}}{a}$ , thereby violating local second law in the early universe. But when  $\zeta = \zeta_0$ ,  $\zeta$  always remains positive through out the evolution of the universe (since  $\zeta_0 > 0$ ) and hence satisfying the local second law of thermodynamics.

However, if one consider the Generalized second law (GSL) which includes the total entropy of the universe plus that of the horizon, it is found that total entropy is always on the increase for total  $\zeta$ , if apparent horizon is considered as the boundary. On taking account of the validity of GSL, it can be reasonably argued that in the early universe where  $\zeta$  becomes negative, the total pressure becomes positive and the viscous matter will act as an ordinary non-relativistic matter causing decelerated expansion. There are conventional dark energy models which act as the non-relativistic matter in the early phases causing decelerated expansion [115–118]. There are also works [105, 119–121], showing that the entropy change can become negative depending on the equation of state of mat-

## 68 Thermodynamics of bulk viscous matter dominated universe

ter. In the current literature, there are publications dealing the problems with negative viscous coefficients [105]. In this reference the authors has point out that the positivity of  $\zeta$  in conventional cosmology is based upon the requirement that the change of entropy in a non-equilibrium system is positive, and they argues that the possibility of allowing for negative values of  $\zeta$  is not so unreasonable in view of the general bizarre properties of the dark energy fluid, as far as temperature is positive. Apart from this our model also satisfies GSL with total  $\zeta$ .

Now we will consider event horizon as the boundary for analyzing the validity of GSL for  $\zeta = \zeta_0$ . The radius of the event horizon is given as,

$$R_E = a \int_a^\infty \frac{da}{Ha^2}, \quad (3.22)$$

where  $a$  is the scale factor and  $H$  is the Hubble parameter given as equation (2.12),

$$H(a) = H_0 \left[ a^{-\frac{3}{2}} \left( 1 - \frac{\tilde{\zeta}_0}{3} \right) + \frac{\tilde{\zeta}_0}{3} \right]. \quad (3.23)$$

$H_0$  is the present value of the Hubble parameter. The radius of the event horizon then obtained as,

$$R_E = \frac{a}{H_0} (4.16 + 2.65 \arctan[0.58 - 1.4\sqrt{a}] - 1.53 \log[0.97 + 1.18\sqrt{a}] + 0.76 \log[0.94 - 1.14\sqrt{a} + 1.38a]). \quad (3.24)$$

The entropy associated with the event horizon is

$$S_E = \frac{A}{4}. \quad (3.25)$$

$A = 4\pi R_E^2$  is the area of the horizon. So entropy becomes

$$S_E = \pi R_E^2. \quad (3.26)$$

The temperature of the event horizon can be defined as  $T_E = \frac{1}{2\pi R_E}$ . Using these we get[122],

$$T_E \dot{S}_E = \dot{R}_E = HR_E - 1. \quad (3.27)$$

The entropy of matter can be obtained using the Gibbs' relation,

$$\begin{aligned} T_m dS_m &= d(\rho_m V) + P dV \\ &= (\rho_m + P) dV + V d\rho_m, \end{aligned} \quad (3.28)$$

where  $T_m$  is the temperature of the bulk viscous matter,  $V = \frac{4}{3}\pi R_E^3$  is the volume enclosed by the event horizon. Using the expression for pressure  $P = -3H\zeta_0 = HH_0\tilde{\zeta}_0$  ( $\tilde{\zeta}_0 = \frac{3\zeta}{H_0}$  is the dimensionless viscous parameter), the conservation equation and the relation  $\dot{R}_E = HR_E - 1$ , we get

$$T_m \dot{S}_m = 4\pi R_E^2 (HH_0\tilde{\zeta}_0 - 3H^2). \quad (3.29)$$

Under equilibrium conditions, the temperature  $T_m$  of the viscous matter and that of the horizon  $T_E$  are equal,  $T_m = T_E = T$ . Adding equations (3.27) and (3.29), we get,

$$T(\dot{S}_E + \dot{S}_m) = 4\pi R_E^2 (HH_0\tilde{\zeta}_0 - 3H^2) + HR_E - 1. \quad (3.30)$$

For GSL to be valid,  $T(\dot{S}_E + \dot{S}_m) > 0$ . We have checked the validity by numerically plotting Eq. (3.30) with respect to  $a$  and is shown in the figure 3.8.

The plot shows that the GSL is violated when we take event horizon as the boundary. So, in our model GSL is satisfied at the apparent horizon but violated at the event horizon. At this juncture, one may note that a more novel GSL was proposed by Bousso et.al [123] regardless of whether an event horizon is present. However, the validity of this new GSL is to be checked for our model.

There are many works in literature in tune with our result regarding the validity of GSL. In references [124, 126], the authors have shown that in general, for an accelerating universe, GSL of thermodynamics holds only in the case where the enveloping surface is the apparent horizon, but not in the case of the event horizon. There are also many other dark

## 70 Thermodynamics of bulk viscous matter dominated universe

---

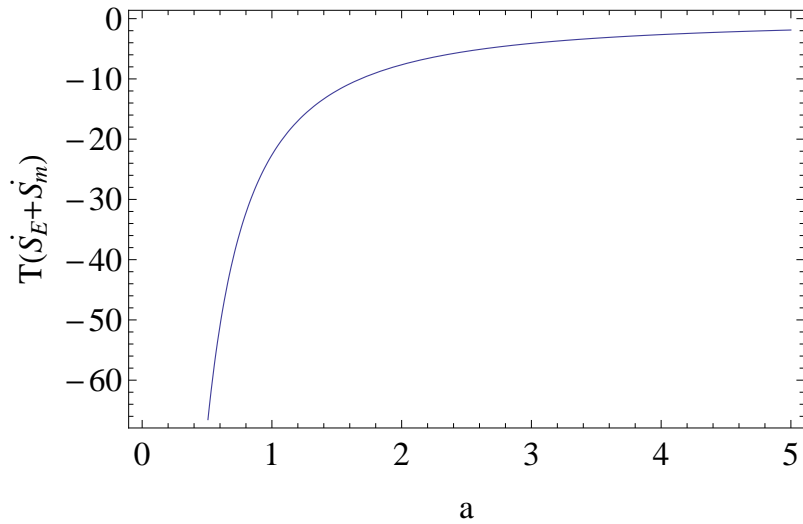


Figure 3.8: Plot of  $T(\dot{S}_E + \dot{S}_m)$  with the scale factor  $a$  when event horizon is considered as the boundary.

energy models which shows the same behavior. Some models are viscous model [125, 127], interacting dark energy model with dark matter [122], Holographic Ricci dark energy model [128, 129], DGP model [130], brane world model [131]. In all these references, it is found that the event horizon in an accelerating universe is not a boundary from the thermodynamical point of view. In lieu of these, apparent horizon can be considered as the proper thermodynamic boundary.

# 4

## Dynamical system analysis of bulk viscous matter dominated universe

*This chapter discuss the asymptotic behavior of the bulk viscous model through phase space analysis in order to check whether the model predicts all the conventional phases of the universe.*

The present chapter is devoted to the dynamical system analysis analysis of the model. A phase space analysis of a cosmological model would indicate the different stages of the universe like (a) a radiation dominated phase, followed by (b) a matter dominated phase, and (c) an accelerated expanding phase, corresponding to the existence of different critical points. So doing a phase space analysis would clearly indicate whether the model predicts the realistic picture regarding the evolution of our universe.

It is difficult to solve exactly the cosmological field equations with more than one cosmic components. Under such condition one often make use of the dynamical system tools to extract the asymptotic properties of the model. For this we write down the cosmological equations as a system of autonomous differential equations and then investigate the equivalent phase space of the model. The critical points of these equations can be

correlated with the solutions of the cosmological field equations and its stability can be determined by examining the system obtained by linearizing about the critical point i.e., from the eigen values of the corresponding Jacobian matrix. The first step is to select suitable dynamic variables for the phase space analysis.

## 4.1 Phase space analysis of bulk viscous matter dominated universe

Here we consider the flat universe with a single component, the bulk viscous matter for carrying out the phase-space analysis. We consider  $u$  and  $v$  as the dimensionless phase space variables which are defined as follows,

$$u = \Omega_m = \frac{\rho_m}{3H^2}, \quad (4.1)$$

$$v = \frac{1}{\frac{H_0}{H} + 1}. \quad (4.2)$$

These phase space coordinates are varying in the range  $0 \leq u \leq 1$  and  $0 \leq v \leq 1$ . Below we describe the dynamical analysis for different cases by which the viscosity is being accounted.

**Case 1: with**  $\zeta = \zeta_0 + \zeta_1 \frac{\dot{a}}{a} + \zeta_2 \frac{\ddot{a}}{a}$

Using Friedmann equations, conservation equation for matter and equation (3.4), we can obtain the autonomous equations satisfied by  $u$  and  $v$  as

$$u' = \frac{(1-u)(2\tilde{\zeta}_0(1-v) + (2\tilde{\zeta}_1 - \tilde{\zeta}_2)v)}{v(2 - \tilde{\zeta}_2)} = f(u, v) \quad (4.3)$$

$$v' = \frac{(1-v)(\tilde{\zeta}_0(1-v) + (\tilde{\zeta}_1 + \tilde{\zeta}_2 - 3)v)}{2 - \tilde{\zeta}_2} = g(u, v) \quad (4.4)$$

where the prime denote the derivative with respect to  $\ln a$ . Using equations (2.31) and (2.35), the deceleration parameter and equation of state parameter, we need them for further use, can be written in terms of  $v$  as

$$q = \frac{1}{2 - \tilde{\zeta}_2} \left( 1 - \tilde{\zeta}_1 - \tilde{\zeta}_0 \frac{1-v}{v} \right), \quad (4.5)$$

$$\omega = \frac{1}{3(2 - \tilde{\zeta}_2)} \left( \tilde{\zeta}_2 - 2\tilde{\zeta}_1 - 2\tilde{\zeta}_0 \frac{1-v}{v} \right). \quad (4.6)$$

The critical points  $(u_c, v_c)$  of the above autonomous equations (4.3) and (4.4) can be obtained by equating  $u' = 0$  and  $v' = 0$ . The stability of the dynamic system in the neighborhood of the critical point can be checked as follows. Linearize the system by considering small perturbations around the critical point  $u \rightarrow u_c + \delta u$ ,  $v \rightarrow v_c + \delta v$ , which satisfy the following matrix equation,

$$\begin{bmatrix} \delta u' \\ \delta v' \end{bmatrix} = \begin{bmatrix} \left( \frac{\partial f}{\partial u} \right)_0 & \left( \frac{\partial f}{\partial v} \right)_0 \\ \left( \frac{\partial g}{\partial u} \right)_0 & \left( \frac{\partial g}{\partial v} \right)_0 \end{bmatrix} \begin{bmatrix} \delta u \\ \delta v \end{bmatrix} \quad (4.7)$$

where the suffix 0 denotes the value evaluated at the critical point  $(u_c, v_c)$ . The Jacobian matrix ( $2 \times 2$  matrix in the right hand side of the equation (4.7)) for the autonomous equations (4.3) and (4.4) is

$$\begin{bmatrix} \left( -\frac{2\tilde{\zeta}_0(v-1) + (\tilde{\zeta}_2 - 2\tilde{\zeta}_1)v}{(\tilde{\zeta}_2 - 2)v} \right)_0 & \left( \frac{2\tilde{\zeta}_0(u-1)}{(\tilde{\zeta}_2 - 2)v^2} \right)_0 \\ 0 & \left( \frac{-2\tilde{\zeta}_0(v-1) + (\tilde{\zeta}_1 + \tilde{\zeta}_2 - 3)(2v-1)}{\tilde{\zeta}_2 - 2} \right)_0 \end{bmatrix} \quad (4.8)$$

If the eigen values of the Jacobian matrix are all negative, then the critical point is stable otherwise the critical point is generally unstable. If all the eigen values are positive then the critical point is an unstable node and if there are both positive and negative eigen values, then the critical point is a saddle point.

For autonomous equations (4.3) and (4.4), there are two critical points  $(u_c, v_c)$  :

1.  $(u_c, v_c) = (1, 1)$

Here  $u = 1$  implies a viscous matter dominated universe and  $v = 1$  corresponds either to  $H_0 = 0$  or  $H \rightarrow \infty$ . Since  $H_0$  cannot be zero, this corresponds to the initial singular state characterized with  $H \rightarrow \infty$ . The Jacobian matrix corresponding to this critical point can be obtained by putting  $u = 1$  and  $v = 1$  in equation (4.8). The eigen values of the Jacobian matrix are

$$\lambda_1 = \frac{2\tilde{\zeta}_1 - \tilde{\zeta}_2}{\tilde{\zeta}_2 - 2}, \quad \lambda_2 = \frac{\tilde{\zeta}_1 + \tilde{\zeta}_2 - 3}{\tilde{\zeta}_2 - 2}. \quad (4.9)$$

Substituting the values of  $\tilde{\zeta}_0$ ,  $\tilde{\zeta}_1$  and  $\tilde{\zeta}_2$  from Table 2.1, we get  $\lambda_1 = 3.88$  and  $\lambda_2 = 3.44$  for the first condition (i.e.,  $\tilde{\zeta}_0 > 0$ ) and  $\lambda_1 = 3.915$  and  $\lambda_2 = 3.457$  for the second condition (i.e.,  $\tilde{\zeta}_0 < 0$ ), which are almost the same except for the slight difference in the decimal places. Since both the eigen values are positive, the critical point is unstable and is a past attractor. The values of equation of state parameter  $\omega$  and deceleration parameter  $q$  (using equations (4.6) and (4.5)) are found to be around 1.3 and 2.4 respectively, for the two cases. This shows that in the early stage of the evolution of the universe, bulk viscous matter will behave almost like a stiff fluid and since  $\omega > 1$ , it may possibly violates the causality [139].

2.  $(u_c, v_c) = (1, \frac{\tilde{\zeta}_0}{\tilde{\zeta}_0 - (\tilde{\zeta}_1 + \tilde{\zeta}_2 - 3)}) = (1, 0.475)$

This also corresponds to a matter dominated universe with  $\frac{H_0}{H} = 1.105$ . The eigen values corresponding to this point are

$$\lambda_1 = -\frac{\tilde{\zeta}_1 + \tilde{\zeta}_2 - 3}{\tilde{\zeta}_2 - 2}, \quad \lambda_2 = -3. \quad (4.10)$$

Using the values of bulk viscous parameters from Table 2.1, we obtain  $\lambda_1 \sim -3.45$  for the two conditions (i.e., for  $\tilde{\zeta}_0 < 0$  and  $\tilde{\zeta}_0 > 0$ ). Since the two eigen values are negative, this critical point is a stable

$(u_c, v_c)$	$\lambda_1$	$\lambda_2$	Stability	$\omega$	$q$
(1, 1)	3.9	3.4	Unstable, Past at- tractor	1.3	2.4
(1, 0.475)	-3.45	-3	Stable, future attractor	-1	-1

Table 4.1: Critical points for case 1, with  $\zeta = \zeta_0 + \zeta_1 \frac{\dot{a}}{a} + \zeta_2 \frac{\ddot{a}}{a}$

node and a future attractor. It is found that  $\omega \sim -1$  and  $q \sim -1$  and it corresponds to de Sitter phase.

The phase space plot for this case is shown in the figure 4.1. From the figure, it is clear that the critical point (1,1) is an unstable past attractor as trajectories emerge from this point. These emerging trajectories finally converges to the critical point (1,0.475), which is the future attractor. So the phase plot analysis of this case suggest a universe which begins from an initial singular state and ends on a de Sitter type universe. This is almost similar to the picture given by the  $\Lambda$ CDM model, in which the universe evolves from an initial singularity to a de Sitter phase through a matter dominated epoch. However, in the initial singular phase,  $\omega > 1$ , thereby having causality problem [139]. So this case cannot be considered as physical. The critical points, their stability and the values of  $\omega$  and  $q$  are summarized in the Table 4.1.

**Case 2: with  $\zeta = \zeta_0 + \zeta_1 \frac{\dot{a}}{a}$**

Using the Friedmann equations and conservation equation for matter we get the autonomous equation for this case as,

$$\begin{aligned}
 u' &= (1 - u) \left( \frac{\tilde{\zeta}_0}{v} + \tilde{\zeta}_1 - \tilde{\zeta}_0 \right), \\
 v' &= \frac{1}{2} (1 - v) (\tilde{\zeta}_0 + (\tilde{\zeta}_1 - \tilde{\zeta}_0 - 3) v).
 \end{aligned}
 \tag{4.11}$$

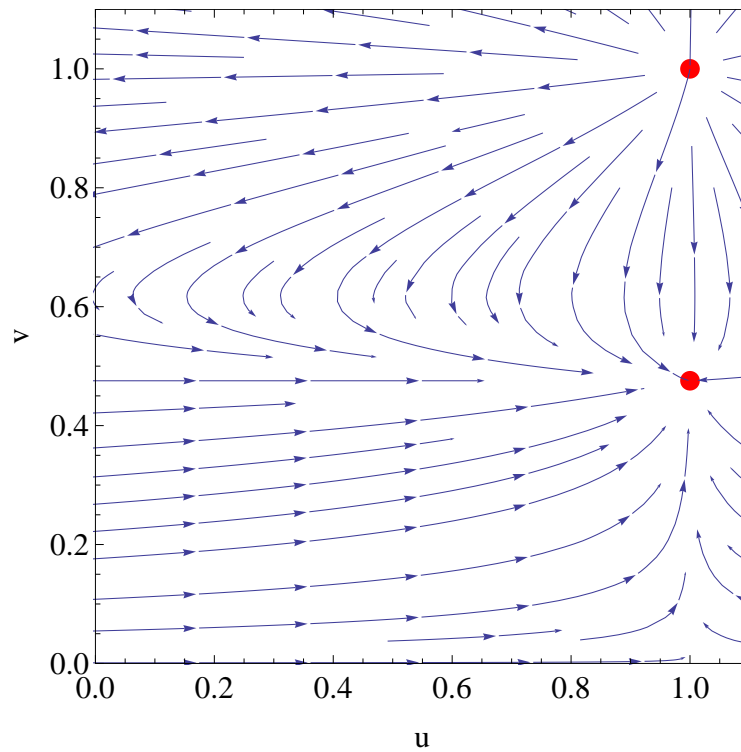


Figure 4.1: The figure shows the phase space structure in the  $u - v$  plane corresponding to the Case 1 ( $\zeta = \zeta_0 + \zeta_1 \frac{\dot{a}}{a} + \zeta_2 \frac{\ddot{a}}{a}$ ). The critical point  $(1,1)$  in the upper right corner of the plot is a past attractor and the point  $(1,0.475)$ , below the first critical point, is a future attractor. The direction of the trajectories is shown by the arrow head.

In this case also there are two critical points  $(u_c, v_c) = (1, 1)$  and  $(1, \frac{\tilde{\zeta}_0}{\tilde{\zeta}_0 - \tilde{\zeta}_1 + 3})$ . There properties are discussed below:

1.  $(u_c, v_c) = (1, 1)$

This is a matter dominated solution representing the initial singular state, since  $v = 1$  implies  $H \rightarrow \infty$ . The critical point is same as that in case 1. The eigen values of the corresponding Jacobian matrix are,

$$\lambda_1 = \frac{3 - \tilde{\zeta}_1}{2} = 3.455, \quad \lambda_2 = -\tilde{\zeta}_1 = 3.91. \quad (4.12)$$

Since the eigen values are all positive, the critical point is an unstable node or can be called as the past attractor. Thus it is a source point of any orbit in the phase space. Using the values of bulk viscous parameters from Table 3.1, we get  $\omega = 1.3$  and  $q = 2.45$  from equations (4.6) and (4.5), respectively. From these values it is clear that the point represent a decelerated phase of the universe. However, this may violate the causality condition since  $\omega > 1$ .

2.  $(u_c, v_c) = (1, \frac{\tilde{\zeta}_0}{\tilde{\zeta}_0 - \tilde{\zeta}_1 + 3}) = (1, 0.475)$

The eigen values of the corresponding Jacobian matrix are,

$$\lambda_1 = \frac{\tilde{\zeta}_1 - 3}{2} = -3.455, \quad \lambda_2 = -3, \quad (4.13)$$

using the value of  $\tilde{\zeta}_1$  from Table 3.1. Since the eigen values are negative, this solution is a stable node and a future attractor. So all trajectories in the phase space tends to meet at this point. The equation of state parameter  $\omega$  and the deceleration parameter  $q$  are both found to be -1, thereby representing a de Sitter epoch.

The phase plot of this case is shown in figure 4.2. The phase space trajectories starts from the critical point (1,1) and ends in the point (1,0.475) in the u-v phase plane. The behavior is same as that in the first case. The results are summarized in Table 4.2.

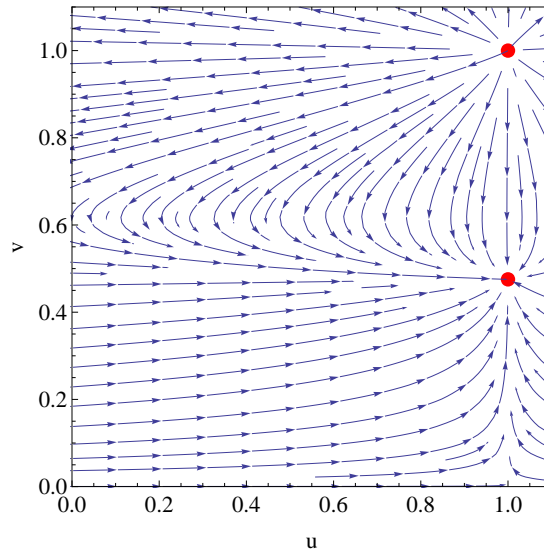


Figure 4.2: The figure shows the phase space structure in the  $u - v$  plane corresponding to the Case 2 ( $\zeta = \zeta_0 + \zeta_1 \frac{\dot{a}}{a}$ ). The critical point  $(1,1)$  in the upper right corner of the plot is a past attractor and the point  $(1,0.475)$ , below the first critical point, is a future attractor. The direction of the trajectories is shown by the arrow head.

$(u_c, v_c)$	$\lambda_1$	$\lambda_2$	Stability	$\omega$	$q$
$(1, 1)$	3.45	3.9	Unstable, Past at- tractor	1.3	2.4
$(1, 0.475)$	-3.45	-3	Stable, future attractor	-1	-1

Table 4.2: Critical points for case 2, with  $\zeta = \zeta_0 + \zeta_1 \frac{\dot{a}}{a}$

**Case 3: with  $\zeta = \zeta_0$**

In this case, the autonomous equation reduces to,

$$\begin{aligned} u' &= (1 - u) \left( \frac{\tilde{\zeta}_0}{v} - \tilde{\zeta}_0 \right) \\ v' &= \frac{1}{2} (1 - v) (\tilde{\zeta}_0 - (\tilde{\zeta}_0 + 3) v). \end{aligned} \tag{4.14}$$

There exists two critical points:

1.  $(u_c, v_c) = (u, 1)$

Here we see that the  $u$  coordinate is variable, which can assume any values ranging from 0 to 1, while  $v$  coordinate is a constant having value 1. As a result the critical point will not be an isolated point (see figure 4.3). It represents an initial state of the universe since  $H \rightarrow \infty$ . The eigen values of the corresponding Jacobian matrix are,

$$\lambda_1 = \frac{3}{2} = 1.5, \quad \lambda_2 = 0. \tag{4.15}$$

Since these values are positive, it is unstable. The value of equation of state parameter and the deceleration parameter are  $\omega = 0$  and  $q = 0.5$ . From these values it is clear that it represents a matter dominated decelerated phase of the universe. Unlike the other two cases, where the values of  $\omega$  corresponds to a stiff fluid, here in this case the value of  $\omega$  indicates the non-relativistic dark matter causing a usual decelerated phase.

2.  $(u_c, v_c) = (1, \frac{\tilde{\zeta}_0}{\tilde{\zeta}_0+3}) = (1, 0.39)$

This corresponds to a matter dominated universe with  $\frac{H_0}{H} = 1.564$ , representing the future phase of the universe. The eigen values are,

$$\lambda_1 = -\frac{3}{2} = -1.5, \quad \lambda_2 = -3. \tag{4.16}$$

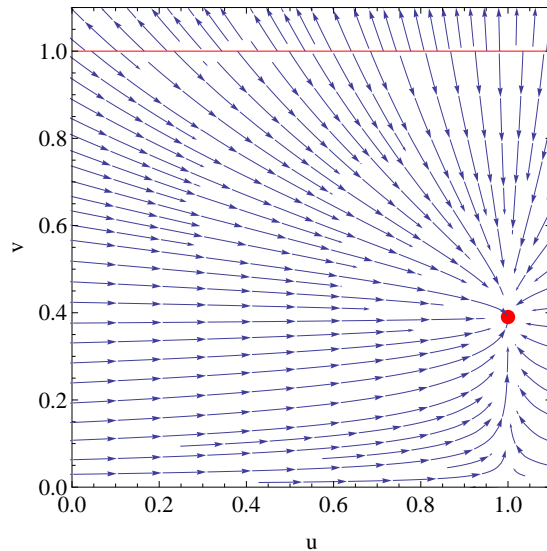


Figure 4.3: The figure shows the phase space structure in the  $u - v$  plane corresponding to the Case 3 ( $\zeta = \zeta_0$ ). The direction of the trajectories is shown by the arrow head.

The point is stable since both the eigen values are negative. The values of the equation of state parameter and the deceleration parameter are  $\omega \sim -1$  and  $q \sim -1$ , which corresponds to a de Sitter phase.

The phase plot diagram is shown in figure 4.3. From the figure it is clear that the phase space trajectories originate from the non-isolated critical point (or rather a critical line), which is a past attractor (representing the matter dominated decelerated epoch of the universe). These trajectories finally converge to the stable critical point  $(1, 0.39)$ , representing the de Sitter phase. This is similar to the behavior of the  $\Lambda$ CDM model. The results of the phase space analysis of the model are summarized in Table 4.3.

$(u_c, v_c)$	$\lambda_1$	$\lambda_2$	Stability	$\omega$	q
$(u, 1)$	1.5	0	Unstable, Past attractor	0	0.5
$(1, 0.39)$	-1.5	-3	Stable, future attractor	-1	-1

Table 4.3: Critical points for case 3, with  $\zeta = \zeta_0$

## 4.2 Phase space analysis of the bulk viscous model including radiation

The realistic picture of the universe have an early radiation dominated phase followed by matter dominated epoch and a late accelerated epoch. In order to know whether the bulk viscous model predicts a prior radiation dominated phase, we study the phase space structure of the model by including radiation as an additional cosmic component. For such a universe, the Friedmann equations becomes,

$$H^2 = \frac{\rho_m + \rho_r}{3}, \quad (4.17)$$

$$2\dot{H} + 3H^2 = HH_0\tilde{\zeta} - \frac{\rho_r}{3}. \quad (4.18)$$

The conservation equation for matter is given by

$$\dot{\rho}_m + 3H(\rho_m - HH_0\tilde{\zeta}) = 0, \quad (4.19)$$

and that for radiation it is,

$$\dot{\rho}_r + 4H\rho_r = 0. \quad (4.20)$$

Equation 4.18 can be modified using the radiation density parameter  $\Omega_r = \frac{\rho_r}{3H^2}$ , then the derivative of  $H$  with respect to time  $t$  becomes

$$\dot{H} = \frac{1}{2} (HH_0\tilde{\zeta} - 3H^2 - \Omega_r H^2) \quad (4.21)$$

Substituting this in equation (2.7), the total dimensionless bulk viscous parameter  $\tilde{\zeta}$  takes the form,

$$\tilde{\zeta} = \frac{1}{2 - \tilde{\zeta}_2} \left[ 2\tilde{\zeta}_0 + (2\tilde{\zeta}_1 - \tilde{\zeta}_2 - \tilde{\zeta}_2\Omega_r) \frac{H}{H_0} \right], \quad (4.22)$$

which will reduce to equation (3.4) for  $\Omega_r = 0$ . The expression for deceleration parameter  $q$  and equation of state parameter  $\omega$  can be obtained by substituting equations (4.21) and (4.22) in equations (2.28) and (2.34) as

$$q = \frac{1}{2 - \tilde{\zeta}_2} \left( 1 - \tilde{\zeta}_1 + \Omega_r - \tilde{\zeta}_0 \left( \frac{H_0}{H} \right) \right), \quad (4.23)$$

$$\omega = \frac{1}{3(2 - \tilde{\zeta}_2)} \left( 2\Omega_r - 2\tilde{\zeta}_1 + \tilde{\zeta}_2 - 2\tilde{\zeta}_0 \left( \frac{H_0}{H} \right) \right), \quad (4.24)$$

which reduces to equations (2.31) and (2.35) for  $\Omega_r = 0$ . In the radiation dominated case (i.e., when  $\Omega_r \rightarrow 1$ , then  $\frac{H_0}{H} \rightarrow 0$ ), the deceleration parameter and the equation of state reduces to,

$$q \sim \frac{2 - \tilde{\zeta}_1}{2 - \tilde{\zeta}_2}, \quad (4.25)$$

$$\omega \sim \frac{2 - 2\tilde{\zeta}_1 + \tilde{\zeta}_2}{3(2 - \tilde{\zeta}_2)}. \quad (4.26)$$

When radiation is the dominant component of the universe, there would be no acceleration in expansion such that  $q > 0$  and  $\omega > -\frac{1}{3}$ . These conditions constrain the bulk viscous parameters as  $\tilde{\zeta}_1 < 2$  and  $\tilde{\zeta}_2 < 2$ . In the extreme limit corresponding to the radiation dominated phase,  $q = 1$  and  $\omega = \frac{1}{3}$  and is corresponding to  $\tilde{\zeta}_1 = \tilde{\zeta}_2$ .

For doing the phase space analysis, we are defining the phase space co-ordinates as

$$\begin{aligned} u &= \Omega_m = \frac{\rho_m}{3H^2}, \\ y &= \Omega_r = \frac{\rho_r}{3H^2}, \\ v &= \frac{1}{\frac{H_0}{H} + 1}. \end{aligned} \quad (4.27)$$

Contrary to the previous discussion, here we take  $\zeta = \zeta_0$  as Case 1,  $\zeta = \zeta_0 + \zeta_1 \frac{\dot{a}}{a}$  as Case 2 and  $\zeta = \zeta_0 + \zeta_1 \frac{\dot{a}}{a} + \zeta_2 \frac{\ddot{a}}{a}$  as Case 3.

**Case 1: with  $\zeta = \zeta_0$**

Using equations (4.19), (4.20) and (4.21), the autonomous equations satisfied by the phase space co-ordinates becomes,

$$\begin{aligned} u' &= \tilde{\zeta}_0(1-u)\left(\frac{1-v}{v}\right) + uy, \\ y' &= \frac{y}{v} \left( \tilde{\zeta}_0(v-1) + v(y-1) \right), \\ v' &= \frac{(1-v)}{2} \left( \tilde{\zeta}_0(1-v) - v(y+3) \right). \end{aligned} \quad (4.28)$$

The Jacobian matrix for this can be obtained from equation (4.37) by setting  $\tilde{\zeta}_1 = \tilde{\zeta}_2 = 0$ . The critical points are,

1.  $(u_c, y_c, v_c) = (0, 1, 1)$

This corresponds to the radiation dominated phase of the universe. The eigen values of the corresponding Jacobian matrix are,

$$\lambda_1 = 1, \quad \lambda_2 = 1, \quad \lambda_3 = 2. \quad (4.29)$$

All the eigen values are positive, indicating an unstable node (past attractor). The equation of state parameter and the deceleration parameter corresponding to this critical point can be obtained by substituting the values of  $u_c$ ,  $y_c$  and  $v_c$  in equations (4.24) and (4.23), respectively, and are found to be  $\omega = \frac{1}{3}$  and  $q = 1$ . These values confirms that the point is the radiation dominated phase of the universe.

2.  $(u_c, y_c, v_c) = (u, 0, 1)$

The eigen values of the corresponding Jacobian matrix are,

$$\lambda_1 = -1, \quad \lambda_2 = 0, \quad \lambda_3 = \frac{3}{2}. \quad (4.30)$$

$(u_c, y_c, v_c)$	$\lambda_1$	$\lambda_2$	$\lambda_3$	Stability	$\omega$	q
$(0, 1, 1)$	1	1	2	Unstable node	$\frac{1}{3}$	1
$(u, 0, 1)$	-1	0	$\frac{3}{2}$	Saddle	0	$\frac{1}{2}$
$(1, 0, \frac{\tilde{\zeta}_0}{\tilde{\zeta}_0+3})$	-4	-3	$-\frac{3}{2}$	Stable node	-1	-1

Table 4.4: Critical points for case 1: with  $\zeta = \zeta_0$

These values shows that the point is a saddle point. The equation of state parameter and deceleration parameter are found to be,  $\omega = 0$  and  $q = \frac{1}{2}$  respectively from equations (4.24) and (4.23), indicating that the universe is matter dominated without accelerating, hence  $u_c \sim 1$ .

3.  $(u_c, y_c, v_c) = (1, 0, \frac{\tilde{\zeta}_0}{\tilde{\zeta}_0+3})$

The eigen values of the corresponding Jacobian matrix are,

$$\lambda_1 = -4, \quad \lambda_2 = -3, \quad \lambda_3 = -\frac{3}{2}. \quad (4.31)$$

The critical point is a stable node, since all the eigen values are negative. From equations (4.24) and (4.23), the equation of state parameter,  $\omega = -1$  and deceleration parameter  $q = -1$ , independent of the value of  $\tilde{\zeta}_0$ . This represent a de Sitter type phase.

Thus this case predicts a universe beginning with a radiation dominated phase (past attractor) and then transit to a decelerated matter dominated phase (saddle point) and then finally evolving to a de Sitter type universe (stable future attractor). Thus it has a close resemblance with the conventional evolution of the universe. The results are summarized in Table 4.4

**Case 2: with**  $\zeta = \zeta_0 + \zeta_1 \frac{\dot{a}}{a}$

In this case the autonomous equations are,

$$\begin{aligned} u' &= \frac{\tilde{\zeta}_0(1-u)}{v} + (1-u)(\tilde{\zeta}_1 - \tilde{\zeta}_0) + uy, \\ y' &= y \left( \frac{\tilde{\zeta}_0(v-1)}{v} + y - 1 - \tilde{\zeta}_1 \right), \\ v' &= \frac{1}{2 - \tilde{\zeta}_2} (1-v) (\tilde{\zeta}_0(1-v) + (\tilde{\zeta}_1 - 3 - y)v). \end{aligned} \quad (4.32)$$

The Jacobian matrix for this autonomous system is given by equation (4.37) provided  $\tilde{\zeta}_2 = 0$ . The critical points are,

1.  $(u_c, y_c, v_c) = (-\tilde{\zeta}_1, \tilde{\zeta}_1 + 1, 1)$

The eigen values of the corresponding Jacobian matrix are,

$$\lambda_1 = \tilde{\zeta}_1 + 1, \quad \lambda_2 = 1, \quad \lambda_3 = 2. \quad (4.33)$$

The point will be unstable node if  $\tilde{\zeta}_1 > -1$ , otherwise it will be a saddle point. The equation of state parameter,  $\omega = \frac{1}{3}$  and deceleration parameter  $q = 1$ , independent of  $\tilde{\zeta}_0$  and  $\tilde{\zeta}_1$ . Hence if  $\tilde{\zeta}_1 = 0$ , the point will indicate an exact radiation dominated universe.

2.  $(u_c, y_c, v_c) = (1, 0, 1)$

This corresponds to a matter dominated initial stage of the universe.

The eigen values of the corresponding Jacobian matrix are,

$$\lambda_1 = -(\tilde{\zeta}_1 + 1), \quad \lambda_2 = -\tilde{\zeta}_1, \quad \lambda_3 = \frac{3 - \tilde{\zeta}_1}{2}. \quad (4.34)$$

The point will be unstable node if  $\tilde{\zeta}_1 < -1$ , a stable one if  $\tilde{\zeta}_1 > 3$  and a saddle point otherwise. For this point, the equation of state,  $\omega = -\frac{\tilde{\zeta}_1}{3}$  and the deceleration parameter  $q = \frac{1 - \tilde{\zeta}_1}{2}$ . If  $\tilde{\zeta}_1 < -1$ , then the values of  $\omega$  and  $q$  will not represent a conventional matter dominated universe. So only if  $\tilde{\zeta}_1 = 0$ , this will represent a conventional matter dominated universe without acceleration.

3.  $(u_c, y_c, v_c) = (1, 0, \frac{\tilde{\zeta}_0}{\tilde{\zeta}_0 - (\tilde{\zeta}_1 - 3)})$

The eigen values are,

$$\lambda_1 = -4, \lambda_2 = -3, \lambda_3 = \frac{1}{2}(\tilde{\zeta}_1 - 3). \quad (4.35)$$

The point will be a stable one if  $\tilde{\zeta}_1 < 3$ , otherwise it will be a saddle point. The equation of state parameter,  $\omega = -1$  and deceleration parameter  $q = -1$ , independent of the values of viscous parameters, representing a de Sitter type universe. So If  $\tilde{\zeta}_1 = 0$ , the point will be represent a stable future attractor with same values of  $\omega$  and  $q$ .

In order to represent a realistic picture, the first critical point must be a unstable (past attractor) radiation dominated phase, the second must be a matter dominated phase without acceleration (saddle point) and the third must corresponds to the stable accelerated phase of the universe. In order to satisfy this,  $\tilde{\zeta}_1$  should be equal to zero. The results of the analysis is given in Table 4.5

**Case 3: with**  $\zeta = \zeta_0 + \zeta_1 \frac{\dot{a}}{a} + \zeta_2 \frac{\ddot{a}}{a}$

In this case the phase space variables satisfy the autonomous equations,

$$\begin{aligned} u' &= \frac{1}{v(2 - \tilde{\zeta}_2)} (2\tilde{\zeta}_0(1 - u)(1 - v) + \\ &\quad v((u - y - 1)\tilde{\zeta}_2 + 2(1 - u)\tilde{\zeta}_1 + 2yu)), \\ y' &= \frac{1}{v(2 - \tilde{\zeta}_2)} 2y (\tilde{\zeta}_0(v - 1) + (y - 1 - \tilde{\zeta}_1 + \tilde{\zeta}_2)v), \\ v' &= \frac{1}{2 - \tilde{\zeta}_2} (1 - v) (\tilde{\zeta}_0(1 - v) + (\tilde{\zeta}_1 + \tilde{\zeta}_2 - 3 - y)v). \end{aligned} \quad (4.36)$$

$(u_c, y_c, v_c)$	$\lambda_1$	$\lambda_2$	$\lambda_3$	Stability	$\omega$	q
$(-\tilde{\zeta}_1, \tilde{\zeta}_1 + 1, 1)$	$\tilde{\zeta}_1 + 1$	1	2	Unstable node if $\tilde{\zeta}_1 > -1$ , otherwise a saddle point	$\frac{1}{3}$	1
$(1, 0, 1)$	$-(\tilde{\zeta}_1 + 1)$	$-\tilde{\zeta}_1$	$\frac{3-\tilde{\zeta}_1}{2}$	Unstable node if $\tilde{\zeta}_1 < -1$ , Stable if $\tilde{\zeta}_1 > 3$ , a saddle point otherwise	$\frac{-\tilde{\zeta}_1}{3}$	$\frac{1-\tilde{\zeta}_1}{2}$
$(1, 0, \frac{\tilde{\zeta}_0}{\tilde{\zeta}_0 - (\tilde{\zeta}_1 - 3)})$	-4	-3	$\frac{1}{2}(\tilde{\zeta}_1 - 3)$	Unstable node if $\tilde{\zeta}_1 < 3$ , otherwise a saddle point	-1	-1

Table 4.5: Critical points for case 2: with  $\zeta = \zeta_0 + \zeta_1 \frac{a}{a}$

$(u_c, y_c, v_c)$	$\lambda_1$	$\lambda_2$	$\lambda_3$	Stability	$\omega$	$q$
$(\tilde{\zeta}_2 - \tilde{\zeta}_1, 1 - (\tilde{\zeta}_2 - \tilde{\zeta}_1), 1)$	$\frac{-2(\tilde{\zeta}_1 - \tilde{\zeta}_2 + 1)}{\tilde{\zeta}_2 - 2}$	1	2	Unstable node if $\tilde{\zeta}_2 < 2$ , Saddle point otherwise	$\frac{1}{3}$	1
$(1, 0, 1)$	$\frac{2(\tilde{\zeta}_1 - \tilde{\zeta}_2 + 1)}{\tilde{\zeta}_2 - 2}$	$\frac{2\tilde{\zeta}_1 - \tilde{\zeta}_2}{\tilde{\zeta}_2 - 2}$	$\frac{\tilde{\zeta}_1 + \tilde{\zeta}_2 - 3}{\tilde{\zeta}_2 - 2}$	Unstable node if (i) $\tilde{\zeta}_2 > 2, \tilde{\zeta}_1 > 1, \tilde{\zeta}_1 - \tilde{\zeta}_2 > -1$ , (ii) $\tilde{\zeta}_2 < 2, \tilde{\zeta}_1 < 1, \tilde{\zeta}_1 - \tilde{\zeta}_2 < -1$	$\frac{-2\tilde{\zeta}_1 + \tilde{\zeta}_2}{3(2 - \tilde{\zeta}_2)}$	$\frac{1 - \tilde{\zeta}_1}{2 - \tilde{\zeta}_2}$ *
$(1, 0, \frac{\tilde{\zeta}_0}{\tilde{\zeta}_0 - (\tilde{\zeta}_1 + \tilde{\zeta}_2 - 3)})$	-4	-3	$-\frac{\tilde{\zeta}_1 + \tilde{\zeta}_2 - 3}{\tilde{\zeta}_2 - 2}$	Stable node if (i) $\tilde{\zeta}_0 > 0, \tilde{\zeta}_2 < 2$ , (ii) $\tilde{\zeta}_0 < 0, \tilde{\zeta}_2 > 2$ , Saddle point otherwise	-1	-1

Table 4.6: Critical points for case 3: with  $\zeta = \zeta_0 + \zeta_1 \frac{\dot{a}}{a} + \zeta_2 \frac{\ddot{a}}{a}$   
 \*When  $\tilde{\zeta}_1 = \tilde{\zeta}_2 = 0$ , the critical point corresponds to  $w = 0, q = \frac{1}{2}$  implying a matter dominated universe without acceleration.

The Jacobian matrix, which we need to calculate the eigen values, for these set of autonomous equation is obtained as,

$$\begin{bmatrix} M_{11} & \left(\frac{\tilde{\zeta}_2 - 2u}{\tilde{\zeta}_2 - 2}\right)_0 & \left(\frac{2\tilde{\zeta}_0(1-u)}{(\tilde{\zeta}_2 - 2)v^2}\right)_0 \\ 0 & M_{22} & \left(\frac{-2\tilde{\zeta}_0 y}{(\tilde{\zeta}_2 - 2)v^2}\right)_0 \\ 0 & \left(\frac{(1-v)v}{\tilde{\zeta}_2 - 2}\right)_0 & M_{33} \end{bmatrix} \quad (4.37)$$

where  $M_{11} = \left(\frac{2\tilde{\zeta}_0(1-v) + (2\tilde{\zeta}_1 - \tilde{\zeta}_2 - 2y)v}{(\tilde{\zeta}_2 - 2)v}\right)_0$ ,  $M_{22} = \left(\frac{2(\tilde{\zeta}_0 - \tilde{\zeta}_0 v + (1 + \tilde{\zeta}_1 - \tilde{\zeta}_2 - 2y)v)}{(\tilde{\zeta}_2 - 2)v}\right)_0$  and  $M_{33} = \left(\frac{2\tilde{\zeta}_0(1-v) + (\tilde{\zeta}_1 + \tilde{\zeta}_2 - 3 - y)(2v-1)}{\tilde{\zeta}_2 - 2}\right)_0$ .

The critical points  $(u_c, y_c, v_c)$  of these equations are

1.  $(u_c, y_c, v_c) = (\tilde{\zeta}_2 - \tilde{\zeta}_1, 1 - (\tilde{\zeta}_2 - \tilde{\zeta}_1), 1)$

For this solution to represent the realistic phase (for example, matter dominated or radiation dominated) of the universe, the bulk viscous parameters should satisfy the condition,  $0 \leq \tilde{\zeta}_2 - \tilde{\zeta}_1 \leq 1$ . The eigen values of the corresponding Jacobin matrix are,

$$\lambda_1 = \frac{-2(\tilde{\zeta}_1 - \tilde{\zeta}_2 + 1)}{\tilde{\zeta}_2 - 2}, \quad \lambda_2 = 1, \quad \lambda_3 = 2. \quad (4.38)$$

The point will be unstable if  $\tilde{\zeta}_2 - 2 < 0$  and a saddle point otherwise. The equation of state parameter and deceleration parameter corresponding to this critical point are,  $\omega = \frac{1}{3}$  and  $q = 1$ .

2.  $(u_c, y_c, v_c) = (1, 0, 1)$

This point corresponds to a matter dominated phase of the universe. The eigen values of the corresponding jacobian matrix are,

$$\lambda_1 = \frac{2(\tilde{\zeta}_1 - \tilde{\zeta}_2 + 1)}{\tilde{\zeta}_2 - 2}, \lambda_2 = \frac{2\tilde{\zeta}_1 - \tilde{\zeta}_2}{\tilde{\zeta}_2 - 2}, \lambda_3 = \frac{\tilde{\zeta}_1 + \tilde{\zeta}_2 - 3}{\tilde{\zeta}_2 - 2}. \quad (4.39)$$

This critical point will be unstable if (i)  $\tilde{\zeta}_2 > 2, \tilde{\zeta}_1 > 1, \tilde{\zeta}_1 - \tilde{\zeta}_2 > -1$  or if (ii)  $\tilde{\zeta}_2 < 2, \tilde{\zeta}_1 < 1, \tilde{\zeta}_1 - \tilde{\zeta}_2 < -1$ . The equation of state parameter

and the deceleration parameter corresponding to this critical point are,  $\omega = \frac{2\tilde{\zeta}_1 - \tilde{\zeta}_2}{3(\tilde{\zeta}_2 - 2)}$  and  $q = \frac{\tilde{\zeta}_1 - 1}{\tilde{\zeta}_2 - 2}$ .

3.  $(u_c, y_c, v_c) = (1, 0, \frac{\tilde{\zeta}_0}{\tilde{\zeta}_0 - (\tilde{\zeta}_1 + \tilde{\zeta}_2 - 3)})$

This also represents a matter dominated universe with  $\frac{H_0}{H} = \frac{3 - (\tilde{\zeta}_1 + \tilde{\zeta}_2)}{\tilde{\zeta}_0}$ .

The eigen values of the Jacobian matrix are,

$$\lambda_1 = -4, \quad \lambda_2 = -3, \quad \lambda_3 = -\frac{\tilde{\zeta}_1 + \tilde{\zeta}_2 - 3}{\tilde{\zeta}_2 - 2}. \quad (4.40)$$

The relation  $\frac{H_0}{H} = \frac{3 - (\tilde{\zeta}_1 + \tilde{\zeta}_2)}{\tilde{\zeta}_0} > 0$  holds if  $\tilde{\zeta}_0 > 0$  and  $\tilde{\zeta}_1 + \tilde{\zeta}_2 < 3$  or if  $\tilde{\zeta}_0 < 0$  and  $\tilde{\zeta}_1 + \tilde{\zeta}_2 > 3$ . Applying this condition to the eigen value  $\lambda_3$  we find that this critical point will be stable (or future attractor) if (i)  $\tilde{\zeta}_2 < 2$  for  $\tilde{\zeta}_0 > 0$  or if (ii)  $\tilde{\zeta}_2 > 2$  for  $\tilde{\zeta}_0 < 0$ . It is a saddle point otherwise. The equation of state parameter,  $\omega = -1$  and deceleration parameter  $q = -1$  implies a de sitter like universe.

The above critical points would represent the realistic evolution of the universe, if, successively, the first critical point is a radiation dominated one, the second one is a matter dominated phase without acceleration and the last one be a matter dominated phase with acceleration. For this, first of all the values of the viscous coefficients must be such that  $\tilde{\zeta}_1 \sim \tilde{\zeta}_2$ . Under this conditions the critical points becomes

1.  $(u_c, y_c, v_c) = (0, 1, 1)$ , corresponding to radiation dominated phase with  $\omega = \frac{1}{3}$  and  $q = 1$
2.  $(u_c, y_c, v_c) = (1, 0, 1)$ , corresponding to matter dominated phase with  $\omega = \frac{\tilde{\zeta}_2 - 1}{3(\tilde{\zeta}_2 - 2)}$  and  $q = \frac{\tilde{\zeta}_2 - 1}{\tilde{\zeta}_2 - 2}$
3.  $(u_c, y_c, v_c) = (1, 0, \frac{\tilde{\zeta}_0}{\tilde{\zeta}_0 - (2\tilde{\zeta}_2 - 3)})$ , corresponding to accelerating phase with  $\omega = -1$  and  $q = -1$ .

Then by analyzing the eigen values, it is found that the first critical point will be a past attractor if  $\tilde{\zeta}_2 < 2$ . Under this condition, the second critical point, corresponding to the matter dominated phase, will be a saddle point. The third critical point, corresponding to the accelerated phase, will be a stable one if  $\tilde{\zeta}_2 < \frac{3}{2}$ . However, under this condition, there is a chance for  $\omega$  and  $q$  to become negative in the case of matter dominated phase corresponding to second set of critical points. This doesn't represent a conventional matter dominated phase of the universe. For this critical point to represent a matter dominated phase without acceleration, it requires  $\omega = 0$  and  $q = \frac{1}{2}$ . This is possible only if  $\tilde{\zeta}_1 \simeq \tilde{\zeta}_2 = 0$ . Due to this conditions, the nature of the first and the last critical points will not be affected. i.e., the first critical point will be a radiation dominated past attractor, the second one will be an unaccelerated matter dominated saddle point and the third will be a stable node corresponding to a de Sitter phase. Thus it predicts a universe starting from a radiation dominated era and then entering a decelerated matter dominated phase and then finally evolving to the de Sitter universe. Thus we see that unless  $\tilde{\zeta}_1 = \tilde{\zeta}_2 = 0$ , the model doesn't predict a prior radiation dominated phase and a decelerated matter dominated phase of the universe. The results are summarized in Table 4.6

### **4.3 Estimate of the bulk viscosity $\zeta = \zeta_0$ of the cosmic fluid**

From the above analysis we have concluded that bulk viscous models will predict all the conventional phases of the universe when viscous coefficient  $\zeta = \zeta_0$ , a constant. In the previous chapter we have also seen that for a universe with such a constant bulk viscosity there arise no problem regarding the validation of local second law of thermodynamics and also

with the entropy maximization condition. The model nicely predicts the evolution of universe with prior decelerated epoch and a late accelerated epoch, evolving towards a state of thermal equilibrium. In this light it is important to know the magnitude of the viscous coefficient  $\zeta_0$ .

We have extracted the value of the dimensional viscous parameter  $\tilde{\zeta}_0$  by constraining the model with the Supernovae observational data, as  $\tilde{\zeta}_0 = 1.92$  corresponding to the present day Hubble parameter value,  $H_0 = 69.61$ . In conventional notation this estimation can be expressed as,

$$\tilde{\zeta}_0 = \frac{24\pi G}{c^2} \frac{\zeta_0}{H_0} = 1.92 \quad (4.41)$$

which implies a value in standard unit as,

$$\zeta_0 \sim 7 \times 10^7 \text{Pa. s.} \quad (4.42)$$

This value is in agreement with the value obtained by Velten and Schwarz [133] and by Brevik [134] Many have also attempted recently to obtain the value of this coefficient [135].

Wang and Meng in reference [136] have studied a bulk viscous model of the late accelerating universe and by using the Hubble parameter data for various redshift, obtained a some what less value for the constant viscosity as  $\zeta_0 \sim 10^5 \text{Pa. s.}$  But owing to the comparatively large uncertainties in the observation of the Hubble parameter, this can only be taken as a lower limit to the value of  $\zeta_0$ . Brevik et al. have analyzed a same model and found a value around  $\zeta_0 \sim 10^6$ [137].

In reference [59], the authors have studied the background evolution and also the evolution of cosmological parameters for the bulk viscous model with constant bulk viscosity. It also predicts an age of universe of around 14.95 Gyr, which is in agreement with the constraint from the oldest globular clusters. In this work the authors are also supporting a value around  $\zeta \sim 10^7$ . Having considered all these we suggest for the

universe a constant viscosity within the range,

$$5 \times 10^5 \text{Pa. s.} < \zeta_0 < 7 \times 10^7 \text{Pa. s.} \quad (4.43)$$

However in [138], the authors have suggested the  $\zeta_0$  in the range  $10^4 \text{Pa. s.} < \zeta_0 < 10^7 \text{Pa. s.}$ , which is in almost agreement with ours. In fact  $10^7$  is high value for the viscosity compared to any ordinary macroscopic system. For instance this range is many orders of magnitude higher than the viscosity of ordinary water at atmospheric pressure and room temperature. But universe, such a vast system, the viscosity associated with the dark matter is not so comparable with an ordinary macroscopic system.

## Appendix

### Statefinder parameter diagnostic for $\zeta = \zeta_0$ (comparison with $\Lambda$ CDM model)

For comparison we have make use of the statefinder parameter diagnostic introduced by Sahni et al [132]. The statefinder parameters  $\{r, s\}$  are defined as,

$$r = \frac{\ddot{a}}{aH^3}, \quad s = \frac{r - 1}{3\left(q - \frac{1}{2}\right)}. \quad (4.44)$$

In terms of  $h = \frac{H}{H_0}$ ,  $r$  and  $s$  can be written as

$$r = \frac{1}{2h^2} \frac{d^2 h^2}{dx^2} + \frac{3}{2h^2} \frac{dh^2}{dx} + 1, \quad (4.45)$$

$$s = -\frac{\frac{1}{2h^2} \frac{d^2 h^2}{dx^2} + \frac{3}{2h^2} \frac{dh^2}{dx}}{\frac{3}{2h^2} \frac{dh^2}{dx} + \frac{9}{2}}. \quad (4.46)$$

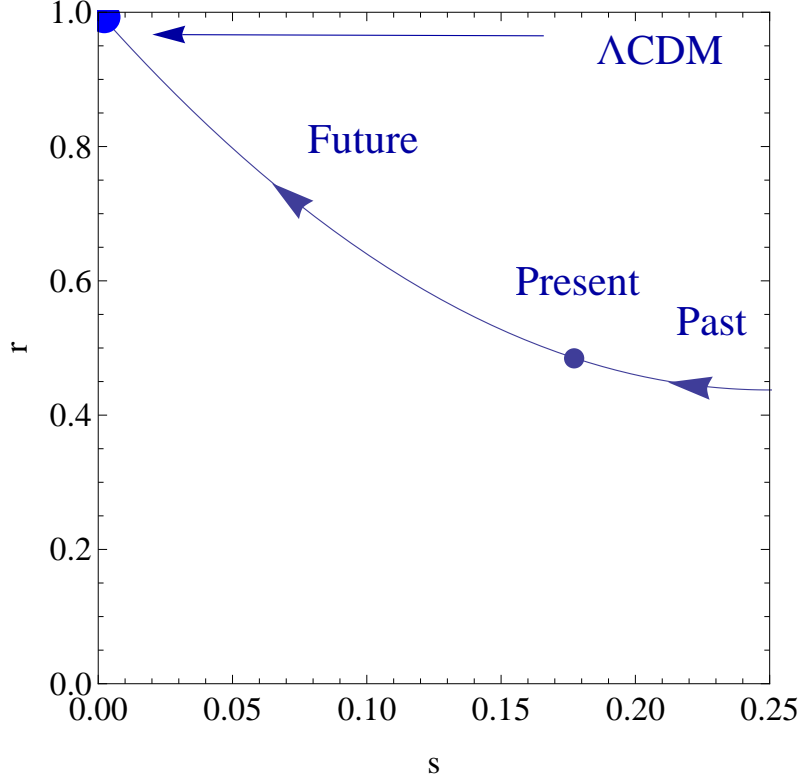


Figure 4.4: The evolution of the model in the  $r$ - $s$  plane for the best estimates of the parameter  $\tilde{\zeta}_0$

Using the expression for  $h$  from equation (3.23) for  $\zeta = \zeta_0$ , these parameters become,

$$r = \frac{3(\tilde{\zeta}_0 - 3)}{4h^2} a^{-\frac{3}{2}} \left( \frac{\tilde{\zeta}_0}{3} - 2h \right) + \frac{3(\tilde{\zeta}_0 - 3)}{2h} a^{-\frac{3}{2}} + 1, \quad (4.47)$$

$$s = - \frac{\frac{3(\tilde{\zeta}_0 - 3)}{4h^2} a^{-\frac{3}{2}} \left( \frac{\tilde{\zeta}_0}{3} - 2h \right) + \frac{3(\tilde{\zeta}_0 - 3)}{2h} a^{-\frac{3}{2}}}{\frac{3(\tilde{\zeta}_0 - 3)}{2h} a^{-\frac{3}{2}} + \frac{9}{2}}. \quad (4.48)$$

The  $\{r, s\}$  plane trajectory of the model with  $\zeta = \zeta_0$  is shown in figure 4.4.

The plot lie in the region  $r < 1, s > 0$ , which is the general behavior of any quintessence model.

# 5

## Bayesian analysis of bulk viscous matter dominated universe

*In this chapter we perform the Bayesian analysis of the model in order to obtain the strength of the model in predicting the given Supernova data when compared with the  $\Lambda$ CDM model.*

### 5.1 Bayesian model comparison

Various models have been proposed to interpret the cosmological observational data which eventually add to our understanding of the evolution of the universe. So there exist, in fact many models explaining the expected evolution of the universe. Contrasting these models among themselves to select the better ones is essential for understanding the true evolution of the universe. Bayesian statistical approach[140–142] is an effective tool to compare the new models with the standard  $\Lambda$ CDM model and also among themselves. The basic approach of this method is originated from the theory of random variables. In general, the relative merit of a random variable can be obtained by calculating the basic probability of it among the ensemble of values obtained theoretically or through repeated obser-

vations. But in cosmology repeated observations are virtually impossible. Here, what one can often do is to form hypothesis or a theory. For making the decision regarding the viability of such a proposed theory one have to assign certain probability to it in contrast to other theories existing for the same purpose. It is in this stage the Bayesian theory help us, so as to assign probability for a certain hypothesis by considering the observational data already available to us. Due to the acquisition of more data, one can in fact adjust the plausibility of the hypothesis using Bayesian theorem. This method have been adopted by many in the past, for instance, Jaffe [143] and Hobson et al. [144] have analysed the relative merits of certain cosmological models. Also John and Narlikar[140] have compared a simple cosmological model with scale factor  $a(t) \propto t$  with standard and inflationary models of the universe. In many models one does not have a prior knowledge about the model parameters for assigning the corresponding probability and in such cases one often starts with a flat prior for the parameter.

According to Bayes's theorem[145], the posterior probability  $p(H_i|D, I)$  of a hypothesis  $H_i$ , given the data  $D$  and assuming any other background information  $I$  to be true, is given as,

$$p(H_i|D, I) = \frac{p(H_i|I)p(D|H_i, I)}{p(D|I)}, \quad (5.1)$$

where  $p(H_i|I)$  is the prior probability, i.e., the probability of  $H_i$  given  $I$  is true and  $p(D|H_i, I)$  is the likelihood for the hypothesis  $H_i$ , which is the probability for obtaining the data  $D$  provided the hypothesis  $H_i$  and  $I$  are true. The factor  $p(D|I)$  helps in normalization.

In Bayesian model comparison, we take the ratios between the posterior probabilities for different models. Let  $M_i$  and  $M_j$  be the two models which we need to compare, then using Bayes theorem the ratio between their

posterior probability  $O_{ij}$  can be written as,

$$O_{ij} = \frac{p(M_i|D, I)}{p(M_j|D, I)} = \frac{p(M_i|I)p(D|M_i, I)}{p(M_j|I)p(D|M_j, I)}. \quad (5.2)$$

Since  $p(D|M_i, I)$  for the data  $D$  is the likelihood for the model  $M_i$ , we re-notate it with  $L(M_i)$ , then the equation (5.2) becomes,

$$O_{ij} = \frac{p(M_i|I)L(M_i)}{p(M_j|I)L(M_j)}. \quad (5.3)$$

If the background information  $I$  does not give any preference to a model over any other, then the prior probabilities becomes equal, so that,

$$O_{ij} = \frac{L(M_i)}{L(M_j)} \equiv B_{ij} \quad (5.4)$$

where  $B_{ij}$  is called the Bayes factor and is thus the ratio of the likelihood of the two models. This factor helps to compare two models with reference to their power in predicting the given data, hence it can be taken as a summary of the evidence provided by the data in favor of one model over the other [146].  $B_{ij}$  less than unity indicates that there is no evidence against the model  $M_j$  when compared with the model  $M_i$  i.e.,  $M_j$  is more strongly supported by the data than  $M_i$ . If  $1 < B_{ij} < 3$ , then the model  $M_i$  is not worth more than a bare mention. If  $3 < B_{ij} < 20$ , the strength of evidence of the model  $M_i$  is positive. If  $20 < B_{ij} < 150$ , the evidence is strong and if  $B_{ij} > 150$ , it is very strong [141].

For a model having one or more free parameters such as  $\alpha, \beta, \dots$  etc, it's likelihood  $L(M_i)$  can be evaluated as

$$L(M_i) = \int d\alpha \int d\beta \dots p(\alpha, \beta, \dots | M_i) L_i(\alpha, \beta, \dots), \quad (5.5)$$

where  $p(\alpha, \beta, \dots | M_i)$  is the prior probability for the set of parameter values  $\alpha, \beta, \dots$  for the model  $M_i$  to be true and  $L_i(\alpha, \beta, \dots)$  is the likelihood for

## 98 Bayesian analysis of bulk viscous matter dominated universe

the combination of the parameters in the model and is usually taken as [141],

$$L_i(\alpha, \beta, \dots) = \exp[-\chi_i^2(\alpha, \beta, \dots)/2] \quad (5.6)$$

where  $\chi_i^2(\alpha, \beta, \dots)$  is the conventional  $\chi^2$ -function. If we assume that the model  $M_i$  has two parameters  $\alpha$  and  $\beta$  having flat prior probabilities in some range,  $[\alpha, \alpha + \Delta\alpha]$  and  $[\beta, \beta + \Delta\beta]$ , respectively, then the flat prior probabilities  $p(\alpha|M_i)$  and  $P(\beta|M_i)$  can be obtained as follows. Plot  $\exp[-\chi_i^2(\alpha, \beta, \dots)/2]$  with  $\alpha$  varying around its value around the one corresponding to the  $\chi_{min}^2$  by taking  $\beta$  as a constant equal to its value corresponding to the  $\chi_{min}^2$ . The width of this Gaussian curve can be taken as  $\Delta\alpha$ . The flat prior probability can then be,  $P(\alpha, M_i) = 1/\Delta\alpha$ . A similar procedure can be adopted to evaluate the prior probability  $P(\beta, M_i)$ . The marginal likelihood of the parameter  $\alpha$  can be obtained as,

$$L_i(\alpha) = \frac{1}{\Delta\beta} \int_{\beta}^{\beta+\Delta\beta} d\beta \exp[-\chi^2(\alpha, \beta)/2]. \quad (5.7)$$

Marginal likelihood of the parameter  $\beta$  can be calculated by adopting the same procedure. This can be extended with the number of parameters. For instance, if we have three parameters,  $\alpha, \beta, \gamma$ , then the marginal likelihood of a parameter, say,  $\alpha$ , can be evaluated as,

$$L_i(\alpha) = \frac{1}{\Delta\gamma} \frac{1}{\Delta\beta} \int_{\gamma}^{\gamma+\Delta\gamma} d\gamma \int_{\beta}^{\beta+\Delta\beta} d\beta \exp[-\chi^2(\alpha, \beta, \gamma)/2]. \quad (5.8)$$

The physical meaning of this marginalized likelihood is that they are the probability of the data given the model type and the parameter, not assuming any particular values for other model parameters. They may find significant use in Bayesian model comparison during a future analysis of the data, by acting as prior probabilities for the respective parameters.

Likelihood of the model is then given as,

$$L(M_i) = \frac{1}{\Delta\alpha} \int_{\alpha}^{\alpha+\Delta\alpha} d\alpha L_i(\alpha). \quad (5.9)$$

## 5.2 Bayesian analysis of bulk viscous models

A fairly detailed description of the method of Bayesian analysis was given in the previous section. In this section we are going into the Bayesian analysis of the different bulk viscous models. For this we consider the following cases for the bulk viscous coefficient separately,

1.  $\zeta = \zeta_0 + \zeta_1 \frac{\dot{a}}{a} + \zeta_2 \frac{\ddot{a}}{a}$ ,  
where viscosity is depending on both the velocity and acceleration of the expansion of the universe.
2.  $\zeta = \zeta_0 + \zeta_1 \frac{\dot{a}}{a}$ ,  
where viscosity is depending only on velocity of the expansion of the universe apart from a constant additive part  $\zeta_0$ . This is equivalent to  $\zeta = \zeta_0 + \zeta_1 \rho^s$ , with  $s = 1/2$ .
3.  $\zeta = \zeta_0$ ,  
where viscosity is pure a constant
4.  $\zeta = \zeta_1 \frac{\dot{a}}{a}$ .  
where viscosity only has the velocity dependent term and is equivalent to  $\zeta = \zeta_1 \rho^s$ , with  $s = 1/2$ .
5.  $\zeta = \zeta_0 + \zeta_2 \frac{\ddot{a}}{a}$   
where viscosity is depending on acceleration apart from an additive constant.

The best estimated values of the parameters  $(\tilde{\zeta}_0, \tilde{\zeta}_1, \tilde{\zeta}_2)$  corresponding to the cases 1, 2 and 3 are already extracted in the Tables 2.1 and 3.1 and that for the cases 4 and 5 are extracted using the same set of data and are given in the Table 5.1. The data used is the SCP “Union” Type Ia

## 100 Bayesian analysis of bulk viscous matter dominated universe

---

Parameters	Bulk viscous models	
	$\zeta = \zeta_1 \frac{\dot{a}}{a}$	$\zeta = \zeta_0 + \zeta_2 \frac{\ddot{a}}{a}$
$\tilde{\zeta}_0$	–	1.275
$\tilde{\zeta}_1$	1.683	–
$\tilde{\zeta}_2$	–	1.593
$H_0$	69.21	70.50
$\chi_{min}^2$	319.31	310.54
$\chi_{d.o.f}^2$	1.04	1.02

Table 5.1: Best estimates of the bulk viscous parameters,  $H_0$  and also  $\chi^2$  minimum value corresponding to the cases 4 and 5 of  $\zeta$ .  $\chi_{d.o.f}^2 = \frac{\chi_{min}^2}{n-m}$ , where  $n = 307$ , the number of data and  $m$  is the number of parameters in the model. The subscript d.o.f stands for degrees of freedom. For the best estimation we have used SCP “Union” 307 SNe Ia data sets.

Supernova data [91] composed of 307 data points from 13 independent data sets and the method used is  $\chi^2$  minimization technique (same as that described in chapter 2). In comparison with the parameters extracted in Table 1 of reference [68], where the authors include non-viscous baryonic matter also, our parameter values are slightly different. For instance, in case 5, with  $\zeta = \zeta_0 + \zeta_2 \frac{\ddot{a}}{a}$ , the value of  $\tilde{\zeta}_0$  and  $\tilde{\zeta}_2$  are 1.275 and 1.593 respectively in our model. While in their case it is 1.59 and 0.05 respectively. In spite of this, there is no change in the general conclusion, that the full viscous model doesn't predicts a conventional evolution of the universe (except, when  $\zeta = \zeta_0$ , a constant). The  $\chi^2$  function is constructed using equation (2.25). After obtaining the  $\chi^2$ , we evaluate the marginal likelihood, using equation (5.8), and likelihood, using equation (5.9), for all the five cases of the model. We kept  $\Lambda$ CDM model as the reference model in order to compare the bulk viscous models and calculate the Bayes factor using equation (5.4). The marginal likelihood of the parameters  $\tilde{\zeta}$  corresponding to the five cases of bulk viscous models are shown in figures 5.1,

5.2, 5.3, 5.4 and 5.5, respectively.

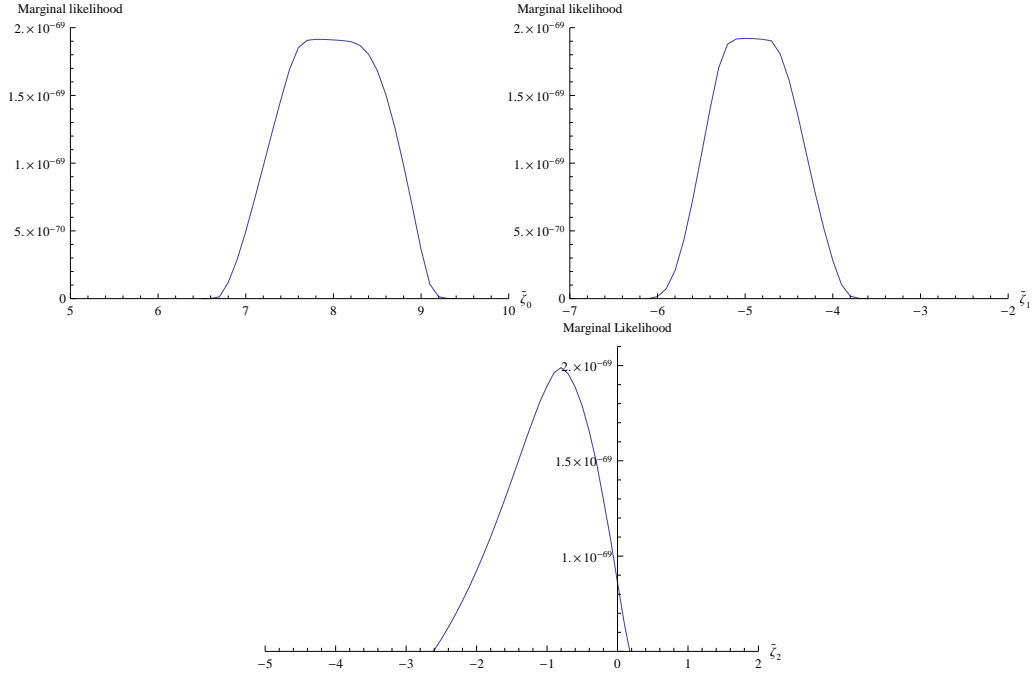


Figure 5.1: Marginal Likelihood of the parameters  $\tilde{\zeta}_0$ ,  $\tilde{\zeta}_1$  and  $\tilde{\zeta}_2$  corresponding to the case 1, when  $\zeta = \zeta_0 + \zeta_1 \frac{\dot{a}}{a} + \zeta_2 \frac{\ddot{a}}{a}$ .

We consider three different priors for the parameters  $\tilde{\zeta}_0$ ,  $\tilde{\zeta}_1$ ,  $\tilde{\zeta}_2$ . The prior probability is chosen by considering the width of the Gaussian curve by varying the corresponding parameter and fixing all others. However due to largeness of the data, there may occur slight discrepancy with the Gaussian curve. Hence we consider three ranges of width in the Gaussian curve, there by obtained three prior values of a parameter. In the present study we find the likelihood range corresponding to three values of  $\exp(-\chi^2(\zeta_0, \zeta_2, \zeta_3)/2)$ . For prior I, corresponds to the range of  $\tilde{\zeta}$ 's for likelihood of about  $1 \times 10^{-70}$ , prior II corresponds to the range of  $\tilde{\zeta}$ 's for likelihood of about  $1 \times 10^{-80}$  and prior III corresponds to the range of  $\tilde{\zeta}$ 's for likelihood of about  $1 \times 10^{-90}$ . Following this we obtained the marginal

## 102 Bayesian analysis of bulk viscous matter dominated universe

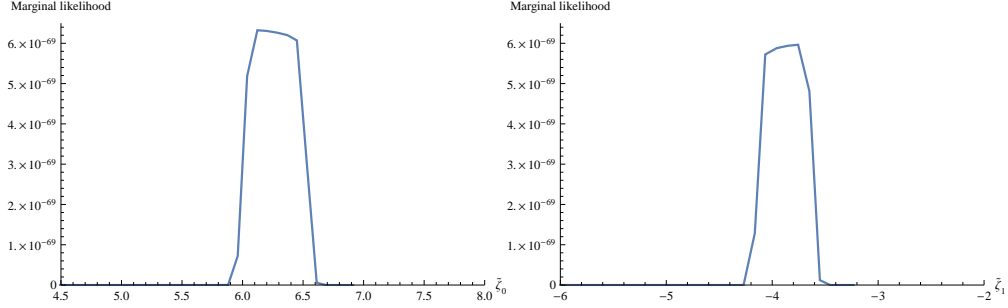


Figure 5.2: Marginal Likelihood of the parameters  $\tilde{\zeta}_0$  and  $\tilde{\zeta}_1$  corresponding to the case 2, when  $\zeta = \zeta_0 + \zeta_1 \frac{\dot{a}}{a}$ .

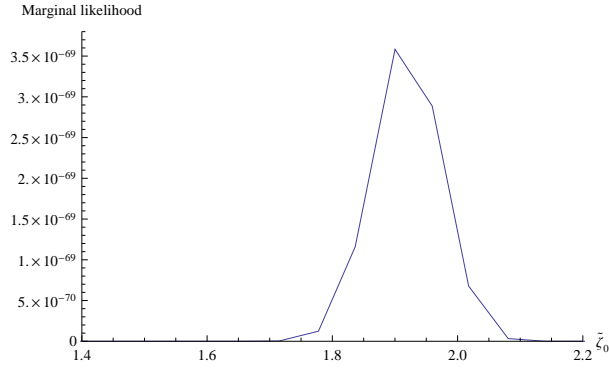


Figure 5.3: Marginal Likelihood of the parameter  $\tilde{\zeta}_0$  corresponding to the case 3, when  $\zeta = \zeta_0$ , a constant.

likelihood of the respective parameters and the respective plots are shown in the figures. The final likelihood of the viscous model was obtained by the procedure discussed previously.

The above procedure was then done for the standard  $\Lambda$ CDM model by considering  $\Omega_m$  and  $\Omega_\Lambda$  as the parameters. In this calculation we took the same three prior ranges for obtaining the marginal likelihood and then the likelihood of the  $\Lambda$ CDM model was obtained.

The likelihood of the viscous model and the standard  $\Lambda$ CDM model are then compared to obtain the Bayes factor for the three different priors. The results are shown in Table 5.2. Usually, the prior probabilities for

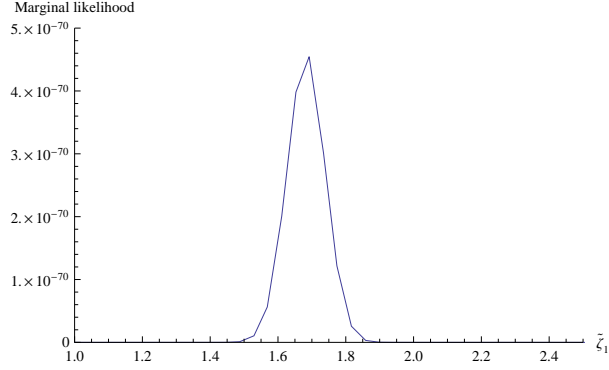


Figure 5.4: Marginal Likelihood of the parameter  $\tilde{\zeta}_1$  corresponding to the case 4, when  $\zeta = \zeta_1 \frac{\dot{a}}{a}$ , a constant.

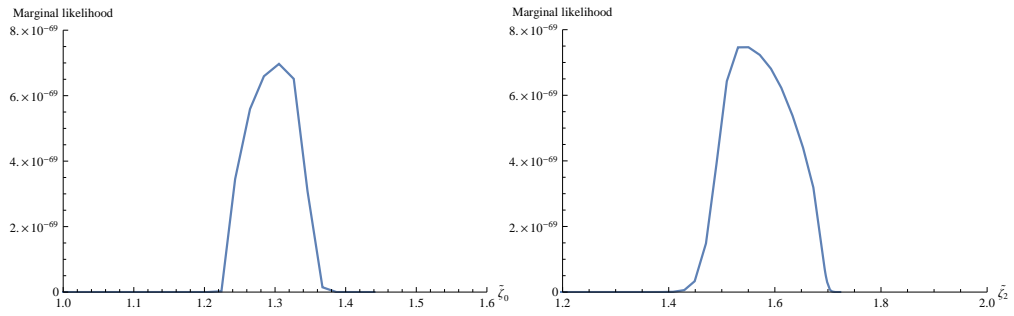


Figure 5.5: Marginal Likelihood of the parameters  $\tilde{\zeta}_0$  and  $\tilde{\zeta}_2$  corresponding to the case 5, when  $\zeta = \zeta_0 + \zeta_2 \frac{\ddot{a}}{a}$ .

the parameters in a model are chosen as the posteriors obtained in the previous measurement/analysis in the same model and this fact is pivotal to the implementation of Bayesian model comparison. But in the first attempt of analyzing a data, it is evident that the parameter's prior we choose crucially affects the result. Such a situation appears in the present case of Bayesian comparison of bulk viscous models. We have used flat prior probabilities for well-known parameters such as matter density, dark energy density, etc., in standard cosmology, but for the parameters in bulk viscous models, the ranges for the flat priors are guessed from the data itself and this is strongly subjective.

## 104 Bayesian analysis of bulk viscous matter dominated universe

Cases	Bulk viscous models $M_i$	Bayes factor $B_{i\Lambda} = \frac{L(M_i)}{L(M_\Lambda)}$		
		Prior I	Prior II	Prior III
1	$\zeta_0 + \zeta_1 \frac{\dot{a}}{a} + \zeta_2 \frac{\ddot{a}}{a}$	0.743	1.372	1.043
2	$\zeta_0 + \zeta_1 \frac{\dot{a}}{a}$	1.86	2.63	3.63
3	$\zeta_0$	0.27	0.32	0.42
4	$\zeta_1 \frac{\dot{a}}{a}$	0.05	0.042	0.052
5	$\zeta_0 + \zeta_2 \frac{\ddot{a}}{a}$	1.65	1.91	1.77

Table 5.2: Bayes factors with respect to  $\Lambda$ CDM model corresponding to three different priors

It can be seen from the Table 5.2 that for the first two cases the Bayes factor depends on the prior, while for the remaining three case such strong dependence on the priors are not evident. For case 2, i.e., when  $\zeta = \zeta_0 + \zeta_1 \frac{\dot{a}}{a}$ , there is an increase in Bayes factor with prior and it exceeds 3, giving more evidence for its increasing strength. The important thing to be noted here is about the value of the Bayes factor for the respective model. For the cases  $\zeta = \zeta_0$  and  $\zeta = \zeta_1 \frac{\dot{a}}{a}$ , the factor is much less than one. While for other cases the values are above one. As per the standard classification, it can be mentioned that, the models for which the Bayes factor is in between 1 and 3, can have only a very feeble advantage over the standard  $\Lambda$ CDM model, however is not worth more than a bare mention.

The SNe Ia data that we have used contains the magnitude of supernovae in the red-shift range  $0.015 < z < 1.55$ . The data predicts a transition from an early decelerated epoch to the late acceleration at a redshift of around  $z \sim 0.5$ . Among the full data set, the low redshift data within the range  $0.015 < z < 0.5$  is often used for deducing the current value of the Hubble parameter. The high redshift data, which were obtained with small interference with the background and with high accuracy, are considered to be the best part of the data [147]. For a critical

Viscous models	$\tilde{\zeta}_0$	$\tilde{\zeta}_1$	$\tilde{\zeta}_2$	$H_0$	$\chi_{min}^2$	$\chi_{d.o.f}^2$
$\zeta_0 + \zeta_1 \frac{\dot{a}}{a} + \zeta_2 \frac{\ddot{a}}{a}$	7.36	-4.73	-1.25	67.41	166.88	1.135
$\zeta_0 + \zeta_1 \frac{\dot{a}}{a}$	4.53	-2.53	–	67.41	166.88	1.13
$\zeta_0$	1.17	–	–	63.06	167.01	1.12
$\zeta_1 \frac{\dot{a}}{a}$	–	0.787	–	61.43	167.09	1.12
$\zeta_0 + \zeta_2 \frac{\ddot{a}}{a}$	1.28	–	1.43	67.41	166.88	1.13

Table 5.3: Best estimates of the bulk viscous parameters,  $H_0$  and also  $\chi^2$  minimum value corresponding to the different cases of  $\zeta$  for high redshift.  $\chi_{d.o.f}^2 = \frac{\chi_{min}^2}{n-m}$ , where  $n = 150$ , the number of data and  $m$  is the number of parameters in the model. The subscript d.o.f stands for degrees of freedom.

Sl. No.	Bulk viscous models $M_i$	Bayes factor $B_{i\Lambda} = \frac{L(M_i)}{L(M_\Lambda)}$	
		Prior I	Prior II
1	$\zeta_0 + \zeta_1 \frac{\dot{a}}{a} + \zeta_2 \frac{\ddot{a}}{a}$	0.79	0.06
2	$\zeta_0 + \zeta_1 \frac{\dot{a}}{a}$	1.044	1.4
3	$\zeta_0$	1.17	1.48
4	$\zeta_1 \frac{\dot{a}}{a}$	1.13	1.42
5	$\zeta_0 + \zeta_2 \frac{\ddot{a}}{a}$	0.733	0.2685

Table 5.4: Bayes factors with respect to  $\Lambda$ CDM model corresponding to two different priors for high redshift.

analysis we have repeated our computation using the high redshift part of the data, corresponding to the red shift range,  $0.5 < z < 1.55$ . For this range, we have extracted the values of the parameters,  $\tilde{\zeta}$ 's corresponding to the above 5 cases using the  $\chi^2$  minimization technique. The results are tabulated in Table 5.3.

The Bayes factor of the bulk viscous models corresponding to the five cases for high redshift data are tabulated in the Table 5.4. Here prior I corresponds to the range of  $\tilde{\zeta}$ 's for likelihood of about  $1 \times 10^{-38}$  and prior II corresponds to the range of  $\tilde{\zeta}$ 's for likelihood of about  $1 \times 10^{-45}$ . The

## 106 Bayesian analysis of bulk viscous matter dominated universe

models corresponding to the cases 1 and 5, where the viscous coefficient depends on the acceleration of the expansion, have Bayes factor less than one for both the priors. As a result these two cases are not worth of any mention against the standard model. This indicates that the dependence of viscosity on the acceleration is not so sensitive. Riess et. al. have found that the magnitude of acceleration is small, since the distance of the high redshift supernovae were on average only 10% – 15% farther than expected in a universe with mass density parameter  $\Omega_m \sim 0.3$ . Such a small acceleration would not have any observable effect on the transport coefficients like that of viscosity. For cases 2, 3 and 4, the Bayes factors are larger than one and it increases slightly with prior. Among these, the third case is of constant viscosity, while for second and fourth cases, the viscous coefficient depends on the velocity of expansion of the universe. As seen from the Table 5.4, the Bayes factors for the cases 2, 3 and 4 are all in the range  $1 < B_{ij} < 3$  and it seems quite difficult to discriminate between them. All these three cases are thus qualified to have bare mention against the  $\Lambda$ CDM model.

# 6

## Bulk viscous matter with cosmological constant

*In this chapter we analyze the viscous model of the universe by including cosmological constant as an additional cosmic component.*

In the preceding chapters we have seen that the bulk viscosity associated with matter can generate the recent acceleration of the universe. The model can predict the conventional evolution, including the radiation dominated epoch, when viscosity coefficient is a constant. However this model too have some problems, among which the prominent one is regarding the prediction of the age of the universe. Meantime the presence of a non-zero cosmological constant cannot be ruled out in verge of the current observational data. Hence it is worth to explore this model in the presence of cosmological constant. In this chapter we consider a universe with cosmological constant having viscous matter ( denoted as  $\Lambda$ vCDM model) [148].

### 6.1 $\Lambda$ vCDM model

We consider a spatially flat universe which follows FLRW metric (equation (2.1)). We assume that universe consists of viscous matter (both dark and

baryonic) and a cosmological constant, which act as the conventional dark energy. We neglect the radiation component since we are dealing with the late time evolution of the universe at which the effect of radiation component is negligibly small. Here also we consider the simplest mechanism for the bulk viscous pressure in accordance with the Eckart formalism [69, 71] and is given by equation (2.2), where we assume the normal pressure  $P$  as zero for the whole matter component of the universe (both dark and baryonic) as it is non-relativistic and  $\zeta$  is the coefficient of bulk viscosity. So the effective pressure is due to the bulk viscosity alone. The coefficient  $\zeta$  is basically a transport coefficient, hence it would depend on the dynamics of the cosmic fluid. As in the previous chapters we assume

$$\zeta = \zeta_0 + \zeta_1 \frac{\dot{a}}{a} + \zeta_2 \frac{\ddot{a}}{\dot{a}}. \quad (6.1)$$

The Friedmann equations governing the bulk viscous universe with cosmological constant are given as,

$$H^2 = \frac{\rho_m + \rho_\Lambda}{3}, \quad (6.2)$$

$$2\frac{\ddot{a}}{a} + \left(\frac{\dot{a}}{a}\right)^2 = \rho_\Lambda - P^*. \quad (6.3)$$

where we have taken  $8\pi G = 1$ .  $\rho_m$  and  $\rho_\Lambda = \frac{\Lambda}{8\pi G}$  are the densities of matter and cosmological constant  $\Lambda$  respectively and overdot represents the derivative with respect to cosmic time  $t$ . We consider separate conservation equations for matter and dark energy due to the absence of any interaction as the density of cosmological constant is constant through out and the equations are as given below,

$$\dot{\rho}_m + 3H(\rho_m + P^*) = 0. \quad (6.4)$$

$$\dot{\rho}_\Lambda = 0. \quad (6.5)$$

This otherwise implies that the equation of state of  $\Lambda$  satisfies  $\omega_\Lambda = -1$ . Using the Friedmann equations (6.2) and (6.3) and also (2.7) and (2.2), we get the differential equation for the Hubble parameter as,

$$\dot{H} = \frac{1}{2 - \tilde{\zeta}_2} (\tilde{\zeta}_0 H H_0 + (\tilde{\zeta}_1 + \tilde{\zeta}_2 - 3) H^2 + 3 H_0^2 \Omega_\Lambda), \quad (6.6)$$

where  $\tilde{\zeta}_0, \tilde{\zeta}_1, \tilde{\zeta}_2$  are the previously defined dimensionless parameters,

$$\tilde{\zeta}_0 = \frac{3\zeta_0}{H_0}, \quad \tilde{\zeta}_1 = 3\zeta_1, \quad \tilde{\zeta}_2 = 3\zeta_2. \quad (6.7)$$

$H_0$  is the present value of the Hubble parameter and  $\Omega_\Lambda$  is the present density parameter of dark energy. Integrating equation (6.6) we can get the expression for the Hubble parameter as,

$$H = H_0 \left[ \frac{(y + \tilde{\zeta}_0) (y - 2(\tilde{\zeta}_{123}) - \tilde{\zeta}_0) e^{\frac{t'y}{2-\tilde{\zeta}_2}} - (y - \tilde{\zeta}_0) (y + 2(\tilde{\zeta}_{123}) + \tilde{\zeta}_0)}{2(\tilde{\zeta}_{123}) \left( e^{\frac{t'y}{2-\tilde{\zeta}_2}} (2(\tilde{\zeta}_{123}) - y) + \tilde{\zeta}_0 \right) - (y + 2(\tilde{\zeta}_{123}) + \tilde{\zeta}_0)} \right], \quad (6.8)$$

where  $\tilde{\zeta}_{123} = \tilde{\zeta}_1 + \tilde{\zeta}_2 - 3$ ,  $t' = H_0(t - t_0)$ ,  $y = \sqrt{\tilde{\zeta}_0^2 - 12\Omega_\Lambda \tilde{\zeta}_{123}}$  and  $t_0$  is the present cosmic time. As  $t - t_0 \rightarrow \infty$ ,  $H \rightarrow H_0 \left[ \frac{y + \tilde{\zeta}_0}{2\tilde{\zeta}_{123}} \right]$ , a constant provided  $\tilde{\zeta}_2 < 2$ . When  $t - t_0$  is small, H evolves as  $H_0 \left[ \frac{2(2-\tilde{\zeta}_2) + H_0(t-t_0)(\tilde{\zeta}_0 + 6\Omega_\Lambda + y)}{2(2-\tilde{\zeta}_2) + H_0(t-t_0)(y - 2\tilde{\zeta}_{123} - \tilde{\zeta}_0)} \right]$ .

Using the definition of the Hubble parameter, we obtained the scale factor from equation (6.8) as,

$$a = e^{\frac{H_0(t-t_0)(y-\tilde{\zeta}_0)}{2\tilde{\zeta}_{123}}} \left[ \frac{y + 2\tilde{\zeta}_{123} + \tilde{\zeta}_0 + e^{\frac{H_0(t-t_0)y}{2-\tilde{\zeta}_2}} (y - 2\tilde{\zeta}_{123} - \tilde{\zeta}_0)}{2y} \right]^{\frac{\tilde{\zeta}_2-2}{\tilde{\zeta}_{123}}}. \quad (6.9)$$

In the absence of cosmological constant,  $\Omega_\Lambda = 0$ , the scale factor reduces to

$$a(t) = \left[ \left( \frac{\tilde{\zeta}_0 + \tilde{\zeta}_{12} - 3}{\tilde{\zeta}_0} \right) + \left( \frac{3 - \tilde{\zeta}_{12}}{\tilde{\zeta}_0} \right) e^{\frac{\tilde{\zeta}_0}{2-\tilde{\zeta}_2} H_0(t-t_0)} \right]^{\frac{2-\tilde{\zeta}_2}{3-\tilde{\zeta}_{12}}}, \quad (6.10)$$

which is the expression obtained in chapter 2. When  $t - t_0$  is small, the scale factor evolves as,

$$a \sim \left[ 1 + \frac{H_0(t - t_0)(y - \tilde{\zeta}_0)}{2\tilde{\zeta}_{123}} \right] \left[ 1 + \frac{H_0(t - t_0)}{2 - \tilde{\zeta}_2}(y - 2\tilde{\zeta}_{123} - \tilde{\zeta}_0) \right]^{\frac{\tilde{\zeta}_2 - 2}{\tilde{\zeta}_{123}}}. \quad (6.11)$$

On the other hand when  $t - t_0$  is very large, scale factor increases exponentially.

The equation of state parameter  $\omega$  and the deceleration parameter  $q$  can be obtained using the relations (2.34) and (2.28), respectively. Using the expression (6.6) and (6.8), we get the expressions for  $\omega$  and  $q$  as,

$$\omega = -1 + \frac{2y^2 (\tilde{\zeta}_0 + \tilde{\zeta}_{123} + 3\Omega_\Lambda)}{3 (\tilde{\zeta}_2 - 2) \left( \text{Sinh} \left[ \frac{t'y}{2(2-\tilde{\zeta}_2)} \right] (\tilde{\zeta}_0 + 6\Omega_\Lambda) + \text{Cosh} \left[ \frac{t'y}{2(2-\tilde{\zeta}_2)} \right] y \right)^2}, \quad (6.12)$$

$$q = -1 + \frac{y^2 (\tilde{\zeta}_0 + \tilde{\zeta}_{123} + 3\Omega_\Lambda)}{(\tilde{\zeta}_2 - 2) \left( \text{Sinh} \left[ \frac{t'y}{2(2-\tilde{\zeta}_2)} \right] (\tilde{\zeta}_0 + 6\Omega_\Lambda) + \text{Cosh} \left[ \frac{t'y}{2(2-\tilde{\zeta}_2)} \right] y \right)^2}. \quad (6.13)$$

The present value of  $\omega$  and  $q$  can be obtained by putting  $t = t_0$  and respectively are,

$$\omega_0 = \frac{2\tilde{\zeta}_0 + 2\tilde{\zeta}_1 - \tilde{\zeta}_2 + 6\Omega_\Lambda}{3(\tilde{\zeta}_2 - 2)}, \quad (6.14)$$

$$q_0 = \frac{\tilde{\zeta}_0 + \tilde{\zeta}_1 - 1 + 3\Omega_\Lambda}{\tilde{\zeta}_2 - 2}. \quad (6.15)$$

The present universe will be accelerating only if  $3\omega_0 + 1 < 0$  and  $q_0 < 0$ . For the universe to be in quintessence region so as to avoid big rip, it should satisfy the relation  $q_0 > -1$ . Following these, in order to guarantee a conventional evolution of the the universe, such that a universe to begin from the Big Bang and then entering in to decelerated epoch and then

making a transition to the accelerated epoch in the past, we obtained the necessary conditions to be satisfied by the  $\tilde{\zeta}$ 's as,

1.  $\tilde{\zeta}_0 > 0$ ,  $\tilde{\zeta}_2 < 2$ ,  $\tilde{\zeta}_0 + \tilde{\zeta}_1 > 1 - 3\Omega_{\Lambda 0}$ ,  $\tilde{\zeta}_1 + \tilde{\zeta}_2 < 3$ ,  $\tilde{\zeta}_0 + \tilde{\zeta}_1 + \tilde{\zeta}_2 < 3 - 3\Omega_{\Lambda 0}$
2.  $\tilde{\zeta}_0 < 0$ ,  $\tilde{\zeta}_2 > 2$ ,  $\tilde{\zeta}_0 + \tilde{\zeta}_1 < 1 - 3\Omega_{\Lambda 0}$ ,  $\tilde{\zeta}_1 + \tilde{\zeta}_2 > 3$ ,  $\tilde{\zeta}_0 + \tilde{\zeta}_1 + \tilde{\zeta}_2 > 3 - 3\Omega_{\Lambda 0}$

If we neglect the cosmological constant i.e.,  $\Omega_{\Lambda 0} = 0$ , then these would reduce to the conditions obtained in the chapter 2 (equations (2.16) & (2.17)) as expected.

## 6.2 The case with constant bulk viscosity

Let us consider the case when bulk viscous coefficient is a constant, i.e., when  $\zeta = \zeta_0$  and  $\zeta_1 = \zeta_2 = 0$ . The expression for Hubble parameter then becomes,

$$H = H_0 \frac{\tilde{y} - \zeta_0 - 6\Omega_{\Lambda} + e^{\frac{1}{2}H_0(t-t_0)\tilde{y}} (\tilde{y} + \zeta_0 + 6\Omega_{\Lambda})}{\tilde{y} + \zeta_0 - 6 + e^{\frac{1}{2}H_0(t-t_0)\tilde{y}} (\tilde{y} - \zeta_0 + 6)}, \quad (6.16)$$

where  $\tilde{y} = \sqrt{\tilde{\zeta}_0^2 + 36\Omega_{\Lambda}}$ . This can be obtained by putting  $\zeta_1 = \zeta_2 = 0$  in the expression for Hubble parameter for the general  $\zeta$ , equation (6.8). Similarly the scale factor for constant viscosity can be obtained from equation (6.9) as,

$$a = e^{\frac{1}{6}H_0(t-t_0)(\tilde{\zeta}_0 - \tilde{y})} \left( \frac{(\tilde{y} + \tilde{\zeta}_0 - 6) + e^{\frac{H_0(t-t_0)\tilde{y}}{2}} (\tilde{y} - \tilde{\zeta}_0 + 6)}{2\tilde{y}} \right)^{\frac{2}{3}}. \quad (6.17)$$

The corresponding equation of state and the deceleration parameter (for constant viscosity) becomes,

$$\omega = \left( -1 - \frac{(\tilde{\zeta}_0 - 3 + 3\Omega_{\Lambda}) \tilde{y}^2}{3 (\tilde{y} \text{Cosh} [\frac{1}{4}t'\tilde{y}] + (\tilde{\zeta}_0 + 6\Omega_{\Lambda}) \text{Sinh} [\frac{1}{4}t'\tilde{y}])^2} \right), \quad (6.18)$$

$$q = \left( -1 - \frac{(\tilde{\zeta}_0 - 3 + 3\Omega_\Lambda) y^2}{2 (\tilde{y} \text{Cosh} [\frac{1}{4} t' \tilde{y}] + (\tilde{\zeta}_0 + 6\Omega_\Lambda) \text{Sinh} [\frac{1}{4} t' \tilde{y}])^2} \right). \quad (6.19)$$

As mentioned before, for an accelerating universe, the present value of equation of state  $\omega_0 < -\frac{1}{3}$  and the present value of the deceleration parameter  $q_0 < 0$ . To avoid big rip, the equation of state parameter  $\omega_0 > -1$ , above the phantom limit. These conditions help us to constrain the value of  $\tilde{\zeta}_0$  as,

$$1 - 3\Omega_\Lambda < \tilde{\zeta}_0 < 3(1 - \Omega_\Lambda). \quad (6.20)$$

From observation  $\Omega_\Lambda$  is constrained in the range  $0.65 - 0.75$ . This constrains the  $\tilde{\zeta}_0$  in between  $-1.25 < \tilde{\zeta}_0 < 1.05$ .

### 6.2.1 Age of the universe

Age of the universe in this case can be obtained by equating  $a = 1$  in the equation (6.17) and is found to be,

$$\text{Age} \equiv \left( \frac{2}{H_0 \tilde{y}} \right) \text{Log} \left[ 1 - \frac{2\tilde{y}}{6 + \tilde{y} - \tilde{\zeta}_0} \right]. \quad (6.21)$$

The plot of age of the universe for different values of  $(\tilde{\zeta}_0, \Omega_\Lambda)$  subjected to the constraint (6.20) are shown in the figure (6.1). The age plot shows reasonably good agreement for  $(\tilde{\zeta}_0, \Omega_\Lambda) = (-0.5, 0.7)$  but the agreement with respect  $(\tilde{\zeta}_0, \Omega_\Lambda) = (0.1, 0.68)$  is slightly less and for the third choice it is not in nice agreement. But corresponding to the best agreement pair the viscosity is negative. Whether is physically feasible or not may evident from the further considerations of the entropy evolution and dynamical system behavior

### 6.2.2 Thermodynamics

We now check the validity of the Generalized second law and maximization of entropy condition in this case. Assuming apparent horizon as

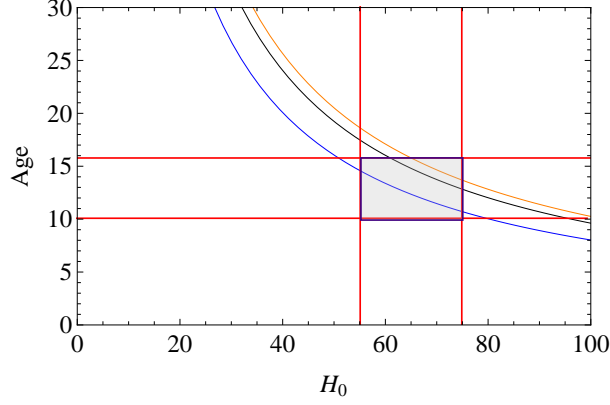


Figure 6.1: The figure shows the variation of age with  $H_0$  for different values of  $(\tilde{\zeta}_0, \Omega_\Lambda)$ . Black line corresponds to  $(\tilde{\zeta}_0, \Omega_\Lambda) = (0.1, 0.68)$ . The orange line and blue line corresponds to  $(\tilde{\zeta}_0, \Omega_\Lambda) = (0.2, 0.7)$  and  $(-0.5, 0.7)$  respectively.

the boundary of the universe and obtaining the horizon entropy using the Bekenstein relation (equation (3.7)) and matter entropy using the Gibbs equation (equation (3.28)), we calculated the expression for the first derivative and second derivative of the total entropy with respect to time. The relation obtained are as follows:

$$\dot{S} = \frac{64\pi^2 e^{t'\tilde{y}} b^2 \tilde{y}^4 \left( \tilde{y} - 6 + \tilde{\zeta}_0 + e^{\frac{1}{2}t'\tilde{y}} (\tilde{y} + 6 - \tilde{\zeta}_0) \right)}{H_0 \left( \tilde{y} - \tilde{\zeta}_0 - 6\Omega_\Lambda + e^{\frac{1}{2}t'\tilde{y}} (6\Omega_\Lambda + \tilde{y} + \tilde{\zeta}_0) \right)^5}, \quad (6.22)$$

$$\ddot{S} = -\frac{384\pi^2 b^2 \tilde{y}^5 e^{\frac{3}{2}t'\tilde{y}} (b\tilde{y} + 2(1 + \Omega_\Lambda)\tilde{y} \text{Cosh}[\frac{1}{2}t'\tilde{y}] + 2d \text{Sinh}[\frac{1}{2}t'\tilde{y}])}{((-1 + e^{\frac{1}{2}t'\tilde{y}})\tilde{\zeta}_0 - 6\Omega_\Lambda + \tilde{y} + e^{\frac{1}{2}t'\tilde{y}}(6\Omega_\Lambda + \tilde{y}))^6}, \quad (6.23)$$

where  $b = \tilde{\zeta}_0 + 3\Omega_{\Lambda 0} - 3$ ,  $d = \tilde{\zeta}_0 + 12\Omega_\Lambda - \tilde{\zeta}_0\Omega_\Lambda$  and  $t' = H_0(t - t_0)$ . The evolution of  $\dot{S}$  and  $\ddot{S}$  with respect to the scale factor for different values of  $\Omega_\Lambda$  and  $\tilde{\zeta}_0$  subjected to the constrain (6.20) are plotted and are shown in figures (6.2) and (6.3) respectively. From the figures, it is clear that GSL and maximization of entropy condition are valid for this model.

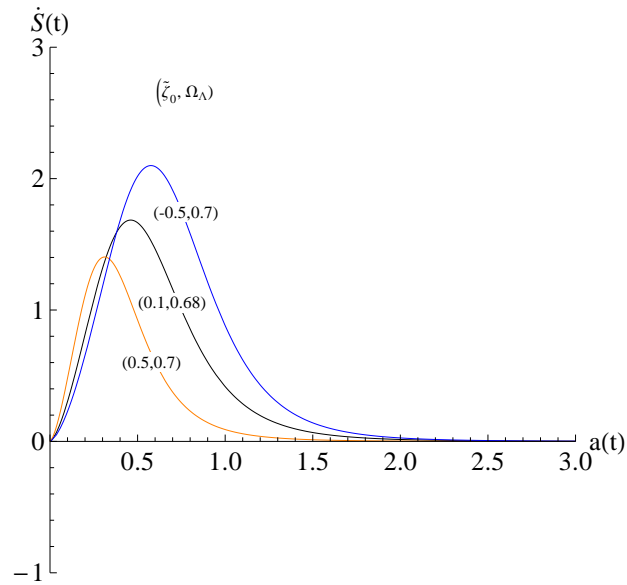


Figure 6.2: Evolution of the first derivative of entropy with the scale factor for different values of  $(\tilde{\zeta}_0, \Omega_\Lambda)$  subjected to the constrain (6.20).

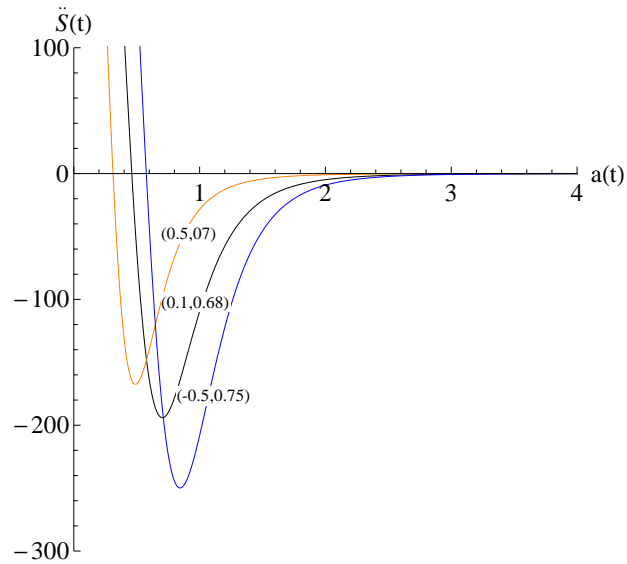


Figure 6.3: Evolution of the second derivative of entropy with the scale factor for different values of  $(\tilde{\zeta}_0, \Omega_\Lambda)$  subjected to the constrain (6.20).

$(u_c, v_c)$	Eigen value $(\lambda_1, \lambda_2)$
$(u, 1)$	$\left(\frac{3}{2}, 0\right)$
$\left(-\frac{\tilde{\zeta}_0(\tilde{\zeta}_0 + \sqrt{\tilde{\zeta}_0^2 + 36\Omega_\Lambda})}{18\Omega_\Lambda}, \frac{\tilde{\zeta}_0 - 6\Omega_\Lambda - \sqrt{\tilde{\zeta}_0^2 + 36\Omega_\Lambda}}{6 + 2\tilde{\zeta}_0 - 6\Omega_\Lambda}\right)$	$\left(-3, \frac{3}{-1 + \frac{\tilde{\zeta}_0}{\sqrt{\tilde{\zeta}_0^2 + 36\Omega_\Lambda}}}\right)$
$\left(\frac{\tilde{\zeta}_0(-\tilde{\zeta}_0 + \sqrt{\tilde{\zeta}_0^2 + 36\Omega_\Lambda})}{18\Omega_\Lambda}, \frac{\tilde{\zeta}_0 - 6\Omega_\Lambda + \sqrt{\tilde{\zeta}_0^2 + 36\Omega_\Lambda}}{6 + 2\tilde{\zeta}_0 - 6\Omega_\Lambda}\right)$	$\left(-3, \frac{3}{-1 - \frac{\tilde{\zeta}_0}{\sqrt{\tilde{\zeta}_0^2 + 36\Omega_\Lambda}}}\right)$

Table 6.1: Critical values and the corresponding eigen values for the bulk viscous model with  $\Lambda$  for  $\zeta = \zeta_0$

### 6.2.3 Phase space analysis

We also studied the asymptotic behavior of the model. We chose  $u$  and  $v$  as the phase space variables, which are defined as

$$\begin{aligned} u &= \Omega_m = \frac{\rho_m}{3H^2}, \\ v &= \frac{1}{\frac{H_0}{H} + 1}, \end{aligned} \quad (6.24)$$

The variables varies in the range  $0 \leq u \leq 1$  and  $0 \leq v \leq 1$  respectively. Using the conservation equation and differential equation for Hubble parameter, we can obtained the autonomous equations for  $u$  and  $v$  as,

$$\begin{aligned} u' &= \frac{(1-v)}{v^2} (v(1-u)\tilde{\zeta}_0 - 3\Omega_\Lambda u(1-v)), \\ v' &= \frac{(1-v)}{2v} (3\Omega_\Lambda(1-v)^2 + \tilde{\zeta}_0 v(1-v) - 3v^2). \end{aligned} \quad (6.25)$$

There are three critical points for the above autonomous equations and we have evaluated the corresponding eigen values, they are listed in the Table 6.1. In order to represent a universe with unstable matter dominated phase and a stable, physically feasible accelerated phase we see that  $\tilde{\zeta}_0$  must be positive subjected to the constrain (6.20). In determining the age corresponding to this model we have noted that, the best fit have

arised both with negative value of  $\zeta_0$  and also with positive value (the black line in the age plot) of  $\zeta_0$ . But the asymptotic analysis presented here, however supports only a positive value for  $\zeta_0$ . Earlier in the analysis without cosmological constant also we conclude that, the case with  $\zeta = \zeta_0$  is preferred over other cases. Thus even though the age prediction has been changed slightly, the present model is also predicting a conventional evolution of the universe with constant viscosity as in the case of the model without cosmological constant.

### 6.3 The case with $\zeta = \zeta_1 H$

Let us consider another special case,  $\zeta = \zeta_1 H$ , where viscosity depends only on the velocity component of the expansion of the universe such that  $\zeta_0 = \zeta_2 = 0$  in equation (2.7). The expression for the Hubble Parameter and the scale factor can be obtained from equations (6.8) and (6.9) by putting  $\zeta_0 = \zeta_2 = 0$  and are as

$$H = \frac{-\left(\sqrt{3}H_0\Omega_\Lambda(6 - 2\tilde{\zeta}_1 - 2\sqrt{3}\eta + 2e^{\sqrt{3}\eta t'}(3 - \tilde{\zeta}_1 + \sqrt{3}\eta))\right)}{\eta\left(6 - 2\tilde{\zeta}_1 - 2\sqrt{3}\eta - 2e^{\sqrt{3}\eta t'}(3 - \tilde{\zeta}_1 + \sqrt{3}\eta)\right)}, \quad (6.26)$$

where  $\eta = \sqrt{(3 - \tilde{\zeta}_1)\Omega_\Lambda}$  and  $t' = H_0(t - t_0)$ .

$$a = 12^{\frac{1}{\tilde{\zeta}_1 - 3}} e^{-\frac{\sqrt{3}\Omega_\Lambda t'}{\eta}} \left( \frac{\tilde{\zeta}_1 - 3 + \sqrt{3}\eta + e^{\sqrt{3}\eta t'}(3 - \tilde{\zeta}_1 + \sqrt{3}\eta)}{\eta} \right)^{\frac{2}{3 - \tilde{\zeta}_1}}. \quad (6.27)$$

From the expression of Hubble parameter and the scale factor, we see that  $\tilde{\zeta}_1 < 3$  must be satisfied for an expanding universe. Combining the above two equations it is easy to obtain the Hubble parameter in terms of the scale factor  $a$ . And it is,

$$H = H_0 \sqrt{\left[ \frac{a^{\tilde{\zeta}_1 - 3}(\tilde{\zeta}_1 - 3 + 3\Omega_\Lambda) - 3\Omega_\Lambda}{\tilde{\zeta}_1 - 3} \right]}. \quad (6.28)$$

Model	$\tilde{\zeta}_1$	$H_0$	$\Omega_\Lambda$	$\Omega_m$	$\chi_{min}^2$	$\chi_{d.o.f}^2$
$\zeta = \zeta_1 \frac{\dot{a}}{a}$	-0.0975	70	0.75	0.25	312.23	1.02

Table 6.2: Best estimates of the bulk viscous parameter  $\tilde{\zeta}_1$ ,  $H_0$ ,  $\Omega_\Lambda$ ,  $\Omega_m = 1 - \Omega_\Lambda$  and also  $\chi^2$  minimum value for  $\zeta = \zeta_1 \frac{\dot{a}}{a}$   $\chi_{d.o.f}^2 = \frac{\chi_{min}^2}{n-m}$ , where  $n = 307$ , the number of data and  $m$  is the number of parameters in the model. The subscript d.o.f stands for degrees of freedom. For the best estimation we have used SCP “Union” 307 SNe Ia data sets.

The explicit form of  $H$  in terms of  $a$ , makes it easier for parameter extraction and hence to compare with bulk viscous model without  $\Lambda$ .

To extract the value of  $\tilde{\zeta}_1$ , we use the Type Ia Supernova data. The method used is the  $\chi^2$  minimization technique, which is described in chapter 2. Using the expression for  $H$  from equation (6.28), we construct the  $\chi^2$  function. In order to make comparison with bulk viscous model without  $\Lambda$  easier, we use the same data set which is the SCP “Union” Type Ia Supernova data [91] composed of 307 data points from 13 independent data sets. We extract the values of  $\Omega_{\Lambda 0}$  and  $H_0$  along with  $\tilde{\zeta}_1$ . The values are given in the Table 6.2.

### 6.3.1 Equation of state parameter and Deceleration parameter

The equation of state parameter  $\omega$  and the deceleration parameter  $q$ , for this model are obtained using the expression for the Hubble parameter (equation (6.28)) and are given as,

$$\omega = \frac{9a^3\Omega_\Lambda - a^{\tilde{\zeta}_1}\tilde{\zeta}_1(\tilde{\zeta}_1 - 3 + 3\Omega_\Lambda)}{-9a^3\Omega_\Lambda + 3a^{\tilde{\zeta}_1}(\tilde{\zeta}_1 - 3 + 3\Omega_\Lambda)}, \quad (6.29)$$

$$q = -1 - \frac{a^{\tilde{\zeta}_1}(-3 + \tilde{\zeta}_1)(\tilde{\zeta}_1 - 3 + 3\Omega_\Lambda)}{-6a^3\Omega_\Lambda + 2a^{\tilde{\zeta}_1}(\tilde{\zeta}_1 - 3 + 3\Omega_\Lambda)}. \quad (6.30)$$

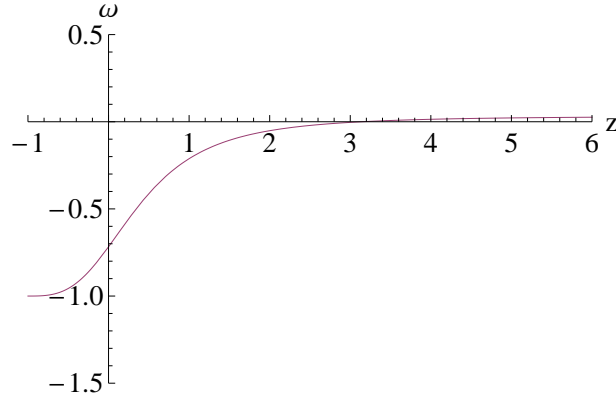


Figure 6.4: Plot of the equation of state with the redshift for the best estimated values of  $\tilde{\zeta}_1$  and  $\Omega_\Lambda$ .

The plot of  $\omega$  and  $q$  for the best estimated values of  $\tilde{\zeta}_1$  and  $\Omega_\Lambda$  are shown in the figures 6.4 and 6.5 respectively. The equation of state is zero in the recent past but slightly above zero in the extreme past of the universe. It decreases to the negative values and finally saturated at  $\omega = -1$  corresponding to a de Sitter epoch in the extreme future. The evolution of the deceleration parameter starts from around  $q \sim 0.5$  in the past, which corresponds to decelerated epoch and decreasing as the universe expands. It saturates at  $q = -1$  corresponding the future de Sitter phase. The present value of  $\omega$  and  $q$  can be obtained by putting  $a=1$  in the expressions given by equation (6.29) and (6.30), respectively and are obtained as,

$$\omega_0 = -\frac{\tilde{\zeta}_1}{3} - \Omega_\Lambda, \quad (6.31)$$

$$q_0 = \frac{1}{2}(1 - \tilde{\zeta}_1 - 3\Omega_\Lambda). \quad (6.32)$$

Using the best estimated values of  $\tilde{\zeta}_1$  and  $\Omega_\Lambda$ , we get  $\omega_0 = -0.7175$  and  $q_0 = -0.57625$ , which is near to concordance value obtained by WMAP observation.

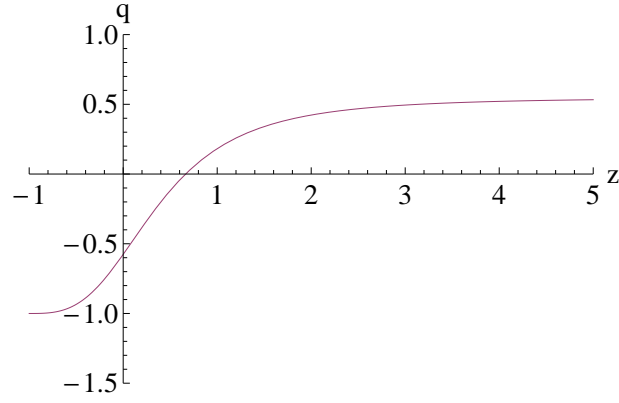


Figure 6.5: Plot of the deceleration parameter with the redshift for the best estimated values of  $\tilde{\zeta}_1$  and  $\Omega_\Lambda$ .

### 6.3.2 Age of the universe

The age of the universe in this model can be obtained by equating the scale factor (equation (6.27)) to one and is found to be

$$Age \equiv \frac{\text{Log} \left[ \frac{3 - \tilde{\zeta}_1 - \sqrt{3} \sqrt{(3 - \tilde{\zeta}_1) \Omega_\Lambda}}{3 - \tilde{\zeta}_1 + \sqrt{3} \sqrt{(3 - \tilde{\zeta}_1) \Omega_\Lambda}} \right]}{\sqrt{3} p \sqrt{-(-3 + \tilde{\zeta}_1) \Omega_\Lambda}}. \quad (6.33)$$

Using the best estimated values for  $\tilde{\zeta}_1$  and  $\Omega_\Lambda$ , the age is found to 13.38Gyr and is matching with the concordance value of the age of the universe obtained from the oldest globular observations. In this way the model is promising in predicting the age. But the problem with this model is the negativity of the viscous coefficient  $\zeta_1$  which causes the violation of the local second law. However in the previous section we have seen that the model with constant viscosity is predicting the age in a reasonable way and also that model is satisfying conditions on entropy evolution, i.e. local second law, generalized second law and the maximization condition of entropy. Hence we are not going into the details of the present case.



# 7

## Conclusions and Future scope

*This chapter concludes the entire work and also describes the future scope.*

In the preceding chapters we have discussed the bulk viscous matter dominated universe, which infact dose two things regarding the late evolution of the universe. First, it explain the late acceleration of the universe without invoking to any exotic dark energy form. Second, it unifies both the dark matter and dark energy. These two things are of utmost importance in the recent times.

Many attempts have been made to understand the nature and evolution of the dark energy which supposed to causes the recent acceleration of the universe. In spite of large volume of work existed in the recent literature, there arised no conclusive consensus regarding either the nature or evolution of dark energy. Therefore attempts have been initiated to explain the late acceleration without advocating for any exotic form of matter. Bulk viscosity associated with the matter sector is seems to a potential candidate to achieve this goal.

In the present thesis we have studied the the bulk viscous matter dominated universe in detail and the study shows that, there is considerable scope in this model. We have also studied the effect of the a cosmological constant in this model. The results of our entire work has been concluded below. We present first a chapter wise summary followed by an overall conclusion. Future scope of the model has also been pointed out.

## 7.1 Conclusions

Recent acceleration in the expansion of universe has been conventionally explained by proposing an exotic form of energy called dark energy. The best choice for the dark energy is cosmological constant which leads to the most successful model of the late universe, the standard  $\Lambda$ CDM model of the universe. But the model failed to predict the extremely low value of the dark energy density and also the mysterious coincidence between the densities of dark energy and dark matter. This lead to the emergence of various varying density dark energy models. In spite of these, the mystery of dark energy as an exotic component has been continued without having any reasonable solution. This ultimately compelled the scientific community to search for possible explanations for the recent acceleration without invoking any exotic component, but by using simple physical phenomenon. Bulk viscous matter is one of the best alternative in this direction. In the present thesis, we presents our studies on the bulk viscous matter dominated universe in the context of the late acceleration of the universe. We give the required introduction and motivation in the introductory chapter.

In **chapter 2**, we have carried out the study of the background evolution of a flat FLRW universe dominated with bulk viscous matter. We assumed that the viscosity has dependence on velocity and acceleration of the expansion of the universe, hence adopted the most general form,  $\zeta = \zeta_0 + \zeta_1 \frac{\dot{a}}{a} + \zeta_2 \frac{\ddot{a}}{a}$ . We have solved the Friedmann equations for the Hubble parameter and the scale factor, which leads to a two set of conditions on the viscosity coefficients, in order to predict the conventional evolution of the universe as,  $(\tilde{\zeta}_0 > 0, \tilde{\zeta}_0 + \tilde{\zeta}_{12} < 3, \tilde{\zeta}_{12} < 3, \tilde{\zeta}_2 < 2)$  and  $(\tilde{\zeta}_0 < 0, \tilde{\zeta}_0 + \tilde{\zeta}_{12} > 3, \tilde{\zeta}_{12} > 3, \tilde{\zeta}_2 > 2)$ .

In constraining the parameters we have used SCP “Union” Type Ia Supernova data set. Following the method of  $\chi^2$  minimization, we have computed  $\chi_{d.o.f}^2$ , the minimum values of  $\chi^2$  function per degrees of free-

dom for both cases of limiting conditions of the bulk viscous parameters and is found to be very near to one, indicating a reasonable goodness-of-fit. We have evaluated the best fit values of the three dimensionless viscous parameters,  $\tilde{\zeta}_0$ ,  $\tilde{\zeta}_1$  and  $\tilde{\zeta}_2$  simultaneously for both cases of limiting conditions of the parameters and are shown in Table 2.1.

For both cases of the best estimate of the viscous parameters, the evolution of the cosmological parameters: the scale factor, deceleration parameter, the equation of state parameter, matter density, curvature scalar are all found to be identical. So these two sets of best estimated values for the parameters cannot be distinguished by using the conventional cosmological parameters.

This model automatically solves the coincidence problem because the bulk viscous matter simultaneously represents dark matter and dark energy sectors.

From the evolution of scale factor, it is found that, for the first limiting conditions of bulk viscous parameters, the transition into the accelerating epoch would be in the recent past if  $\tilde{\zeta}_0 + \tilde{\zeta}_1 > 1$ . On the other hand if  $\tilde{\zeta}_0 + \tilde{\zeta}_1 < 1$ , the transition takes place in the future and if,  $\tilde{\zeta}_0 + \tilde{\zeta}_1 = 1$ , the transition takes place at the present time. For the second limiting conditions of parameters, the above conditions are getting reversed such that when  $\tilde{\zeta}_0 + \tilde{\zeta}_1 > 1$ , the transition will takes place in the future, when  $\tilde{\zeta}_0 + \tilde{\zeta}_1 < 1$ , the transition would occur in the recent past and when  $\tilde{\zeta}_0 + \tilde{\zeta}_1 = 1$ , the transition takes place at the present time.

We have also obtained the age of the universe and is found to be around 10.90 Gyr for the best estimates of the parameters. Compared to the age predicted from oldest galactic globular clusters ( $12.9 \pm 2.9$  Gyr), the present value is relatively less, but it is within the limit of the predicted age.

It is found that for the best estimates of the model parameters, the

universe entered the accelerating phase in the recent past at a red shift  $z_T = 0.49_{-0.057}^{+0.075}$  for the first limiting conditions and  $z_T = 0.49_{-0.066}^{+0.064}$  for the second limiting conditions. This is found to be agreeing only with the lower limit of the corresponding  $\Lambda$ CDM range,  $z_T = 0.45 - 0.73$  [94]. The present value of the deceleration parameter is found to be about  $-0.68_{-0.06}^{+0.06}$  and  $-0.68_{-0.05}^{+0.066}$  for the two cases respectively and is comparable with the observational results which is around  $-0.64 \pm 0.03$ .

We have analyzed the equation of state parameter for the best estimates of the bulk viscous parameters only. The equation of state parameter  $\omega \rightarrow -1$  as  $z \rightarrow -1$ , which means that the bulk viscous matter dominated universe behaves like the de Sitter universe in future. It is also clear that the equation of state parameter of this model doesn't cross the phantom divide and thereby free from big rip singularity. The present value of the equation of state parameter is around  $-0.78_{-0.045}^{+0.03}$  and  $-0.78_{-0.043}^{+0.037}$  for the best fit of viscosity parameters corresponding to the two limiting conditions respectively. This value is comparatively higher than that predicted by the joint analysis of WMAP+BAO+H0+SNe data, which is around -0.93 [11, 98].

From the expression for matter density, it is clear that it diverges as the scale factor tends to zero, which indicates the existence of Big-Bang at the origin. This is further confirmed by obtaining the curvature scalar which also becomes infinity at the origin.

Since the model predicts the late acceleration of the universe as like the standard  $\Lambda$ CDM model, we have analyzed the model using statefinder parameters to distinguish it from other standard dark energy models especially from  $\Lambda$ CDM model. The evolution of the present model in the  $\{r, s\}$  plane is shown in figure 4.4 and it shows that the evolution of the  $\{r, s\}$  parameter is in such a way that  $r > 1, s < 0$ , a feature similar to the Chaplygin gas model. The present position of the bulk viscous model in

the  $r$ - $s$  plane corresponds to  $\{r_0, s_0\} = \{1.25, -0.07\}$ . Hence the model is distinguishably different from the  $\Lambda$ CDM model.

In next chapter, **chapter 3**, we analyse the thermodynamical evolution of the model. The evolution of the total bulk viscous parameter is studied corresponding to both the limiting conditions as given by equations (2.16) and (2.17) and are also found to be identical. In the initial epoch of the expansion, the total bulk viscosity is found to be negative and hence violating the local second law of thermodynamics. But it become positive from  $z \leq 0.8$ , from there onwards the local second law is satisfied. However we found that the generalized second law is satisfied throughout the evolution of the universe, which safeguard the second law in the model. We also checked the entropy maximization condition for the model and found that the entropy of the universe is bounded and hence the universe behaves as an ordinary macroscopic system in this model.

In addition to the general form for bulk viscous coefficient  $\zeta = \zeta_0 + \zeta_1 \frac{\dot{a}}{a} + \zeta_2 \frac{\ddot{a}}{a}$ , we considered two special cases: (1)  $\zeta = \zeta_0 + \zeta_1 \frac{\dot{a}}{a}$ , where the viscous coefficient doesn't depends on acceleration and (2)  $\zeta = \zeta_0$ , where the viscous coefficient is a constant. We first extracted the values of the viscous parameters using the same data and technique as we used for the general form. The results are tabulated in Table 3.1. GSL and entropy maximization condition are also found to be valid for these two cases. However, local second law is found to be valid only for the case  $\zeta = \zeta_0$ .

In the **chapter 4**, we have done the phase space analysis of the model corresponding to the three cases of the bulk viscosity coefficient:

- (i)  $\zeta = \zeta_0$ ,
- (ii)  $\zeta = \zeta_0 + \zeta_1 \frac{\dot{a}}{a}$ ,
- (iii)  $\zeta = \zeta_0 + \zeta_1 \frac{\dot{a}}{a} + \zeta_2 \frac{\ddot{a}}{a}$ .

First we have considered a single component universe, containing bulk

viscous matter alone. By formulating the suitable dynamical equations, the possible critical points have been enumerated and then their stability analyses were performed. The phase space plot for each cases are constructed. It is found that, for all the three cases, there exists a prior decelerated epoch, which is an unstable node and a late stable accelerating epoch, similar to the de Sitter phase. For case (iii) the equation of state,  $\omega$  becomes greater than one for the initial state, which may cause violation of causality [139]. The same situation was found for case (ii) (i.e., for  $\zeta = \zeta_0 + \zeta_1 \frac{\dot{a}}{a}$ ) also. But for the first case (i),  $\zeta = \zeta_0$ , no such causality violation arise. This makes case (i) favorable over the other two.

We repeat the above analysis for a two component universe consisting of radiation and bulk viscous matter. Our main aim here is to check whether the present model successfully predicts a prior conventional radiation dominance. It is found that the model corresponding to case (i), at which  $\zeta = \zeta_0$ , predicts an early radiation dominated phase, represented by a past attractor fixed point. The model then successfully account for a transit into a decelerated matter dominated phase (saddle point) and then finally evolving to a de Sitter type universe (stable future attractor) which expands exponentially. However the other two cases, with  $\zeta = \zeta_0 + \zeta_1 \frac{\dot{a}}{a}$  and  $\zeta = \zeta_0 + \zeta_1 \frac{\dot{a}}{a} + \zeta_2 \frac{\ddot{a}}{a}$ , failed to predicts a prior radiation dominated phase and conventional decelerated matter dominated phase of the universe. Which again increases one's confidence in case (i) as a viable model of the universe.

By considering the case (i)  $\zeta = \zeta_0$ , a model with constant bulk viscosity, as a prominent model of the late universe, which can successfully accommodate an early radiation phase, we then tried to extract out the constant viscous coefficient of our universe. Using the latest supernovae type Ia we computed a value for the constant viscosity around  $\zeta_0 \sim 7 \times 10^7$  Pa. s. There are other references which supports our prediction in this

regard. However, there exist some references which predicts values from  $10^5 \text{Pa.s.}$  onwards. In this light we finally concluded to proposes a range for the constant viscosity for our universe as  $5 \times 10^5 \leq \zeta_0 \leq 7 \times 10^7 \text{ Pa. s.}$  From the previous chapter we have seen that, the thermodynamics considerations also strongly supports a universe with constant viscosity. All these are printing towards a positive situation that it is possible to understand the recent acceleration of the universe without invoking to any exotic form or matter/energy.

In **chapter 5** we devoted our analysis in contrasting the bulk viscous model of the universe with the standard  $\Lambda\text{CDM}$  model using the method of Bayesian analysis. Through Bayesian analysis one is able to find, to what extend a model under consideration is superior over some other or say some previous standard model. Here we made a detailed analysis by considering five separate cases of bulk viscous models:

- (1)  $\zeta = \zeta_0 + \zeta_1 \frac{\dot{a}}{a} + \zeta_2 \frac{\ddot{a}}{a},$
- (2)  $\zeta = \zeta_0 + \zeta_1 \frac{\dot{a}}{a},$
- (3)  $\zeta = \zeta_0,$
- (4)  $\zeta = \zeta_1 \frac{\dot{a}}{a},$
- (5)  $\zeta = \zeta_0 + \zeta_2 \frac{\ddot{a}}{a}.$

The respective parameters were evaluated using the “Union” data of Supernovae Type Ia. then we have obtained the likelihood for all the five models. The likelihood for the  $\Lambda\text{CDM}$  model is also obtained for the same data set. We have then obtained the Bayes factor for all the five cases, see Table 5.2. The primary results indicate that the model corresponding to case 2, i.e.,  $\zeta = \zeta_0 + \zeta_1 \frac{\dot{a}}{a}$  have a Bayes factor just above 3, and thus have slight advantage over the  $\Lambda\text{CDM}$  model compared with other cases. However the results from the analysis of thermodynamics and dynamical system behavior shows that this model is not so promising. For the model corresponding to cases 1 and 5 , the Bayes factor is just above one and

can just have a bare mention, in contrast to the standard model. The model corresponding to case 3, with constant viscosity, also seems to fail in standing against the standard model in this primary analysis.

Among the supernovae data for a wide range of redshifts, those corresponding to high redshifts, say  $z > 0.5$  were obtained with less background interference compared to the lower redshift region. Since Bayes method is relying on the probabilities, the accuracy of the data is a matter of great concern. Hence we restrict to supernovae data with relatively high redshifts,  $z > 0.5$  for pursuing the Bayesian analysis to get more feasible results. The results consequent to this have a marked deviation from the previous one. The Bayes factor for the constant bulk viscosity  $\zeta = \zeta_0$  (case 3) and models corresponding to cases 2 and 4 also are having a slight advantage over other cases when compared with the standard  $\Lambda$ CDM model. Since Bayes factors of the cases 2, 3 and 4, are all in the range  $1 < B_{ij} < 3$ , it is difficult to discriminate among themselves. However in chapter 4, we have found out that only the case 3 will have asymptotically stable end de Sitter phase and also accounting for an early radiation phase. Taking account of this, it can be concluded that, among the cases 2, 3 and 4, which are having almost same Bayes factor, the case 3 can be preferred over the other cases.

**Chapter 6** is dealing with the bulk viscous model with an additional cosmic component, the cosmological constant  $\Lambda$ . As there can exist a non-zero cosmological constant in the present universe, it is worth checking it's effects on a bulk viscous matter universe. Since we have some slight issues with the prediction of age in the pure bulk viscous matter dominated universe, the inclusion of cosmological constant may help us in solving this issue at least to some extend. We have solved the resulting Friedmann equation for the Hubble parameter and studied the evolution of other prominent cosmological parameters. It was found that the age of

the resulting universe has been increased substantially as expected, thus solves the age issue to certain extent. We also found that the model with constant viscosity and cosmological constant is thermodynamically viable as it is satisfying both the generalized second law and the entropy maximization condition. Regarding the phase-space evolution of this model, we have found that, the model predicts an unstable prior decelerated epoch followed by an accelerated epoch for positive definite value for the viscous coefficient  $\zeta_0$ . In addition we have also considered the case  $\zeta = \zeta_1 \frac{\dot{a}}{a}$  with  $\Lambda$ , evaluated the value of  $\tilde{\zeta}_1$  and obtained the evolution of the cosmological parameters. We have obtained the age of the universe for this case and is found to be in the range of age from the oldest globular cluster.

**To summarize** the main results, following the drawbacks of the standard  $\Lambda$ CDM model we consider bulk viscous matter dominated model as an alternative to explain the recent acceleration of the universe. We assume a flat universe with a single component, the bulk viscous matter and used the most general form for the bulk viscous coefficient as,  $\zeta = \zeta_0 + \zeta_1 \frac{\dot{a}}{a} + \zeta_2 \frac{\ddot{a}}{a}$ . It was found that the model can successfully predicts the transition into late acceleration phase and gives the expected background evolution of the universe. In particular the model with constant viscosity,  $\zeta_0$  can account for the evolution of the universe right from the radiation dominated epoch up to the last de Sitter epoch. However the model predicts a relatively less age for the present universe and a high value for the current equation of state parameter. Even though the thermal evolution of the model has got a problem with the local second law in the case of the full viscosity coefficient, the model corresponding to  $\zeta = \zeta_0$  is again free from such inconsistencies. We compared the model with the standard  $\Lambda$ CDM model using Bayesian probability analysis and found that the model with constant viscosity can be qualified to make a relatively good mention against the standard model. Since cosmological

constant is a possible component of the universe, we have also checked the status of bulk viscous model with cosmological constant and found that the age has been substantially increased.

### 7.1.1 Future scope

The relevance of the present model is that, it can explain the late acceleration of the universe without having the conventional exotic dark energy. Here we are using one of the natural effect that can arise in the matter sector of the universe, the bulk viscosity to cause the late acceleration. Especially the model with constant bulk viscosity in the range  $5 \times 10^5 \leq \zeta_0 \leq 7 \times 10^7$  is seems to explain the conventional evolution of our universe First of all it needs to sharpen values of the parameters Contrasting the model with the latest data on Supernova observation and other data from Plank collaborator and CMB is essential, particularly to extract the value of the viscous coefficient  $\zeta_0$  can be the prime future agenda of this model.

An important effect with which the model is to be contrasted with is the Integrated Sachs-Wolfe effect(ISW). The ISW Effect is refers to the change in the energy of a CMB photon as it passes through the evolving gravitational potential wells [102]. For large time, the behavior of  $a$ , the scale factor tends to that of the  $\Lambda$ CDM model for which the gravitational potential,  $\phi \sim 1 + z$ . So compared to the time of decoupling ( $z \sim 1090$ ), the potential will be diluted at later times which consequentially causes the ISW effect. We have presented a brief argument regarding the ISW effect in the present model in the Appendix section included in Chapter 2. But more detailed analysis is needed in this effect to get a mature conclusion.

Another important area which need an extensive investigation is on the effect of the bulk viscous model in the structure formation. Even

though the standard  $\Lambda$ CDM model fits fairly well with the corresponding observational data, there exist problems, like missing satellites [149], the cusp-core problem [150] etc. Thus a perturbative study of the density contrast in the viscous model is essential to know whether the model leads to the formation of large scale structures and thereby solves the problem faced by the standard model. In addition to the general relativistic case, the work may be extended to Newtonian and Neo-Newtonian approaches as well.

The viscous theory we used in the present work is the Eckart approach. As pointed out in the thesis, the theory is only a first order approach to the causal theory. So using full causal and relativistic theory like Israel-Stewart model or with its truncated version one can throw more light into the further feasibility of the viscous universe model in predicting the late time acceleration of the universe. Please refer some of the latest works in this regard [151, 152].

Yet another interesting scope is to study the effects of viscosity in one of the important process took place in the early stage of the universe, the primordial nucleosynthesis. The primordial nucleosynthesis model predicts the primordial abundances of the light elements, except some relatively small issues with Lithium. One may include the viscosity effect in such calculations to see whether it give some positive output towards such kind of issues.



# Bibliography

- [1] S. Perlmutter et al., *Measurements of  $\Omega$  and  $\Lambda$  from 42 High-Redshift Supernovae*, *Astrophys. J.* **517** 565 (1999).
- [2] A. G. Riess et al., *Observational Evidence from Supernovae for an Accelerating Universe and a Cosmological Constant*, *Astron. J.* **116** 1009 (1998).
- [3] Jayant V Narlikar, *Introduction to cosmology*, Cambridge University Press (1993)
- [4] G. F. Hinshaw, et.al., *Nine-Year Wilkinson Microwave Anisotropy Probe (WMAP) Observations: Cosmological Results*, *Astrophys. J. Suppl. Ser.* **208** 19 (2013).
- [5] Planck collaboration, *Planck 2018 results. VI. Cosmological parameters*, *arXiv:1807.06209v1 [astro-ph.CO]* 17 Jul 2018.
- [6] Supernova Search Team collaboration, A.G. Riess et al., *Type Ia supernova discoveries at  $z \lesssim 1$  from the Hubble space telescope: evidence for past deceleration and constraints on dark energy evolution*, *Astrophys. J.* **607** 665 (2004).
- [7] A.G. Riess et al., *New Hubble space telescope discoveries of type Ia supernovae at  $z \lesssim 1$ : narrowing constraints on the early behavior of dark energy*, *Astrophys. J.* **659** 98 (2007).
- [8] C. L. Bennett et al., *First-Year Wilkinson Microwave Anisotropy Probe (WMAP) Observations: Preliminary Maps and Basic Results*, *Astrophys. J. Suppl. Ser.* **148** 1 (2003).
- [9] Tegmark et al., *Cosmological parameters from SDSS and WMAP*, *Phys. Rev. D* **69** 103501 (2004).

- [10] Seljak et al., *Cosmological parameter analysis including SDSS Ly $\alpha$  forest and galaxy bias: Constraints on the primordial spectrum of fluctuations, neutrino mass, and dark energy*, *Phys. Rev. D* **71** 103515 (2005).
- [11] E. Komatsu et al., *Seven-Year Wilkinson Microwave Anisotropy Probe (WMAP) Observations: Cosmological Interpretation*, *Astrophys. J. Suppl.* **192** 18 (2011).
- [12] D. J. Eisenstein et al., *Detection of the baryon acoustic peak in the large-scale correlation function of SDSS luminous red galaxies*, *Astrophys. J.* **633** 560 (2005).
- [13] E.J. Copeland, M. Sami and S. Tsujikawa, *Dynamics of Dark energy*, *Int. J. Mod. Phys. D* **15** 1753 (2006).
- [14] E. Carretta, R. G. Gratton, G. Clementini, and F. Fusi Pecci, *Distances, ages and epoch of formation of globular clusters*, *Astrophys. J.* **533** 215 (2000).
- [15] A. A. Penzias and R. W. Wilson, *A measurement of excess antenna temperature at 4080-Mc/s*, *Astrophys. J.* **142** 419 (1965).
- [16] G. F. Smoot et al., *Structure in the COBE differential microwave radiometer first year maps*, *Astrophys. J.* **396** L1 (1992).
- [17] D. Spergel et al., *First year Wilkinson Microwave Anisotropy Probe (WMAP) observations: Determination of cosmological parameters*, *Astrophys. J. Suppl.* **148** 175-194 (2003).
- [18] D. Spergel et al., *Wilkinson Microwave Anisotropy Probe (WMAP) three year results: implications for cosmology*, *Astrophys. J. Suppl.* **170** 377 (2007).

- 
- [19] E. Komatsu et. al., *Five-Year Wilkinson Microwave Anisotropy Probe (WMAP) Observations: Cosmological Interpretation*, *Astrophys. J. Suppl.* **180** 330 (2009).
- [20] Luca Amendola and Shinji Tsujikawa, *Dark energy Theory and Observations*, *Cambridge University Press* (2010).
- [21] M. Colless, et al., *The 2dF Galaxy Redshift Survey: spectra and redshifts*, *MNRAS* **328** 1039 (2001).
- [22] Pierre-Henri Chavanis and Suresh Kumar, *Comparison between the Logotropic and  $\Lambda$ CDM models at the cosmological scale*, *JCAP* **05** 018 (2017).
- [23] V. Springel, C. S. Frenk and S. D. M. White, *The large-scale structure of the Universe*, *Nature* **440** 1137 (2006).
- [24] S. Weinberg, *The cosmological constant problem*, *Rev. Mod. Phys.* **61** 01 (1989).
- [25] S.M. Carroll, W.H. Press and E.L. Turner, *The cosmological constant*, *Annu. Rev. Astron. Astrophys.* **30** 499 (1992).
- [26] S.M. Carroll, *The cosmological constant*, *Living Rev. Rel.* **4** 01 (2001).
- [27] T. Padmanabhan, *Cosmological constant: the weight of the vacuum*, *Phys. Rept.* **380** 235 (2003).
- [28] I. Zlatev, L.-M. Wang, and P. J. Steinhardt, *Quintessence, cosmic coincidence, and the cosmological constant*, *Phys. Rev. Lett.* **82** 896 (1999).
- [29] P.J. Steinhardt, *Cosmological challenges for the 21st century*, in *Critical problems in physics*, V.L. Fitch and D.R. Marlow eds. Princeton University Press, Princeton U.S.A. (1997).

- 
- [30] P.J. Steinhardt, L.-M. Wang and I. Zlatev, *Cosmological tracking solutions*, *Phys. Rev. D* **59** 123504 (1999).
- [31] H.E.S. Velten, R.F. vom Marttens and W. Zimdahl, *Aspects of the cosmological “coincidence problem”*, *Eur. Phys. J. C* **74**: 3160 (2014).
- [32] Hongya Liu and Paul S. Wesson, *Universe Models with a Variable Cosmological “Constant” and a “Big Bounce”*, *The Astrophysical Journal* **562**: 1-6 (2001).
- [33] B. Ratra and P. Peebles, *Cosmological Consequences of a Rolling Homogeneous Scalar Field*, *Phys. Rev. D* **37** 3406 (1988).
- [34] R. Caldwell, R. Dave, and P. J. Steinhardt, *Cosmological imprint of an energy component with general equation of state*, *Phys. Rev. Lett.* **80** 1582-1585 (1998).
- [35] R. Caldwell and E. V. Linder, *The limits of quintessence*, *Phys. Rev. Lett.* **95** 141301 (2005).
- [36] C. Armendariz-Picon, V. Mukhanov, and P. J. Steinhardt, *Essentials of  $k$  essence*, *Phys. Rev. D.* **63** 103510 (2001).
- [37] T. Chiba, T. Okabe and M. Yamaguchi, *Kinetically driven quintessence*, *Phys. Rev. D.* **62** 023511 (2000).
- [38] C. Armendariz-Picon, T. Damour and V. Mukhanov,  *$k$ -Inflation*, *Phys. Lett. B.* **458** 209 (1999).
- [39] A.Y. Kamenshchik, U. Moschella and V. Pasquier, *An alternative to quintessence*, *Phys. Lett. B.* **511** 265 (2001).
- [40] H. Sandvik, M. Tegmark, M. Zaldarriaga, and I. Waga, *The end of unified dark matter ?*, *Phys. Rev. D.* **69** 123524 (2004).

- [41] S. M. Carroll, V. Duvvuri, M. Trodden, and M. S. Turner, *Is cosmic speed - up due to new gravitational physics?*, *Phys. Rev. D* **70** 043528 (2004).
- [42] S. Nojiri and S. D. Odintsov, *Introduction to modified gravity and gravitational alternative for dark energy*, *Int. J. Geom. Meth. Mod. Phys.* **4** 06 (2006).
- [43] S. Nojiri, S. D. Odintsov, and M. Sasaki, *Gauss-Bonnet dark energy*, *Phys. Rev. D* **71** 123509 (2005).
- [44] S. Nojiri and S. D. Odintsov, *Modified Gauss-Bonnet theory as gravitational alternative for dark energy*, *Phys. Lett. B* **631** 01 (2005).
- [45] G. Cognola et.al., *Dark energy in modified Gauss-Bonnet gravity: Late-time acceleration and the hierarchy problem*, *Phys. Rev. D* **73** 084007 (2006).
- [46] Eric. V. Linder, *Einstein's Other Gravity and the Acceleration of the Universe*, *Phys. Rev. D* **81** 127301 (2010).
- [47] G. R. Bengochea and R. Ferraro, *Dark torsion as the cosmic speed-up*, *Phys. Rev. D* **79** 124019 (2009).
- [48] Ratbay Myrzakulov, *Accelerating universe from  $F(T)$  gravity*, *Eur. Phys. J. C* **71** 1752 (2011).
- [49] C. W. Misner, *The Isotropy of the Universe*, *Astrophysical Journal* **151** 431 (1968).
- [50] George L. Murphy, *Big-Bang Model Without Singularities*, *Phys. Rev. D* **8** 4231 (1973).
- [51] T. Padmanabhan and SM Chitre, *Viscous universes*, *Phys. Lett. A* **120** 433 (1987).

- 
- [52] Ioav Waga and Rossana C. Falcão and Rajat Chanda, *A bulk viscosity driven inflationary model*, *Phys. Rev. D* **33** 1839 (1986).
- [53] Baolian Cheng, *Bulk viscosity in the early universe*, *Phys. Lett. A* **160** 329 (1991).
- [54] O. Grøn, *Viscous inflationary universe models*, *Astrophys. Space Sci.* **173** 191 (1990).
- [55] R. Maartens and V. Mendez, *Nonlinear bulk viscosity and inflation*, *Phys. Rev. D* **55** 1937 (1997).
- [56] J. C. Fabris, and S. V. B. Gonalves, and R. de S Ribeiro, *Bulk viscosity driving the acceleration of the Universe*, *Gen. Relat. Gravit.* **38** 495 (2006).
- [57] Baojiu Li and John D. Barrow, *Does bulk viscosity create a viable unified dark matter model?*, *Phys. Rev. D* **79** 103521 (2009).
- [58] W. S. Hipólito-Ricaldi and H. E. S. Velten, and W. Zimdahl, *Viscous dark fluid universe*, *Phys. Rev. D* **82** 063507 (2010).
- [59] Arturo Avelino and Ulises Nucamendi, *Can a matter-dominated model with constant bulk viscosity drive the accelerated expansion of the universe?*, *JCAP* **04** 006 (2009).
- [60] Arturo Avelino and Ulises Nucamendi, *Exploring a matter-dominated model with bulk viscosity to drive the accelerated expansion of the Universe*, *JCAP* **08** 009 (2010).
- [61] R. Colistete Jr., J.C. Fabris, J. Tossa and W. Zimdahl, *Bulk viscous cosmology*, *Phys. Rev. D* **76** 103516 (2007).

- 
- [62] R. Maartens, *Causal thermodynamics in relativity, in proceedings of Hanno Rund Workshop on Relativity and Thermodynamics*, South Africa June 1996, unpublished [astro-ph/9609119] [SPIRES].
- [63] W. Zimdahl, D. J. Schwarz, A. B. Balakin and D. Pavón, *Cosmic antifriction and accelerated expansion*, *Phys. Rev D* **64** 063501 (2001).
- [64] H. Okumura and F. Yonezawa, *New expression of the bulk viscosity*, *Physica A* **321** 207 (2003).
- [65] P. Ilg and H. C. Ottinger, *Nonequilibrium relativistic thermodynamics in bulk viscous cosmology*, *Phys. Rev. D* **61** 023510 (2000).
- [66] J. R. Wilson, G. J. Mathews and G. M. Fuller, *Bulk viscosity, decaying dark matter, and the cosmic acceleration*, *Phys. Rev. D* **75** 043521 (2007).
- [67] G.J. Mathews, N.Q. Lan and C. Kolda, *Late decaying dark matter, bulk viscosity and the cosmic acceleration*, *Phys. Rev. D* **78** 043525 (2008).
- [68] A. Avelino et.al, *Bulk Viscous Matter-dominated Universes: Asymptotic Properties*, *JCAP*, **08** 12 (2013).
- [69] S. Weinberg, *Gravitation and cosmology: principles and applications of the general theory of relativity*, John Wiley & sons Inc., New york U.S.A. (1972).
- [70] C. W. Misner, K. S. Thorne and J. A. Wheeler, *Gravitation*, W.H. Freeman and Company, U.S.A. (1973).
- [71] C. Eckart, *The thermodynamics of irreversible processes. III. Relativistic theory of the simple fluid*, *Phys. Rev.* **58** 919 (1940)

- 
- [72] L. D. Landau and E. M. Lifshitz, *Fluid Mechanics* Addison-Wesley, Reading U.S.A. (1959).
- [73] W. Israel, *Nonstationary irreversible thermodynamics: A causal relativistic theory*, *Ann. Phys. (N.Y.)* **100** 310 (1976).
- [74] W. A. Hiscock and L. Lindblom, *Generic instabilities in first-order dissipative relativistic fluid theories*, *Phys. Rev. D* **31** 725 (1985).
- [75] W. A. Hiscock and L. Lindblom, *Linear plane waves in dissipative relativistic fluids*, *Phys. Rev. D* **35** 3723 (1987).
- [76] W. Israel and J. M. Stewart, *Transient relativistic thermodynamics and kinetic theory*, *Ann. Phys. (N.Y.)* **118** 341 (1979).
- [77] W. Israel and J. M. Stewart, *On transient relativistic thermodynamics and kinetic theory. II*, *Proc. R. Soc. Lond. A* **365** 43 (1979).
- [78] G. M. Kremer and F. P. Devecchi, *Viscous cosmological models and accelerated universes*, *Phys. Rev. D* **67** 047301 (2003).
- [79] M. Cataldo, N. Cruz and S. Lepe, *Viscous dark energy and phantom evolution*, *Phys. Lett. B* **619** 5 (2005).
- [80] M. G. Hu and X. H. Meng, *Bulk viscous cosmology: statefinder and entropy*, *Phys. Lett. B* **635** 186 (2006).
- [81] W. A. Hiscock and J. Salmonson, *Dissipative Boltzmann-Robertson-Walker cosmologies*, *Phys. Rev. D* **43** 3249 (1991).
- [82] W. Zimdahl, *Bulk viscous cosmology*, *Phys. Rev. D*, **53** 5483 (1996).
- [83] M. Zakari and D. Jou, *Equations of state and transport equations in viscous cosmological models*, *Phys. Rev. D*, **48** 1597 (1993).

- [84] D. Pavón, D. Jou and J. Casas-Vázquez, *On a covariant formulation of dissipative phenomena*, *Ann. Inst. Henri Poincaré* **36** 79 (1982).
- [85] L. N. Liebermann, *The second viscosity of liquids*, *Phys. Rev.* **75** 1415 (1949).
- [86] J. Ren and Xin-He Meng, *Cosmological model with viscosity media (dark uid) described by an effective equation of state*, *Phys. Lett. B* **633** 1 (2006).
- [87] J.P. Singh, Pratibha Singh and Raj Bali, *Bulk viscosity and decaying vacuum density in Friedmann universe*, *Int J Theor Phys*, **51** 3828 (2012).
- [88] Shinichi Nojiri and Sergei D. Odintsov, *Inhomogeneous Equation of State of the Universe: Phantom Era, Future Singularity and Crossing the Phantom Barrier*, *Phys. Rev. D* **72** 023003 (2005).
- [89] S. Capozziello, V. F. Cardone, E. Elizalde, S. Nojiri and S. D. Odintsov, *Observational constraints on dark energy with generalized equations of state*, *Phys. Rev.* **73** 043512 (2006).
- [90] Xu Dou and Xin-He Meng, *Scalar perturbation of the viscosity dark fluid cosmological mode*, arXiv:0911.5401
- [91] M. Kowalski et al., *Improved Cosmological Constraints from New, Old and Combined Supernova Datasets*, *Astrophys. J.* **686** 749 (2008).
- [92] M. Tegmark et al., *Cosmological constraints from the SDSS luminous red galaxies*, *Phys. Rev. D* **74** 123507 (2006).
- [93] WMAP Collaboration, G. Hinshaw et. al., *Five-year Wilkinson Microwave Anisotropy Probe observations: Data Processing, sky maps and basic results*, *AstroPhys. J. Suppl.* **180** 225 (2009).

- [94] U. Alam, V. Sahni and A.A Starobinsky, *The case for dynamical dark energy revisited*, *JCAP* **0406** 008 (2004).
- [95] P. Praseetha and T. K. Mathew, *Interacting modified holographic Ricci dark energy model and statefinder diagnosis in flat universe*, *Int. J. Mod. Phys. D* **23** 1450024 (2014).
- [96] J. S. Alcaniz and J. A. S. Lima, *New limits on  $\Omega_\Lambda$  and  $\Omega_M$  from old galaxies at high redshift*, *Astrophys. J.* **521** L87 (1999).
- [97] I. Brevik, E. Elizalde, S. Nojiri and S.D. Odintsov, *Viscous little rip cosmology*, *Phys.Rev. D* **84** 103508 (2011).
- [98] L.P. Chimanto and M. G. Richarte, *Interacting dark matter and modified holographic Ricci dark energy induce a relaxed Chaplygin gas*, *Phys. Rev. D* **84** 123507 (2011).
- [99] V. Sahni, T. D. Saini, A. A. Starobinsky, and U. Alam, *Statefinder? A new geometrical diagnostic of dark energy*, *JETP Lett.* **77** 201 (2003).
- [100] B. Wu Ya, S. Li, M. H. Fu and J. He, *A modified Chaplygin gas model with interaction*, *Gen. Relativ. Gravity* **39** 653 (2007).
- [101] D. J. Liu and W. Z. Liu, *Statefinder diagnostic for cosmology with the abnormally weighting energy hypothesis*, *Phys. Rev. D* **77** 027301 (2008).
- [102] R.K. Sachs and A.M. Wolfe, *Perturbations of a Cosmological Model and Angular Variations of the Microwave Background*, *Astrophys. J.* **147** 73 (1967).
- [103] Asantha Cooray, *Integrated Sachs-Wolfe effect: Large scale structure correlation*, *Phys. Rev. D* **65** 103510 (2002).

- [104] S. Weinberg, *Entropy generation and the survival of protogalaxies in an expanding universe*, *Astrophys. J.* **168** 175 (1971).
- [105] I. Brevik and O. Grøn, *Universe Models with Negative Bulk Viscosity*, *Astrophys. Space Sci.* **347** 399 (2013).
- [106] J. D. Bekenstein, *Generalized second law of thermodynamics in black-hole physics*, *Phys. Rev. D* **9** 3292 (1974).
- [107] G. W. Gibbons and S. W. Hawking, *Cosmological event horizons, thermodynamics, and particle creation*, *Phys. Rev. D* **15** 2738 (1997).
- [108] G. L. Sewell, *On the generalised second law of thermodynamics*, *Phys. Lett. A* **122** 309 (1987).
- [109] T. K. Mathew, R. Aiswarya and K. S. Vidya, *Cosmological horizon entropy and generalized second law for flat Friedmann universe*, *Eur. Phys. J. C* **73** 2619 (2013).
- [110] A. Sheykhi, *Thermodynamics of interacting holographic dark energy with the apparent horizon as an IR cutoff* *Class.Quantum Grav.* **27** 025007 (2010).
- [111] P. C. W. Davis, *Cosmological horizons and the generalised second law of thermodynamics*, *Class. Quantum Grav.* **4** L225 (1987).
- [112] M. R. Setare and A. Sheykhi, *Viscous dark energy and generalized second law of thermodynamics*, *Int. J. Mod. Phys. D* **19** 1205 (2010).
- [113] H. B. Callen, *Thermodynamics and an introduction to Thermostatistics*, 2nd Edition, John Wiley & Sons, New York, (1960).
- [114] Diego Pavon and Ninfa Radicella, *Does the entropy of the Universe tend to a maximum?*, *Gen. Relativ. Gravit.* **45** 63 (2013).

- [115] M. C. Bento, O. Bertolami and A.A. Sen, *Generalized Chaplygin Gas, Accelerated Expansion and Dark Energy-Matter Unification*, *Phys. Rev. D* **66** 043507 (2002).
- [116] A. Addazi, A. Marcian and S. Alexander, *A Unified picture of Dark Matter and Dark Energy from Invisible QCD*, *arXiv: 1603.01853* (2016).
- [117] V. Gorini et.al., *The Chaplygin gas as a model for dark energy*, *arXiv:0403062* (2004).
- [118] W. Zimdahl et. al., *Viscous dark fluid universe: A unified model of the dark sector?*, *Int. J. Mod. Phys. Conf. Ser.* **03** 312 (2011).
- [119] N. Radicella and D. Pavón, *The generalized second law in universes with quantum corrected entropy relations*, *Phys. Lett. B* **691** 121 (2010).
- [120] N. Radicella and D. Pavón, *A thermodynamic motivation for dark energy*, *Gen. Rel. Grav.* **44** 685 (2012).
- [121] En-Kun Li, Yu Zhang, Jin-Ling Geng, and Peng-Fe Duan, *Generalized holographic Ricci dark energy and generalized second law of thermodynamics in Bianchi Type I universe* *Gen. Rel. Grav.* **47** 136 (2015).
- [122] K Karami, S Ghaffari and M M Soltanzadeh, *The generalized second law of gravitational thermodynamics on the apparent and event horizons in FRW cosmology* *Class. Quantum Grav.* **27** 205021 (2010).
- [123] R. Bousso and N. Engelhardt, *Generalized Second Law for Cosmology* *Phys. Rev. D* **93** 024025 (2016).
- [124] Jia Zhou et.al., *The generalized second law of thermodynamics in the accelerating universe*, *Phys. Lett. B* **652** 86 (2007).

- [125] M. R. Setare and A. Sheykhi, *Viscous dark energy and generalized second law of thermodynamics*, *Int. J. Mod. Phys. D* **19** 1205 (2010).
- [126] B. Wang, Y. Gong and E Abdalla, *Thermodynamics of an accelerated expanding universe*, *Phys. Rev. D* **74** 083520 (2006).
- [127] M. Akbar, *Viscous Cosmology and Thermodynamics of Apparent Horizon*, *Chin. Phys. Lett.* **25** 4199 (2008).
- [128] Titus K. Mathew, P. Praseetha, *Holographic dark energy and generalized second law*, *Mod. Phys. Lett. A* **29** 1450023 (2014).
- [129] P Praseetha and Titus K Mathew, *Entropy of holographic dark energy and the generalized second law*, *Class. Quantum Grav.* **31** 185012 (2014).
- [130] A. Sheykhi, B. Wang and R. G. Cai, *Thermodynamical properties of apparent horizon in warped DGP braneworld*, *Nucl. Phys. B* **779** 1 (2007).
- [131] A. Sheykhi, B. Wang and R. G. Cai, *Deep connection between thermodynamics and gravity in Gauss-Bonnet braneworlds*, *Phys. Rev. D* **76** 023515 (2007).
- [132] V. Sahni, T.D. Saini, A.A. Starobinsky, U. Alam, *Statefinder-A new geometrical diagnostic of dark energy*, *JETP Lett.* **77** 201 (2003).
- [133] H. Velten and D. J. Schwarz, *Dissipation of dark matter*, *Phys. Rev. D* **86** 083501 (2012).
- [134] I. Brevik, *Viscosity-Induced Crossing of the Phantom Barrier*, *Entropy* **17** 6318 (2015).

- [135] B. D. Norman and I. Brevik, *Characteristic properties of two different viscous cosmology models for the future universe*, *Mod.Phys.Lett. A* **32** 1750026 (2017).
- [136] J. Wang and X. Meng, *Effects of New Viscosity Model on Cosmological Evolution*, *Mod. Phys. Lett. A* **29** 1450009 (2014).
- [137] B. D. Normann and I. Brevik, *General Bulk-Viscous Solutions and Estimates of Bulk Viscosity in the Cosmic Fluid*, *Entropy*, **18** 215 (2016).
- [138] I. Brevik, *Temperature variation in the dark cosmic fluid in the late universe*, *Mod. Phys. Lett. A* **31** 1650050 (2016).
- [139] G. F. R. Ellis, R. Maartens and M. A. H. MacCallum, *Causality and the speed of sound*, *Gen Relativ Gravit* **39** 1651 (2007).
- [140] Moncy V John and J. V. Narlikar, *Comparison of cosmological models using Bayesian theory*, *Phys. Rev. D.*, **65** 043506 (2002).
- [141] P. S. Drell, T. J. Lorendo and I. Wasserman, *Type Ia Supernovae, evolution, and the cosmological constant*, *Astrophys. J.*, **530** 593 (2000).
- [142] Moncy V John , *Cosmography, decelerating past, and cosmological models: learning the Bayesian way*, *Astrophys. J.* **630** 667 (2005).
- [143] A. Jaffe,  *$H_0$  and Odds on Cosmology*, *Astrophys. J.*, **471** 24 (1996).
- [144] M.P. Hobson, S.L. Bridle and O. Lahav, *Combining cosmological datasets: hyperparameters and Bayesian evidence*, *Mon.Not.Roy.Astron.Soc.*, **335** 377 (2002).
- [145] Rev. T. Bayes, *An essay toward solving a problem in the doctrine of chances*, *Phil. Trans. R. Soc.*, **53** 370 (1763).

- 
- [146] R. E. Kass and A. E. Raftery, *Bayes factors*, *Journal of the American Statistical Association*, **90** 773 (1995).
- [147] Bertram Schwarzschild, *High-Redshift Supernovae reveal an epoch when cosmic expansion was slowing down*, *Physics Today*, **57**, 6, 19 (2004).
- [148] N. Mostafapoor and O. Grøn, *Viscous  $\Lambda$ CDM universe models*, *Astrophys. Space Sci.*, **333** 357 (2011).
- [149] B. Moore et. al., *Dark Matter Substructure in Galactic Halos*, *Astrophys. J.*, **524** L19 (1999).
- [150] J. F. Navarro, C. S. Frenk and S. D. White, *The Structure of Cold Dark Matter Halos*, *Astrophys. J.*, **462** 563 (1996).
- [151] N D Jerin Mohan, Athira Sasidharan and Titus K Mathew, *Bulk viscous matter and recent acceleration of the universe based on causal viscous theory*, *Eur. Phys. J. C*, **77** 849 (2017).
- [152] N D Jerin Mohan, Athira Sasidharan and Titus K Mathew, *Dynamical system analysis and thermal evolution of the causal dissipative model*, *arXiv:1807.04041* (2018).